

CHAPTER 3 DEPTH DETERMINATION

1. INTRODUCTION

Depth determination is a fundamental task for a hydrographer, which requires specific knowledge of the medium, of underwater acoustics, of the plethora of devices available for depth measurement, of complementary sensors for attitude and heave measurement and proper procedures to achieve and meet the internationally recommended standards for accuracy and coverage as articulated in IHO publication S-44 5th Edition.

Lead line and sounding pole were the earliest methods used for directly measuring water depth. Their easy principles of operation ensured their continued use over many centuries.

Single beam echo sounders, derived from military sonars, were a major development and have been used in hydrographic surveying since the mid 1900s.

During the last decade, hydrographic surveying has experienced a conceptual change in depth measurement technology and methodology. Multibeam echo sounders (MBES) and airborne laser sounding systems (ALS) now provide almost total seafloor coverage and depth measurement. The high data density and high acquisition rates have led to huge bathymetric data sets and much ancillary data.

The state of the art of the depth measurement equipment was evaluated by the working group on S-44 preparing the 4th Edition in 1998 as follows:

“Single beam echo sounders have reached a sub-decimetre accuracy in shallow water. The market offers a variety of equipment with different frequencies, pulse rates etc. and it is possible to satisfy most users' and, in particular, the hydrographers' needs. (...)

Multibeam echo sounder technology is developing rapidly and offers great potential for accurate and total seafloor search if used with proper procedures and provided that the resolution of the system is adequate for proper detection of navigational hazards.

Airborne laser sounding is a new technology which can offer substantial productivity gains for surveys in shallow, clear water. Airborne laser systems are capable of measuring depths to 50 m or more.”

Despite these new technologies, single beam echo sounders (SBES) still remain, for the present, the traditional equipment used on hydrographic surveys worldwide. These echo sounders have also evolved from analogue to digital recording, with greater precisions and higher accuracies and with specific features which allow a wider variety of purposes to be met. The use of digital echo sounders along with motion sensors, satellite positioning systems (such as GPS) and software for data acquisition have combined to optimize productivity with corresponding reductions in personnel for survey operations.

MBES have become a valuable tool for depth determination when full seafloor ensonification is required. An increasing number of National Hydrographic Offices (NHO) has adopted multibeam technology as the methodology of choice for the collection of bathymetric data for new chart production. The acceptance of

multibeam data for use in published nautical charts is a sign of growing confidence in the technology. Notwithstanding their impressive capabilities, it is vital that planners, operators and checkers have indepth knowledge of MBES operating principles, as well as practice in data interpretation and validation.

Airborne laser sounding systems are being used by a few NHOs; these systems have, by far, the highest data acquisition rates and are particularly suited to near shore and shallow water areas. However, the high costs for the assets involved in data collection and their operation do not currently allow a more general use.

In this Chapter, Section 2 covers the broad acoustic fundamentals necessary for the understanding of sea water acoustic waves and physical characteristics, acoustic wave propagation and acoustic parameters. Section 3 deals with motion sensors. Section 4 covers transducer characteristics, their classification with regard to beam pattern, principles of operation and their installation. Section 5 describes the acoustic systems of single beam echo sounders and swath systems, both multibeam and interferometric sonars, with regard to their characteristics, principles of operation, installation and operational use. Finally, Section 6 explains non-acoustic systems, such as airborne laser and electromagnetic induction systems, remote sensing systems and classic mechanical devices.

The terminology used in this chapter follows, as far as possible, the Hydrographic Dictionary [IHO SP-32 5th Edition, 1994].

2. ACOUSTIC AND MOTION SENSORS FUNDAMENTALS

Sea water is the medium in which hydrographic measurements normally take place, therefore knowledge of sea water's physical properties and of acoustic waves propagation is important for full comprehension of the contents and aim of this chapter.

2.1 Sea water acoustic waves and physical characteristics

Despite electromagnetic waves having an excellent propagation in a vacuum and air, they hardly penetrate nor propagate through liquids. However, acoustic waves, either sonic or ultra-sonic, achieve good penetration and propagation through all elastic media once these media can be made to vibrate when exposed to pressure variations. The majority of the sensors used for depth determination use acoustic waves.

2.1.1 Acoustic field

The acoustic waves consist of subtle variations of the pressure field in the water. Sea water particles move longitudinally, back and forth, in the direction of the propagation of the wave, producing adjacent regions of compression and expansion, similar to those produced by longitudinal waves in a bar.

The intensity of the acoustic wave, **I**, is the amount of energy per second crossing a unit area. The acoustic intensity is given by:

$$I = \frac{p_e^2}{\rho c} \quad (3.1)$$

where ρ is the water density, c is the sound velocity in the water and p_e is the effective acoustic pressure³⁰, given by the root mean square of the peak pressure amplitude, P , i.e.:

$$p_e = \frac{P}{\sqrt{2}}$$

The acoustic wave intensity is computed using average acoustic pressure rather than instantaneous values. The acoustic pressure and intensity, due to their wide range variation, are usually expressed in logarithmic scales referred to pressure and intensity levels, the decibel scale being the most common logarithmic scale.

The acoustic intensity level, **IL**, is given by:

$$IL = 10 \log_{10} \frac{I}{I_{Ref}} \quad (3.2)$$

where I_{Ref} is the reference intensity.

The acoustic intensity level is alternatively expressed by,

$$IL = 20 \log_{10} \frac{p_e}{p_{Ref}} \quad (3.3)$$

where p_{Ref} is the reference pressure³¹.

2.1.2 Sonar Equation

The sonar³² equation is used to study and express the detection capability and performance of echo sounders as a function of operating conditions [Urick, 1975].

The sonar equation for echo sounders defines the signal or echo detection as the Echo Excess (**EE**),

$$EE = SL - 2 TL - (NL - DI) + BS - DT \quad (3.4)$$

where **SL** = source level, **TL** = transmission loss, **NL** = noise level, **DI** = directivity index, **BS** = bottom backscattering strength and **DT** = detection threshold.

In this section each term of the sonar equation is presented and studied to enable a better understanding of the processes involved in acoustic signal propagation and echo detection.

The acoustic wave intensity I_r at a distance r from the transmitter is obtained by,

³⁰ Pascal (Pa) is the unit of pressure in the International System (SI).

³¹ In underwater acoustics reference pressure is usually adopted as 1 μ Pa.

³² Sound Navigation and Ranging.

$$I_r = \frac{p_r^2}{\rho c} \text{ W/m}^2 \quad (3.5)$$

Where p_r is the effective pressure at the distance r from the source and ρc is the acoustic impedance³³ (considering a sound velocity of 1500 m/s and sea water density of 1026 kg/m³ the acoustic impedance is $\rho c = 1.54 \cdot 10^6 \text{ kg/m}^2\text{s}$).

The Source Level (SL) gives the acoustic signal intensity level referred to the intensity of a plane³⁴ wave with root mean square (rms) pressure 1 μPa , for a point located 1 metre away from the centre of the source (transmitter), i.e.:

$$\text{SL} = 10 \cdot \log_{10} \frac{I_1}{I_{\text{Ref}}} \quad (3.6)$$

The Transmission Loss (TL) takes into account the losses of acoustic intensity due to geometry, i.e. from spreading losses, proportional to r^2 and the losses due to absorption, proportional to the coefficient of absorption, dependent on the physical and chemical sea water properties and on the acoustic frequency (see 2.3.1).

The spreading loss is caused by the geometry of the beam with its cone shape (Figure 3.1). The increase in area results in the decrease of power per unit of area.

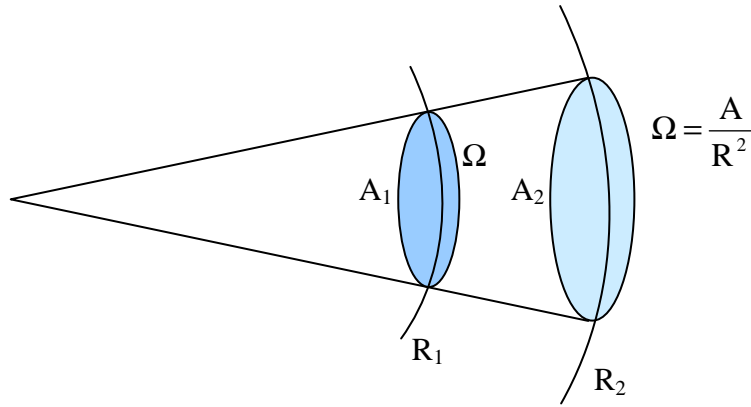


Fig. 3.1 "Spreading loss due to beam geometry"

The power, Π , of the acoustic pulse is equal to Intensity x Area:

$$\Pi = I_1 \cdot A_1 = I_2 \cdot A_2$$

where $A_1 = \Omega \cdot R_1^2$ and $A_2 = \Omega \cdot R_2^2$, being Ω the solid angle³⁵.

³³ Acoustic impedance corresponds to the resistance of the medium to the wave propagating through it, i.e., a proportionality factor between the velocity and the acoustic pressure.

³⁴ Plane waves occur in a small region away from the source where wave fronts (points where vibrations are in phase), are approximately plane and have negligible change in amplitude.

Therefore, the relation of intensities is given by:

$$\frac{I_1}{I_2} = \left(\frac{R_2}{R_1} \right)^2 \quad (3.7)$$

If one considers the reference intensity at $R_1 = 1$ m, the distance at which the source level (SL) is determined, the logarithmic ratio of the intensities relates to the transmission loss due to spreading is:

$$10 \cdot \log_{10} \frac{I}{I_{\text{Ref}}} = 10 \cdot \log_{10} \frac{1}{R_2^2} = -20 \cdot \log_{10} R_2 \quad (3.8)$$

Hence, the transmission loss is given by:

$$TL = 20 \log_{10} r + ar \quad (3.9)$$

where r is the distance to the transducer and a the absorption coefficient.

The Noise Level (NL) is dependent on the environmental spectral noise level (N_0) and on the transducer bandwidth during reception (w),

$$NL = N_0 + 10 \log_{10} w \quad (3.10)$$

The noise in the ocean is generated by several sources [Urick, 1975] such as: waves, rain, seismic activity, thermal noise, living organisms and man-made.

Besides noise, it is also important to take into account the combined affect of the backscattering acoustic energy created by various marine bodies; these include surface waves, air bubbles, marine life, materials in suspension, etc. This contribution is known as the Reverberation Level (RL).

Transducers usually have the capacity to concentrate the energy within a conical shape (Figure 3.2). This property can be quantified, for the sonar equation, as the ratio from the intensity within the beam to the intensity of an omni directional point source with the same power.

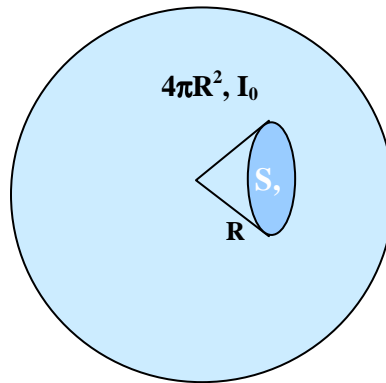


Fig. 3.2 "Ensonified surfaces from an omni directional source and directional source"

³⁵ The solid angle, Ω , is the space enclosed by a conical surface. The value, expressed in steradian (sr), is obtained as $\Omega = S/R^2$, where S is the spherical surface with centre in the apex of the cone and radius R .

Therefore, considering the same power for the omni directional and directional sources:

$$\Pi = I_0 \cdot 4\pi R^2 = I \cdot S \quad (3.11)$$

The ratio of intensities is given by:

$$\frac{I}{I_0} = \frac{4\pi R^2}{S} \quad (3.12)$$

and the Directivity Index (DI) is obtained by:

$$DI = 10 \log_{10} \frac{I}{I_{Ref}} = 10 \log_{10} \frac{4\pi R^2}{S} \quad (3.13)$$

For an array with length, L , and wave length, λ , (with $L \gg \lambda$) the Directivity Index is given by:

$$DI = 10 \log_{10} (2L/\lambda) \quad (3.14)$$

The acoustic energy returned from the seafloor is the energy used by sonar systems, as well as the remote means by which to deduce some seafloor properties. Knowledge of the beam angle and the sound velocity profile in the water column allows one to obtain backscatter strength corrected for absorption and spherical spreading.

Each particle on the seafloor can be likened to a reflector and the seabed return as the sum of the energy contributions from the water-seabed interface and from the volume of sediments, due to some energy penetration into the sediments. However, the contribution from the volume of sediments is less significant when using high frequencies.

The seabed Backscattering Strength (**BS**) is usually described as the logarithmic sum of intrinsic backscattering strength per unit area or backscatter index (**SB**), which is dependent on the reflective properties of the seafloor and the effective instantaneous scattering area **A**, the area of the seafloor which contributes to the backscattered signal:

$$BS = SB + 10 \log_{10} A \text{ dB}. \quad (3.15)$$

The limits of the backscattering area are defined by the beam geometry, particularly by the beam width (of the transmit beam) in the along-track direction at normal incidence or nadir, ϕ_T , and by the beam width (of the receive beam) in the across-track direction at nadir, ϕ_R .

For the off-nadir directions, the backscattering area is bounded by the beam width, ϕ_T , and by the transmitted pulse length τ (Figure 3.3). The seafloor backscattering strength may be given by:

$$BS = \begin{cases} SB + 10 \cdot \log_{10}(\phi_T \phi_R R^2) & \text{beam width constrict} \\ SB + 10 \cdot \log_{10}\left(\frac{c\tau}{2\sin\beta} \phi_T R\right) & \text{pulse length constrict} \end{cases} \quad (3.16)$$

where R is the slant range from the transducer to the point on the seafloor, c is the velocity of the sound and β is the beam angle with reference to the vertical.

The backscatter coefficient, SB , is usually partially dependent upon the angle of incidence, the largest variation being near nadir and typically follows a Lambert's law [Urlick, 1975 and de Moustier, 1993] dependence at larger angles of incidence. It is common to define:

$$\begin{aligned} SB &= BS_N, \text{ for normal incidence } (\beta = 0^\circ) \\ SB &= BS_O \cdot \cos^2 \beta, \text{ for oblique incidence } (\beta > 10\text{-}25^\circ) \end{aligned}$$

Typically, BS_N will be about -15 dB and BS_O about -30 dB. These values may change within ± 10 dB or even more depending on seabed type and roughness.

Looking at the beam footprint (ensonified area), Figure 3.3, the instantaneous ensonified area, A , is a function of the transmitted beam width, ϕ_T . The number of samples per beam depends on the sampling interval (τ_s).

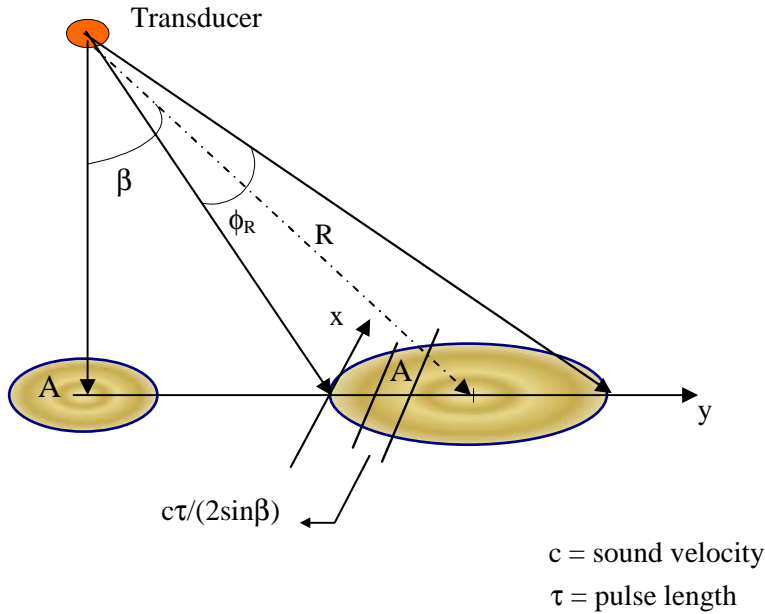


Fig. 3.3 "Backscatter samples"

The Detection Threshold (DT) is a system dependent parameter which establishes the lowest level above which the echo sounder can detect the returning echoes.

2.1.3 Temperature

The temperature at the sea surface varies with the geographic position on the earth, with the season of the year and the time of the day [Pickard and Emery, 1990]. The temperature field distribution is a complex one and can not be predicted with enough accuracy for hydrographic surveys; through the water column the behaviour of the temperature is also very complex. Such unpredictability necessitates a comprehensive distribution of sound velocity profile casts, both temporally and spatially, to maintain a representative currency of the sound velocity profiles for the survey area.

The depth measurement is quite sensitive to variations of the sound velocity profile; a variation of one degree Celsius in temperature translates to approximately 4.5 m/s in sound velocity variation.

The temperature variation is the dominant factor for sound velocity variation between the surface and the lower limit of the thermocline³⁶, thereafter pressure becomes the principal influence.

2.1.4 Salinity

The salinity is a measure of the quantity of dissolved salts and other minerals in sea water. It is normally defined as the total amount of dissolved solids in sea water in parts per thousand (ppt or ‰) by weight.

In practice, salinity is not determined directly but is computed from chlorinity, electrical conductivity, refractive index or some other property whose relationship to salinity is well established. As a result of the Law of Constancy of Proportions, the level of chlorinity in a sea water sample is used to establish the sample's salinity³⁷.

The average salinity of sea water is around 35 ‰. The rate of variation of sound velocity is approximately 1.3 m/s for a 1 ‰ alteration in salinity. Typically the salinity is measured with a CTD cast (Conductivity, Temperature and Depth) using the observable electrical conductivity, see 2.2.1.2.

2.1.5 Pressure

The pressure also impacts significantly on the sound velocity variation. Pressure is a function of depth and the rate of change of sound velocity is approximately 1.6 m/s for every alteration of 10 atmospheres, i.e. approximately 100 metres of water depth³⁸.

The pressure has a major influence on the sound velocity in deep water.

2.1.6 Density

Water density is dependent upon the previous parameters, i.e. temperature, salinity and pressure.

Fifty percent of the ocean waters have a density between 1027.7 and 1027.9 kg/m³. The largest influence on density is compressibility with depth. Water with a density of 1028 kg/m³ at the surface would have a density of 1051 kg/m³ at a depth of 5000 metres.

³⁶ The thermocline is also called discontinuity layer or thermal layer. The thermocline corresponds to a vertical negative temperature gradient in some layers of the water column, which is appreciably greater than the gradients above and below it. The main thermoclines in the ocean are either seasonal, due to heating of the surface water in summer, or permanent.

³⁷ A joint committee (IAPO, UNESCO, ICES, and SCOR) proposed the universal adoption of the following equation for determining salinity from chlorinity: $S = 1.80655 Cl$.

³⁸ This is derived by the hydrostatic principle, i.e., $p(z) = p_0 + \rho gz$.

2.2 Salinity, Temperature, and Sound Velocity Determination

This subsection describes the instrumentation used for salinity, temperature and sound velocity determination as well as their operating principles and the calculation for mean sound velocity.

2.2.1 Instrumentation

2.2.1.1 Sound Velocity Profiler is the most common instrument used to measure the sound velocity profile through the water column. This instrument has one pressure sensor to measure depth, a transducer and a reflector a certain distance, d , apart. The sound velocity is calculated by the equation $c = 2d/\Delta t$, where Δt is the two-way travel time of the acoustic signal between the transducer and the reflector (similar to the depth measurement performed by echo sounders).

2.2.1.2 CTD is an electronic instrument with sensors for conductivity, temperature and depth. This instrument records the salinity by directly measuring the electrical conductivity of the sea water.

Sound velocity in the water varies with the medium's elasticity and density, which are dependent upon the salinity, temperature and pressure. With the information from the CTD (salinity, temperature and pressure) it is possible to calculate the sound velocity in the water based on empirical equations. One simple equation with adequate accuracy was presented by Coppens [Kinsler et al., 1982]:

$$C(Z, T, S) = 1449.05 + T[4.57 - T(0.0521 - 0.00023 \cdot T)] + \quad (3.17) \\ + [1.333 - T(0.0126 - 0.00009 \cdot T)](S - 35) + \Delta(Z)$$

where T is the temperature in degrees Celsius ($^{\circ}\text{C}$), S is the salinity in parts per thousand (ppt), Z is the depth in km, and $\Delta(Z) \approx 16.3 \cdot Z + 0.18 \cdot Z^2$.

This equation is valid for a latitude of 45° . For other latitudes, Z should be replaced by $Z[1 - 0.0026 \cdot \cos(2\phi)]$, being ϕ the latitude.

2.2.1.3 Thermistors are elements whose electrical resistance depends on their temperature, which depends on the amount of heat radiation³⁹ falling on it from the sea. Thermistor chains are used to measure the water temperature at several depths through the water column. These chains, usually moored, consist of several thermistor elements, regularly spaced along a cable. A data logger samples each element sequentially and records the temperatures as a function of time.

2.2.2 Instrument operation

Important for successful operation of a sound velocity profiler, before deployment, the profiler should have the correct parameters entered with the required recording settings and be calibrated with the correct atmospheric offset in order to generate reliable depth measurements.

It should be stressed that, during the atmospheric offset calibration, a sound velocity profiler should not be in a pressurised compartment or the calibration will produce biased offsets and thus erroneous depth measurements.

³⁹ The heat radiation rate is given by Stefan's Law which states that the rate of emission of heat radiation from an object is proportional to the fourth power of its absolute temperature.

Before deployment, the profiler should be in the water for approximately 15 minutes for thermal stabilisation and during a sound velocity cast, it is recommended a constant deployment speed is maintained.

2.2.3 Data recording and processing

Sound velocity profiles should be edited and carefully checked for anomalous depths and sound velocity readings.

In general, velocity profilers record both depth and sound velocity, both downwards and upwards. The two profiles should be compared to confirm they are similar after which the profiles are often meaned to create the final profile, although this not necessarily required, in any event the readings should be compared and additional information removed to allow sorting into ascending or descending order.

2.2.4 Sound velocity computation

After the sound velocity profile has been validated, it can be applied to the survey file. The computation is used to correct depth measurements with sound velocity profile data.

For beams near the vertical, specific case of single beam echo sounders, it is accurate enough to use the average sound velocity in the water column. However, away from nadir, it is necessary to perform ray tracing to take account of the beam curvature due to any refraction phenomenon encountered; this is the procedure used in MBES (see 5.2.1.8.1).

For a signal transmitted vertically (i.e., $\theta_0 = 0^\circ$), the harmonic mean sound velocity, c_h for a depth z_n is obtained by:

$$c_h(z_n) = \frac{z_n}{\sum_{i=1}^n \frac{1}{g_i} \ln \left(\frac{c_i}{c_{i-1}} \right)} \quad (3.18)$$

where g_i is the constant gradient at layer i , given by:

$$g_i = \frac{c_i - c_{i-1}}{z_i - z_{i-1}}.$$

2.3 Sea water sound propagation

This section focuses on sound propagation namely attenuation, reflection, and refraction.

2.3.1 Attenuation

Attenuation is the loss in energy of a propagating wave due to absorption, spherical spreading and scattering by particles in the water column.

The absorption is the result of dissociation and association of some molecules in the water column; magnesium sulphate ($MgSO_4$) is a major source of absorption in salt water. The rate of absorption is dependent on the physical and chemical properties of sea water and on the acoustic frequency being transmitted. From Figure 3.4 it can be seen that above a frequency of 100 kHz the absorption coefficient increases with the increase of temperature; thus, it can be expected that sonar range will vary with the water temperature.

The spherical spreading is dependent on the geometry; for a solid angle the acoustic energy spreads over a larger area as the distance from the source increases.

Both losses by absorption and spherical spreading are taken into account in the sonar equation (see 2.1.2). However, losses from scattering depend upon particles or bodies present in the water column; scattering is chiefly due to marine organisms, a major source of which is the deep scattering layer (DSL) which consists of a layer of plankton whose depth varies throughout the day.

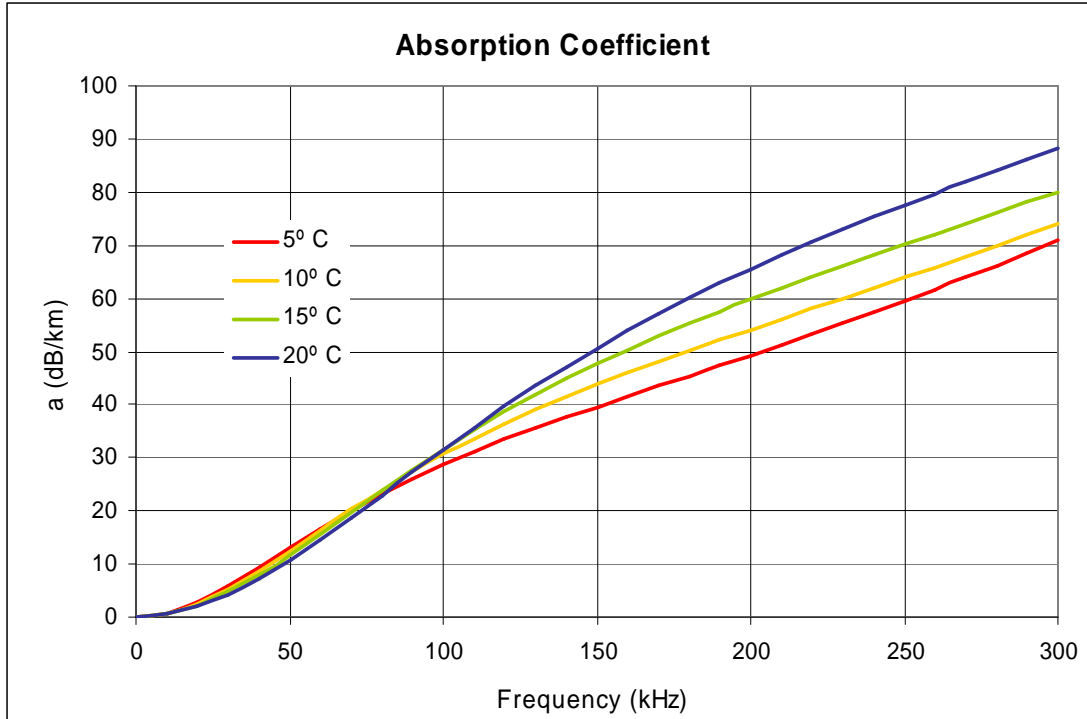


Fig. 3.4 "Absorption coefficient"

2.3.2 Refraction and reflection

Refraction is the process in which the direction of propagation of the acoustic wave is altered due to a change in sound velocity within the propagating medium or as the energy passes through an interface, representing a sound velocity discontinuity between two media.

According to Snell's Law and considering two media (Figure 3.5) with different sound velocities, c_1 and c_2 ; if c_1 is greater than c_2 , the direction of the acoustic wave propagation is altered and the transmit angle will be smaller than the angle of incident. In contrast, if c_1 is smaller than c_2 , the direction of the acoustic wave propagation is changed and the transmit angle will be greater than the angle of incident. For normal incidence no refraction occurs.

For normal incidence and smooth seabeds, the reflection coefficient⁴⁰ for the pressure, \mathcal{R} , is obtained by the ratio of the amplitude pressure of the reflected wave by the amplitude pressure of the incident wave [Kinsler et al., 1982].

⁴⁰ It is also possible to define reflection coefficients for power and intensity. For normal incidence the reflection coefficient for power and intensity is the square of the reflection coefficient for the pressure.

$$\mathfrak{R} = \frac{P_R}{P_I} = \frac{\rho_2 c_2 - \rho_1 c_1}{\rho_2 c_2 + \rho_1 c_1} \quad (3.19)$$

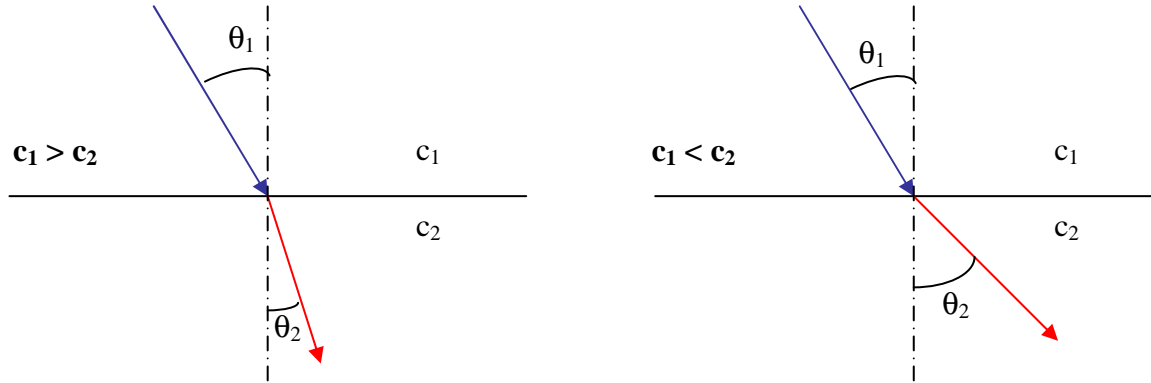


Fig. 3.5 "Refraction principle"

For general conditions, the ratio of acoustic intensity reflected and transmitted depends mainly on:

- Contrast between the acoustic impedances of the media;
- Seafloor roughness;
- Acoustical frequency.

2.4 Acoustic parameters

The characteristics of an echo sounder are determined by the transducers, namely the directivity, beam width, beam steering and side lobes level. In this subsection each of these parameters is analyzed.

2.4.1 Frequency

The echo sounder's acoustic frequency is the parameter which determines the range and the sound penetration of sediments. The attenuation of the acoustic signal in the water is proportional to the frequency. The higher the frequency is, the higher the attenuation will be and, consequently, the lower the range and the penetration into the seafloor.

The beam width is dependent on the acoustic wave length and on the size of the transducer. For the same beam width a lower frequency will require a larger transducer.

The frequencies of bathymetric echo sounders are typically:

- Waters shallower than 100 metres: frequencies higher than 200 kHz;
- Waters shallower than 1500 metres: frequencies from 50 to 200 kHz;
- Waters deeper than 1500 metres: frequencies from 12 to 50 kHz;

The frequencies for sediment echo sounders are below 8 kHz.

2.4.2 Band width

Taking f_0 as the frequency of maximum power transmission (resonance frequency) and f_1 and f_2 as the frequencies corresponding to one half of that power, the band width is the frequency interval between these frequencies (Figure 3.6), i.e. $W = f_2 - f_1$

The transducer's quality factor, Q , is given by,

$$Q = \frac{f_0}{W} \quad (3.20)$$

From the definitions above one can see that Q and W have reciprocal variation. Hence, to optimize the transmission power, the transducer should transmit close to the resonance frequency and therefore have a small band width, i.e. a high quality factor value.

During reception it is necessary to have good echo discrimination from any other signal. Although, it must be well defined in the frequency range, the transducer band width should satisfy $W \geq 1/\tau$, where τ is the pulse duration.

The optimized solution is to have a transmission transducer with high Q and a reception transducer operating in the same frequency of resonance but with a low Q .

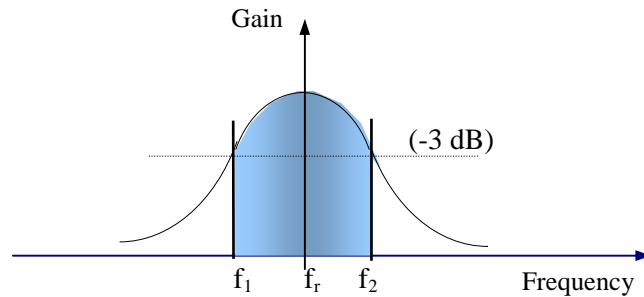


Fig. 3.6 "Transducer band width"

2.4.3 Pulse length

The pulse length determines the energy transmitted into the water; for the same power, the longer the pulse length, the higher the energy put into the water will be and thus the greater the range that can be achieved with the echo sounder.

To take advantage of the transducer resonant frequency, the pulse duration should be at least half its natural period. The drawback of longer pulses is the decrease in vertical resolution of two adjacent features (Figure 3.7).

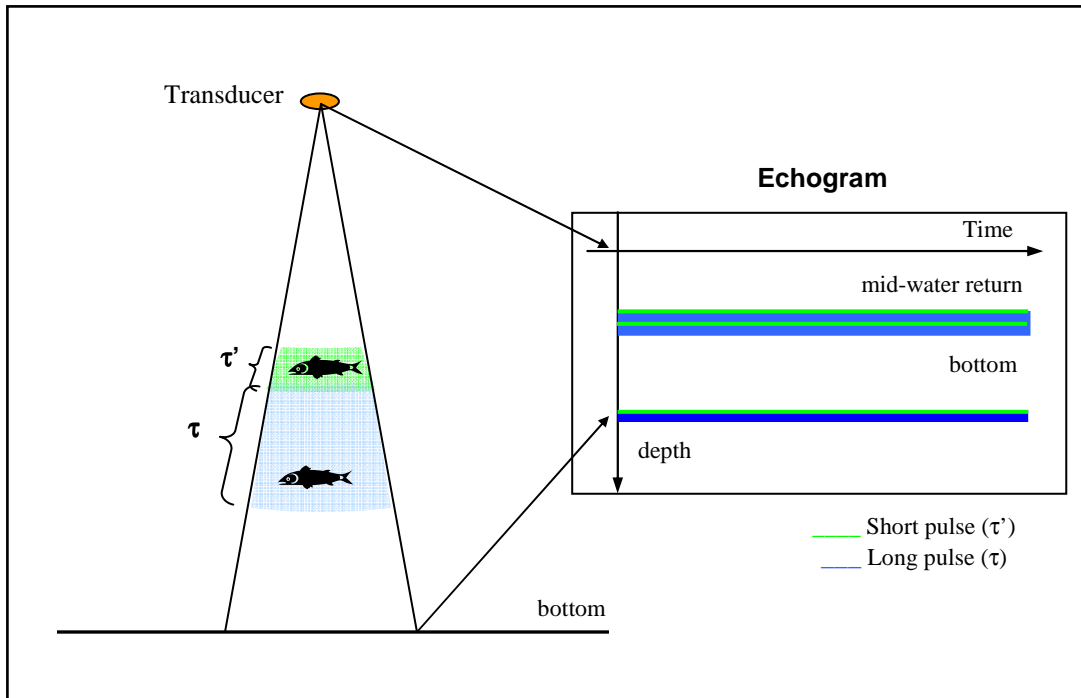


Fig. 3.7 "Resolution as a function of pulse length"

3. MOTION SENSORS

Being able to correct the observed depths and their positioning for vessel motion, i.e. attitude (roll, pitch, and heading) and heave was a considerable achievement and advance in hydrographic surveying quality and accuracy. For this purpose inertial sensors with a heading sensor (usually a gyro or fluxgate compass) or inertial sensors with the integration of GPS information are used to measure the attitude and heave of the survey vessel.

The attitude of the vessel consists of three rotations about the conventional three orthogonal axes defined for the vessel. Hereafter the vessel co-ordinate system is defined as a right-hand system with the x axis pointing towards the bow, the y axis pointing towards starboard and the z axis pointing downwards. In this reference system roll corresponds to a rotation about the x axis (the roll is positive when the starboard side is down), pitch corresponds to a rotation about the y axis (the pitch is positive when the bow is up), and yaw corresponds to a rotation about the z axis (the yaw is positive for a clockwise rotation).

To transform the collected data, referred to the vessel reference frame, to the local co-ordinate system it is necessary to perform rotations according to the sensed attitude. Hereafter, by convention, the local co-ordinate system is defined as a left-hand system with the x axis pointing to East, the y axis pointing to North, and the z axis pointing downwards.

This next section covers the fundamentals of motion sensing and measurement accuracy.

3.1 Principles of operation

3.1.1 Inertial sensors

Inertial sensors or Inertial Measurement Units (IMU) are the most common sensors used in hydrography for roll, pitch and heave measurements. These sensors apply Newton's laws for motion and consist of three accelerometers, mounted in tri-orthogonal axes, and three angular rate sensors placed in the same frame which thus experience the same angular motions as the vessel (strap down system). The output from this triad of accelerometers provides a good estimation of the gravity vector, the direction from which small angular displacements of the vessel are measured. The triad of angular rate sensors measures the angular displacements (i.e., roll, pitch, and yaw).

The heave is determined by the double integration of the linear acceleration sensed by the vertical accelerometer.

The data from the accelerometers are low-pass filtered to remove high frequency variations from the apparent vertical due to swell, quick turns or sudden velocity variations. On the other hand, the data from the angular rate sensors are high-pass filtered to remove the low frequency movements. Therefore the filter output is the platform attitude with frequency above the selected cut-off frequency (usually, cut-off frequencies of 5 to 20 seconds are acceptable).

When the vessel undergoes any systematic acceleration, whose duration exceeds the time constant of the low-pass filter applied to the accelerometers, such as prolonged turns or velocity variation, the centripetal or tangential acceleration are perceived as prolonged horizontal accelerations which can not be filtered out by the low-pass filter. The result is the deflection of the apparent vertical from the true vertical with the consequent errors on angular measurements (pitch and roll).

The combination from the two filters (low- and high-pass filters) and the relationship between the two pass bands establishes the sensor characteristics.

These inertial sensors, especially for heave, are very sensitive to the interval of time used for the integration. The equivalent cut-off frequency should be tuned to an adequate value, in order to detect the longer waves without dumping or attenuating the shorter ones.

3.1.2 Inertial sensors with the integration of GPS information

The integration of GPS information provides a means of determining the vessel's heading through the use of two GPS antennas in a base line, usually oriented longitudinally to the vessel's bow.

The velocity and rate of turn information provided by a GPS receiver and by the angular rate sensors can be used to compute the centripetal acceleration. Taking into account this information, roll and pitch measurements are compensated for the deflection of the apparent vertical. The output from this sensor is roll and pitch of higher accuracy which is not susceptible to any horizontal accelerations.

3.2 Roll, pitch, and heave measurement

Since the mid 1990s, affordable and accurate motion sensors have been utilised in hydrographic surveying. It is now considered an essential requirement not only for multibeam but also for single beam surveys when using automatic data acquisition systems. These sensors are used to compensate the vessel's motion for roll, pitch and heave.

The calculated depths must take into consideration the data from the motion sensor, i.e. the value from the oscillation of the survey vessel about the longitudinal axis (roll - θ_R), the value from the oscillation of the survey vessel about the transversal axis (pitch - θ_P), the vessel's heading (α) and the vertical oscillation (heave) see Figure 3.8 and Annex A.

3.3 Heading

The recording and application of vessel heading is essential for swath surveying systems. However, for single beam surveys the effect of heading variation (yaw) during a rotation is not significant if the positioning antenna and the transducer are located in the same vertical axis. When the positioning antenna and the transducer are not in the same vertical axis, for accurately positioned depths, it is necessary to take account of the vessel's heading.

For real-time heading measurement, several methods and equipment are available, such as: gyro compasses, fluxgate compasses and carrier-phase DGPS.

The heading measurement based on carrier-phase is conducted in the inertial sensors which integrates DGPS information. This solution allows for high accuracies.

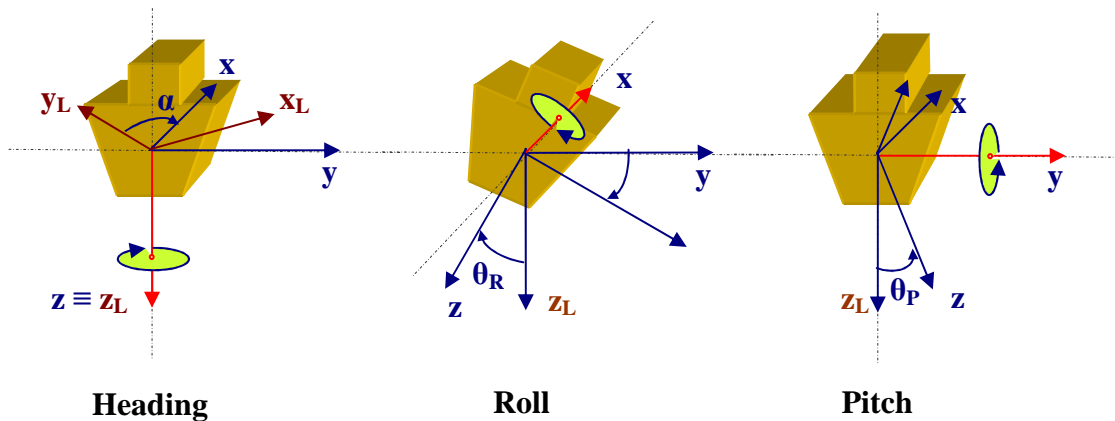


Fig. 3.8 "Vessel attitude"

3.4 Accuracy of measurement

The accuracy of roll, pitch, heave and heading should be as higher as possible. Presently available motion sensors are sufficiently accurate to be used in almost all survey orders. However, during horizontal accelerations of the survey vessel, either centripetal or tangential accelerations, inertial sensors, when used alone, have measurement biases due to the deviation of the apparent vertical.

For MBES it is recommended the inertial sensors are combined with the integration of DGPS information so that the effect of horizontal accelerations can be minimised. Usual systems accuracies, at 95% confidence level, are 0.05° for roll and pitch, 0.2° for heading and 10 centimetres or 10% of heave height whichever is greater.

During vessel turns the heave measurement is degraded due to the centripetal acceleration. Typically it is necessary to wait an interval of ten times the cut-off period to regain accurate measurements after the turn to allow stabilisation and settling of the measuring unit.

4. TRANSDUCERS

The transducers⁴¹ are one of the echo sounders' components; it is transducer characteristics which dictate some of the operating features of an echo sounder. For this reason it is particularly important to study their operating principles, characteristics and related issues such as: beam width, directivity, beam steering, installation and coverage.

The transducers are the devices used for transmission and reception of the acoustic pulses. They operate by converting electrical energy into mechanical energy, i.e. transducers convert electrical pulses from a signal generator to longitudinal vibrations which propagate into the water column as a pressure wave [Seippel, 1983]. During the reception, reciprocally, the pressure waves are converted into electrical signals.

This section describes transducer classifications with regard to: operating principles, beam, beam width, and installation, at the end of the section the assessment of the ensonification is presented.

4.1 Classification with Regard to Operation

Transducers are classified with regard to their operating principle, i.e. magnetostrictive, piezoelectric, and electrostrictive.

4.1.1 Magnetostrictive

These transducers have an axis of iron with a coil of nickel. A D.C. (direct current) current or pulse through the axis generates a magnetic field in the coil which produces a contraction and consequently a reduction of its diameter. When the electric current along the axis stops the coil returns to its original size.

The application of an A.C. (alternating current) signal generates contractions and expansions according to the characteristics of the applied signal. The amplitude of the induced vibration will be a maximum if the frequency is equal or harmonically related to the transducer material's natural frequency or frequency of resonance⁴².

This type of transducer is, however, less efficient than transducers which operate with the piezoelectric effect.

4.1.2 Piezoelectric

These transducers are made from two plates with a layer of quartz crystals between. The application of an electric potential across the plates produces a variation in the thickness of the quartz layer (piezoelectric effect). Alteration of the electric potential causes vibration of the quartz and consequently vibration of the entire unit. Reciprocally, the mechanical compression of the crystal produces a potential

⁴¹ The transducer is the device, underwater antenna, used to transmit acoustic pulses and to receive them back. In particular, if the device is used only for transmission it is called a projector and if it is exclusively used for reception, operated in passive mode, it is called a hydrophone.

⁴² This phenomenon corresponds to the re-enforcement or prolongation of any wave motion, such as acoustic waves. The frequency of resonance is the frequency at which a transducer vibrates more readily.

difference between opposite crystal faces. The amplitude of the vibration will be a maximum if the frequency of the electric potential matches the quartz natural frequency.

4.1.3 Electrostrictive

These transducers are based on the same principle of the piezoelectric transducers. However, the materials used (usually polycrystalline ceramics or certain synthetic polymers) do not have naturally piezoelectric characteristics, therefore during the manufacturing processes they need to be polarized.

Electrostrictive transducers are used almost exclusively these days. These transducers are lighter, reversible and can be arranged in arrays. These arrays with a set of small elements, when properly arranged, allow, according to the product theorem (see 4.2, equation 3.26), similar characteristics to a single piece transducer.

4.2 Beam width

The pressure amplitude generated by a transducer, in polar co-ordinates, is given by the product:

$$P(r, \theta) = P_{ax}(r) \cdot h(\theta) \quad (3.21)$$

Where θ is the angle referred to the beam axis, line of maximum pressure amplitude and intensity, r is the range from a particular point to the transducer, $P_{ax}(r)$ is the pressure amplitude in the acoustic beam axis, and $h(\theta)$ is the directional factor which corresponds to the relative signal strength. The directional factor is normalized for $\theta = 0$, i.e. $h(0) = 1$, hence $P(r, 0) = P_{ax}(r)$.

The transducer directivity is usually represented by a beam pattern diagram $B(\theta) = h^2(\theta)$ or in a logarithmic scale as: $b(\theta) = 10 \cdot \log_{10}(B(\theta)) = 20 \cdot \log_{10}(h(\theta))$.

The transducer can be characterized by its beam width b_w ; this is commonly defined by the angle at the -3 dB level, that is to say, the angular aperture corresponding to half power referred to the beam axis $b_w = 2\theta_{-3dB}$, see Figure 3.9.

The depth measurement is performed in any direction within the cone defined by the beam width.

The beam width is related to the physical dimensions of the transducer and to the frequency of the acoustic pulses. For instance, the beam width at the -3 dB level from a circular piston transducer, with a D diameter, can be approximated by:

$$b_w = 60 \lambda / D \text{ (degrees)}, \quad (3.22)$$

and for a rectangular face transducer, with length L and width W , the beam widths at the -3 dB level in the two dimensions can be respectively approximated by:

$$b_w = 50 \lambda / L \text{ and } b_w = 50 \lambda / W \text{ (degrees)}, \quad (3.23)$$

For a linear array of N omni directional transducer elements, with a distance d apart, the sum of the signals from the elements generates a directional beam pattern diagram (figures 3.10 and 3.11).

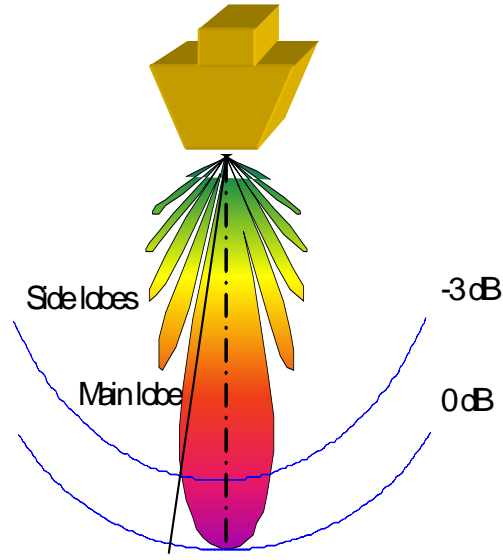


Fig. 3.9 "Beam width defined by the angle at a -3dB level"

The acoustic axis direction is perpendicular to the face of the transducer array. The beam width, at the -3 dB level, is given approximately by:

$$b_w = 50 \lambda / ((N-1)d) \text{ (degrees)} \quad (3.24)$$

where λ is the acoustic wavelength.

The directional factor of the array of transducer elements is given by [Kinsler et al., 1982]:

$$h_{\text{array}}(\theta) = \left| \frac{\sin(N\pi \frac{d}{\lambda} \sin \theta)}{N \cdot \sin(\pi \frac{d}{\lambda} \sin \theta)} \right| \quad (3.25)$$

Product theorem – is a law of acoustics which defines the directional factor of an array of N transducer elements as the product of the directional factor of the transducer element by the directional factor of the array, i.e.

$$h(\theta) = h_e(\theta) \cdot h_{\text{array}}(\theta) \quad (3.26)$$

and the pressure amplitude is given by:

$$P(r, \theta, \phi) = P_{\text{ax}}(r) \cdot h_e(\theta, \phi) \cdot h_{\text{array}}(\theta, \phi). \quad (3.27)$$

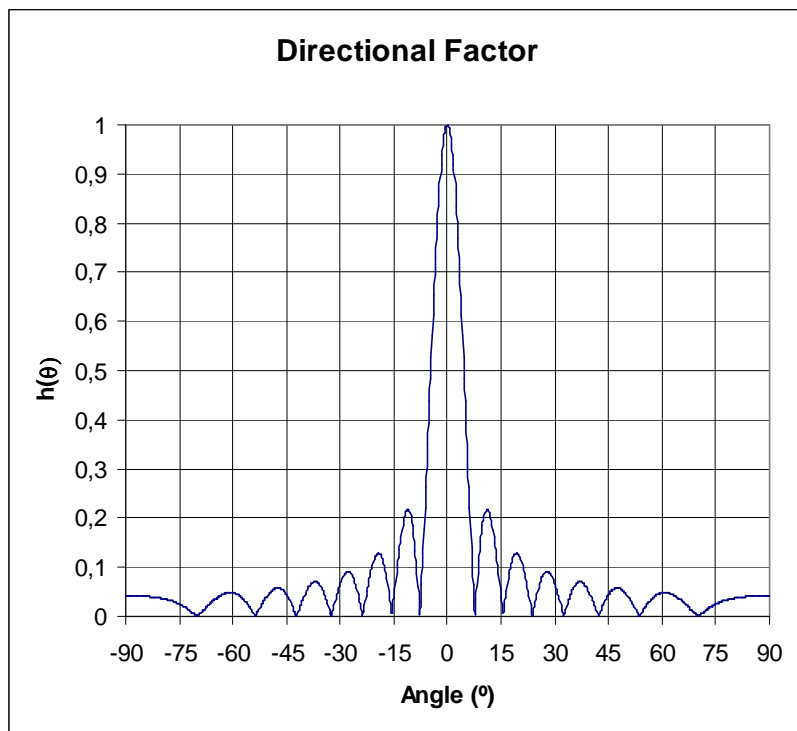


Fig. 3.10 "Directional factor"

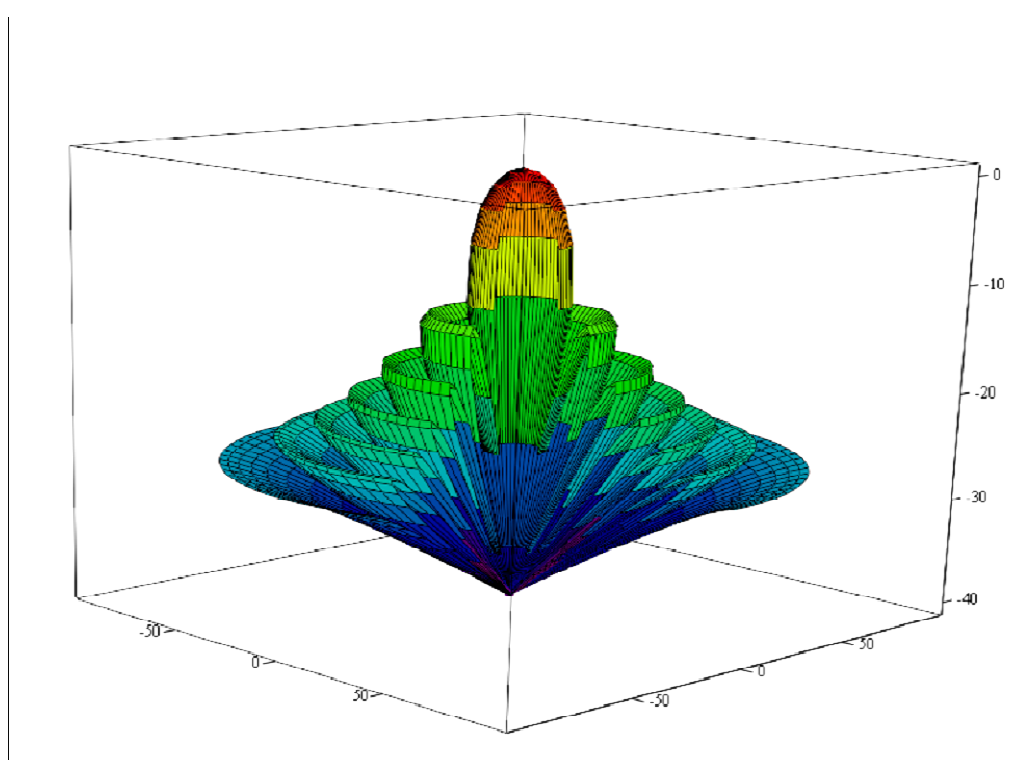


Fig. 3.11 "Beam pattern of a beam perpendicular to the transducer face"

For a linear element, the directional factor is:

$$h_{\text{linear}}(\theta) = \left| \frac{\sin(\pi \frac{L}{\lambda} \sin \theta)}{\pi \frac{L}{\lambda} \sin \theta} \right| \quad (3.28)$$

The directional factor for an array is only valid for the far field, i.e. in the area where two waves generated by a central and an outer element from the same array have a phase difference smaller than 180 degrees.

$$k \sqrt{R^2 + \left(\frac{L}{2}\right)^2} - kR \leq \pi \quad (3.29)$$

where k is the wave number, i.e. $k = 2\pi/\lambda$.

For instance, for a frequency of 100 kHz and a linear transducer array with $L = 0.5$ m, the far field corresponds to distances greater than 4.0 metres. This is usually the restriction for the minimum depth measurement.

In the near field, interfering processes create a more complex representation of the acoustic pressure.

The transducer or transducer array beam axis is normal to the transducer face. To form beams not normal to the face of the array, it is necessary to steer the beam. This process is achieved through beam steering techniques.

One array with N omni directional elements may steer a beam by introducing a phase or time delay in each element. The corresponding directional factor is (Figure 3.12):

$$h_{\text{array}}(\theta) = \left| \frac{\sin \left[N\pi \frac{d}{\lambda} (\sin \theta - \sin \theta_{\text{ax}}) \right]}{N \cdot \sin \left[\pi \frac{d}{\lambda} (\sin \theta - \sin \theta_{\text{ax}}) \right]} \right| \quad (3.30)$$

The result of this equation is the beam axis steered to the direction θ_{ax} (Figure 3.13)

Beam steering can be accomplished by introducing a time delay or phase difference to the elements of the array (equation 3.31).

Beam steering has two aims: beam stabilization and beam forming during the reception phase.

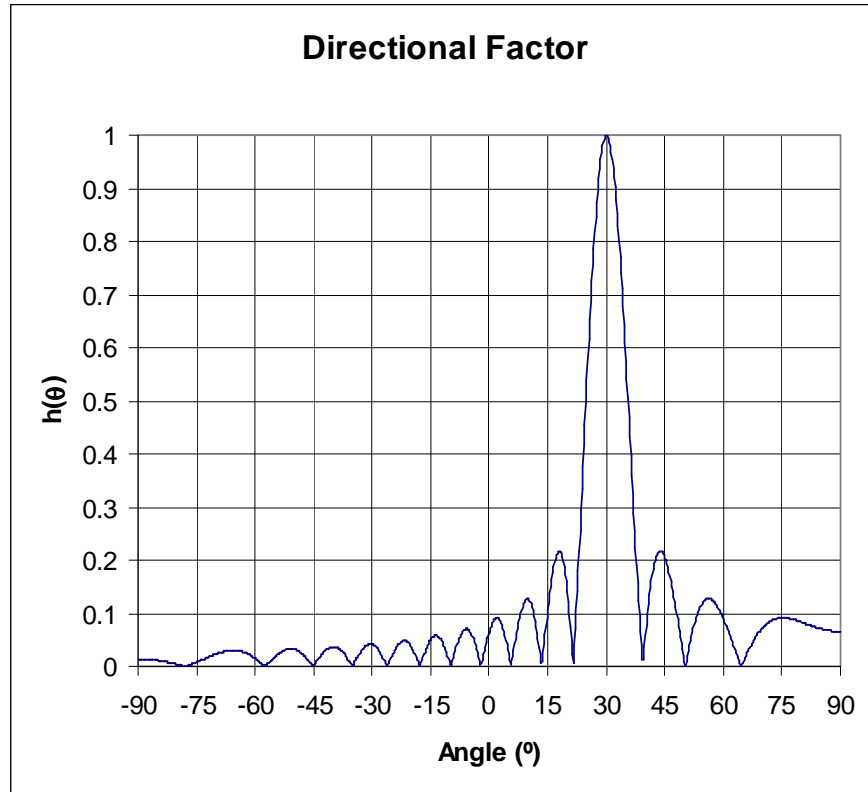


Fig. 3.12 "Directional factor of a beam steered 30 degrees"

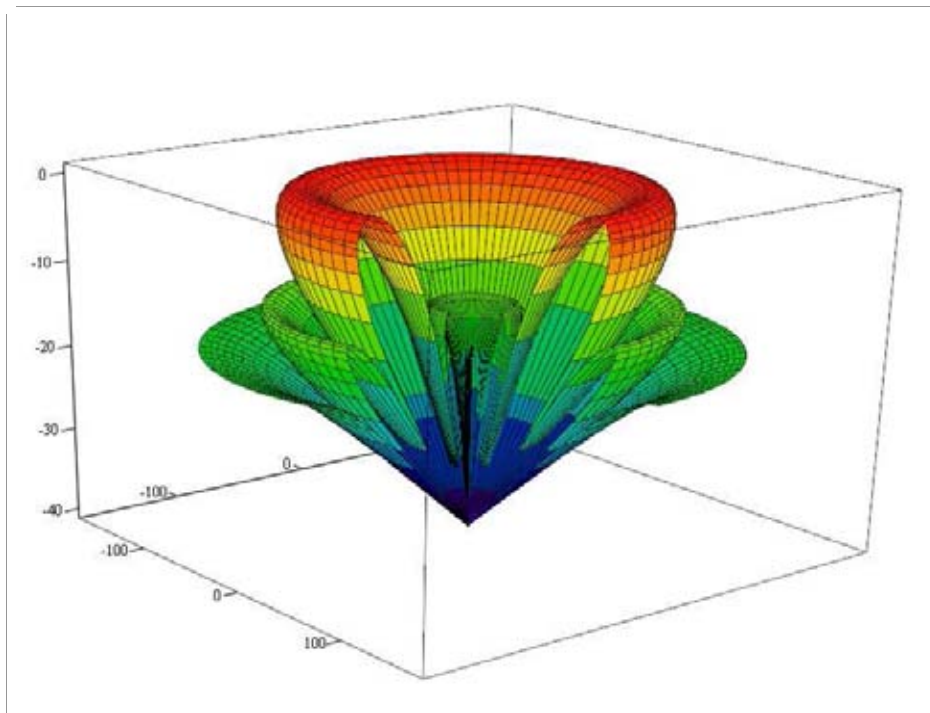


Fig. 3.13 "Beam pattern of a beam steered 30 degrees"

For beam stabilization, it is necessary to measure the angle referred to the normal direction to the array, being the time delay obtained from:

$$\Delta t_n = \frac{nd}{c} \sin(\theta_{ax}) \quad (3.31)$$

During beam forming, the signals from each element of the array are copied for each beam, the time delay applied to one element from a particular channel or beam is:

$$\Delta t_{n,i} = \frac{nd}{c} \sin(\theta_{ax_i}) \quad (3.32)$$

where **i** is the order of the beam and **n** is the number of the transducer element.

Considering two dimensionless elements transmitting a pulse with the same frequency but with a time delay, the acoustical axis is steered to the direction where the wave fronts, coming from the two elements, arrive at the same time (Figure 3.14).

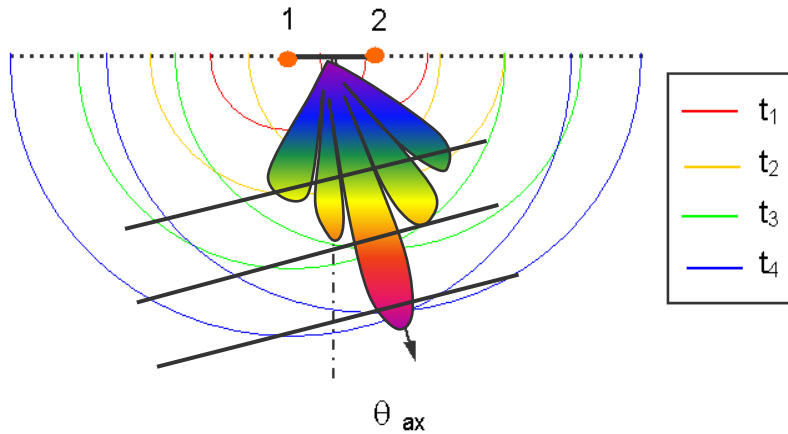


Fig. 3.14 "Illustration of a beam steered θ_{ax} with two transducer elements."

The beam width, usually defined at the -3 dB level, increases with the steering angle, i.e.

$$b_{w_i} = 50 \frac{\lambda}{(N-1)d \cdot \cos(\theta_{ax_i})} \text{ (degrees)} \quad (3.33)$$

Due to the beam's conical shape, when steered, its intersection with the plane of an assumed flat seabed results in a hyperbolic footprint (Figure 3.15).

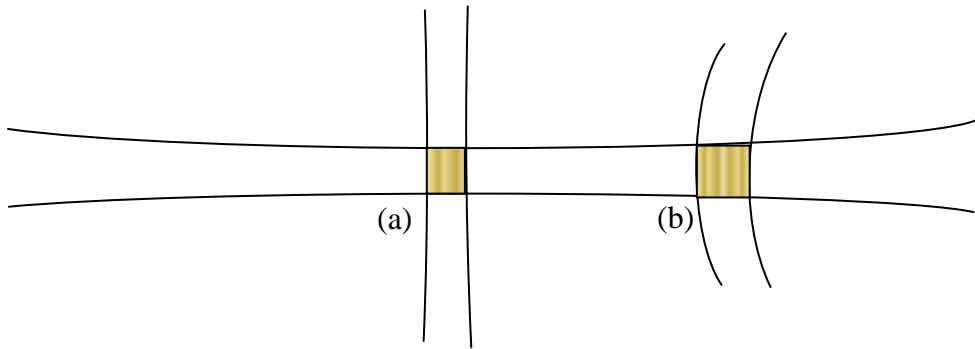


Fig. 3.15 "Linear (a) and hyperbolic (b) footprint."

Side lobes have undesirable effects, such as the detection of echoes corresponding to those lobes. This is the general case for MBES using large beam angles where the erroneous detection is made at the nadir or in the case of rocky spots (Figure 3.16). This effect results in wavy bathymetric contours which sometimes can be identified as an “omega” shape. Lobe reduction is vital for the successful operation of MBES; it is achieved using shading functions, applied during echo reception, corresponding to variable gain applied to the transducer elements.

Considering all transducer elements with the same amplitude, the side lobes will have approximately -13 dB. The technique used to reduce the side lobes consists of superimposing a window, which amplifies the signals from different elements with different gains. These windows are usually symmetric to the centre of the array.

The Dolph-Chebyshev window is quite often used; this window has the advantage of optimising the level of the side lobes for particular beam widths; it produces the same amplitude level for all side lobes.

The disadvantage of windows superimposition is the resultant reduction of the directivity.

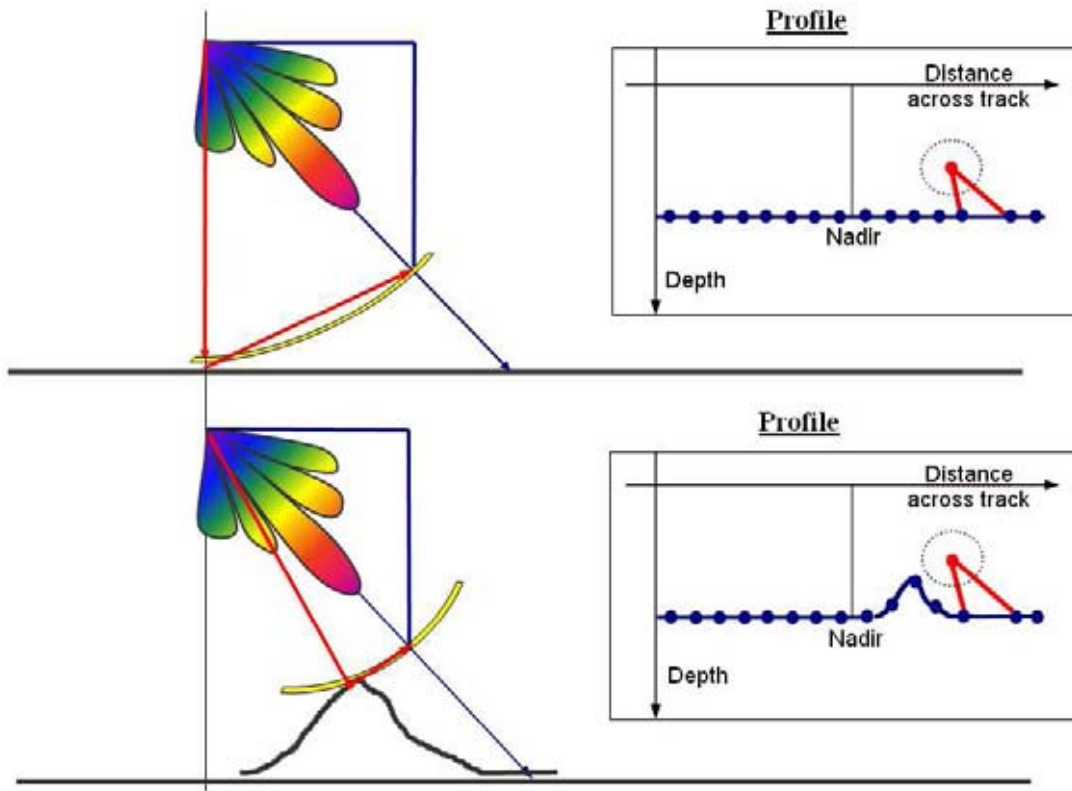


Fig. 3.16 "Depth measurement corresponding to side lobes producing both incorrect depth determination and positioning."

4.3 Classification with Regard to Beam

Echo sounders can be divided into single beam and multibeam. SBES may have transducers either with a single transducer piece or an array. MBES have transducer arrays built up from several elements. As mentioned before, this is a result of the need for beam forming in multiple directions and, sometimes, beam steering to compensate for platform attitude.

4.3.1 Single beam

Single beams require only a transducer, for both transmission and reception, but a transducer array may be used particularly when stabilization is required. Knowledge of roll and pitch angles are needed for beam stabilization.

Beam width is a function of the transducer dimensions and acoustic wave length. The higher the frequency and the larger the transducer is, the narrower the beam will be. Thus to have a narrow beam in low frequencies, a large transducer is required.

The transducer selected for SBES may have a narrow beam when high directivity is required or a wide beam when directivity is not the main concern but the detection of minimum depths or obstacles on the seafloor is the priority.

Wide beams have the capacity to detect echoes within a large solid angle, which is useful for the detection of hazards to navigation requiring further investigation. These beams are usually not stabilized, for common sea conditions the attitude of the transducer does not impact on the measurements.

On the other hand, narrow beams, typically 2° to 5° , are usually required for high resolution mapping (Figure 3.17). These beams might be stabilized in order to measure the depth vertically below the transducer.

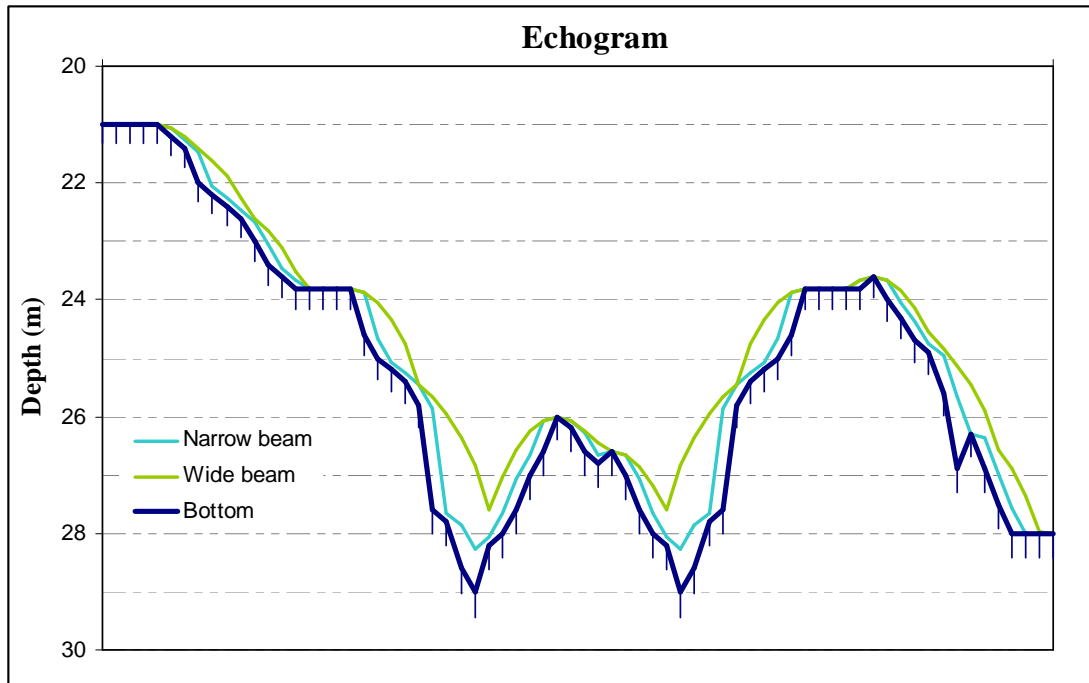


Fig. 3.17 "Illustration of depth measurement using a single narrow- and wide-beam."

4.3.2 Multibeam

MBES usually have separated transducer arrays for transmission and reception, i.e. one projector and one hydrophone, where the first is oriented longitudinally and the second is oriented transversally to the vessel's bow. The most common is to have only one transmitted beam with a fan shape, narrow along track and broad across track.

The reception transducer forms several beams, in predefined directions, narrow across track and broad along track, guaranteeing, regardless of the attitude of the surveying platform, intersection between the transmission and the reception beams.

The reduction of side lobes is essential for correct depth measurement and positioning of MBES. It is common to have side lobes below -20 dB.

4.4 Classification with Regard to Installation

The installation of the transducers on board the survey vessel can be undertaken in several ways. The decision on the way in which the transducer should be installed depends on system portability, keeping it free from vessel noise sources, including turbulent water flow under the keel, and the need to lower it

close to the sea floor. The transducer installation can be keel mounted, towed or portable. Each of these is described in the following paragraphs.

4.4.1 Keel mounted

This is the common installation for single beam and multibeam transducers in large vessels, particularly for those designed for deep water surveys.

The installation on the keel can be optionally chosen from:

- 4.4.1.1 Flush mounted – the transducer is mounted with the face in the hull plane. This option is used either in single beam or multibeam transducers. The advantage is that it does not require a special structure for the installation; the disadvantage may be the vessel noise.
- 4.4.1.2 Blister – the transducer is mounted in a structure with a small hull shape. This option is used for both single and multibeam transducers. The advantage is the reduction in hull water flow effect at the transducers face; the disadvantage is the need for a special structure for the installation.
- 4.4.1.3 Gondola - the transducer is mounted in a special gondola shaped structure (Figure 3.18). This option is used for multibeam transducers, particularly for deep water operation. The advantages are the reduction of vessel noise and the elimination of hull water flow noise at the transducer face as it passes in between the hull and the gondola; the disadvantages are the need for a special structure for the installation and consequently an increase in the vessel's draught of the order of a metre.

4.4.2 Towed

The transducer installation in a towed fish is used for side scan sonars when it is essential to have good stability of the transducer, reduction of vessel noise and the ability to lower the transducer close to the seabed.

4.4.3 Portable

This method of installation is commonly used either on single beam and multibeam transducers in small vessels, specifically aimed at shallow water surveys. This installation can be achieved either on the side or over the bow (Figure 3.19) of the vessel. The support structure for the transducer should be rigid and resistant to torque.

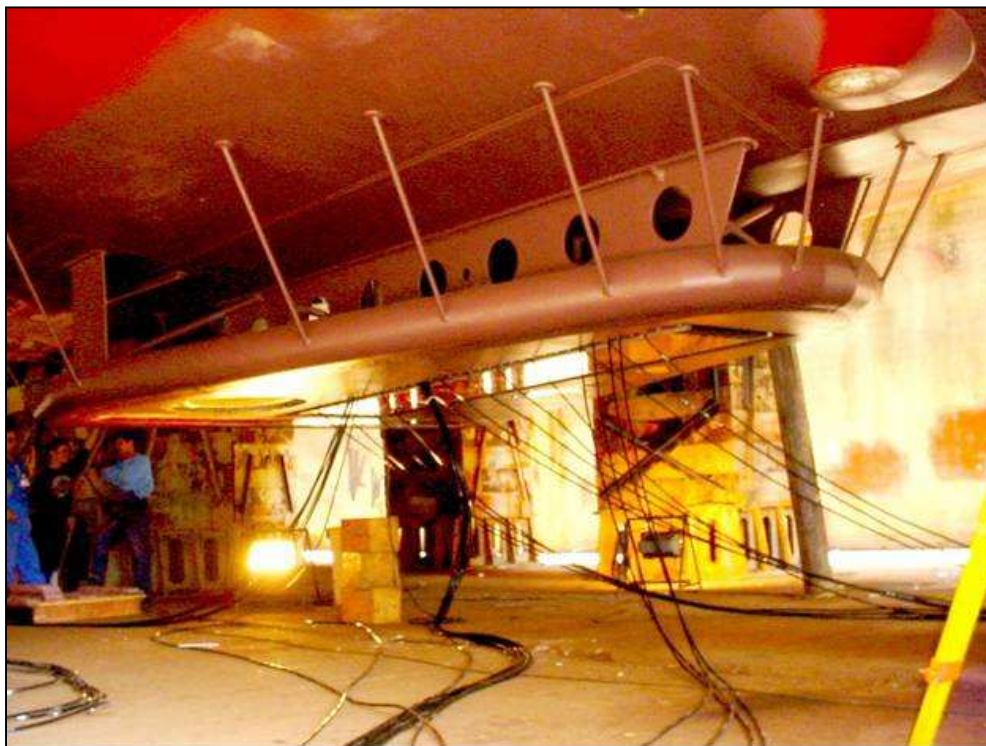


Fig. 3.18 "Gondola installation"



Fig. 3.19 "Transducer installation over the bow"

4.5 Coverage

The seafloor coverage, i.e. the ensonified area by SBES, is the area within the beam, where the footprint size is given by (Figure 3.20):

$$a = 2 \cdot z \cdot \tan\left(\frac{\phi}{2}\right) \quad (3.34)$$

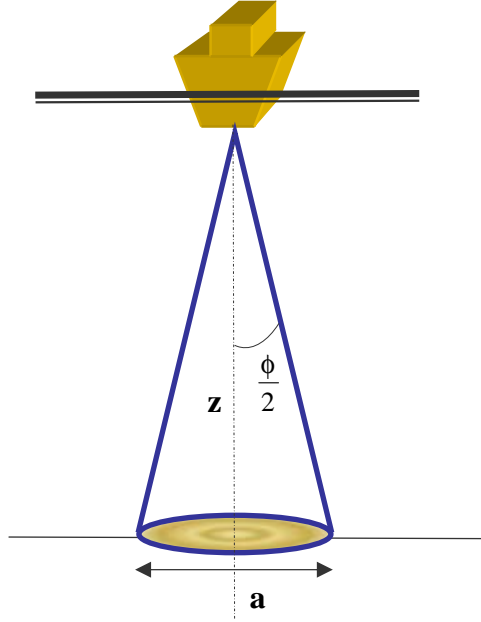


Fig. 3.20 "Single beam coverage"

For multibeam echo sounders, the ensonified area is the result of the intersection of the transmitted and received beam patterns and is dependent upon beam pointing angle, beam width, depth and mean slope of the seafloor. The ensonified area for each beam can be approximated by an ellipse. Taking a flat and levelled seafloor, the length of this ellipse in the athwart ships direction is approximately given by a_y ,

$$a_y = \frac{2z}{\cos^2(\beta)} \tan\left(\frac{\phi_R}{2}\right) \quad (3.35)$$

where z is the mean depth, β is the beam pointing angle and ϕ_R is the width of the reception beam in the athwart ships direction. In the presence of a slope, defined by an angle ζ , the length of the acoustic footprint is approximately:

$$a_y = \frac{2z}{\cos(\beta)\cos(\beta - \zeta)} \tan\left(\frac{\phi_R}{2}\right) \quad (3.36)$$

The width or dimension of the footprint ellipse in the fore-aft direction, for a flat seafloor, is approximately given by a_x ,

$$a_x = \frac{2z}{\cos(\beta)} \tan\left(\frac{\phi_T}{2}\right) \quad (3.37)$$

where ϕ_T is the width of the transmitted beam.

The coverage of the seafloor is a function of the dimension of the ensonified areas, beam spacing across-track, ping rate, ship's speed, yaw, pitch and roll. In order to achieve full coverage of the seafloor, the ensonified areas from consecutive pings must overlap one another, so that every single point on the seafloor is ensonified, at least, by one acoustic pulse.

The width of the swath for a flat seafloor is given by,

$$S_w = 2z \cdot \tan\left(\frac{\Delta\theta}{2}\right) \quad (3.38)$$

where $\Delta\theta$ is the angular coverage between the outer beams of the MBES, effectively used for hydrographic purposes.

5. ACOUSTIC SYSTEMS

In this section, the acoustic systems applied in hydrographic surveying are described. These systems are divided according to their ability to cover the seafloor, i.e. SBES and swath systems, either multibeam or interferometric sonar⁴³.

5.1 Single beam echo sounders

These echo sounders are devices for depth determination by measuring the time interval between the emission of a sonic or ultrasonic pulse and the return of its echo from the seabed.

Traditionally, the main purpose of the echo sounder is to produce a consistent and high resolution vertical seabed profile on echo trace. The echo trace, after a cautious interpretation, is sampled and digitized manually to produce soundings.

During the last decade, the technology applied in SBES has progressively improved with automatic digitisers, recorders without moving parts and annotation of positions on the echo trace. Recently, built-in computers and signal processors have allowed more sophisticated real time signal processing and data presentation on graphical colour displays, rather than a paper recorder.

5.1.1 Principles of operation

An echo sounder works by converting electrical energy, from the pulse generator, into acoustic energy. As the transducers do not transmit in all directions, the acoustic energy is projected into the water in the form of a vertically oriented beam.

⁴³ A system of determining distance of an underwater object by measuring the interval of time, between transmission of an underwater sonic or ultrasonic signal and the echo return. The name sonar is derived from the words Sound Navigation and Ranging.

The acoustic pulse travels through the water column and hits the seabed. The interaction with the sea floor results in reflection, transmission and scattering.

The reflected energy which returns to the transducer, the echo, is sensed by the transducer. The strength of the echo decreases rapidly with time, for that reason the echo is automatically adjusted in accordance with its energy level using the Automatic Gain Control (AGC) set in the factory and the Time Variable Gain (TVG) to compensate for the echo's decrease as a function of time. After amplification the electric signal is passed to an envelope detector and compared to the threshold setting to filter the noise from the signal. The output signal is then visualized or recorded.

The resultant observable is the time interval between pulse transmission and echo reception, t , being the measured depth given by:

$$z_m = \frac{1}{2} \cdot t \cdot \bar{c} \quad (3.39)$$

where \bar{c} is the mean sound velocity in the water column.

5.1.1.1 Echo sounder parameters need to be set correctly in order to obtain high accuracy and a clear record of the seabed. The most important parameters are:

- a) **Power** – The operating range of the echo sounder depends on pulse length, frequency and transmitted power. To optimize the use of the echo sounder, the transmitted power should be kept at the lowest values consummate with adequate detection. Increases in power will result in high levels of echoes but also in higher reverberation levels, creating a poor record. The power is limited by cavitation⁴⁴ phenomenon and by the braking stress of the transducer material.
- b) **Gain** – The gain entails signal amplification. The amplification of the signal also amplifies the noise and consequently the data record may be confused. It is recommended that the gain is adjusted according to the seabed type and to the transmission power.
- c) **Register intensity** – This parameter is used in analogue echo sounders to adjust the recording intensity.
- d) **Pulse length** – The pulse length is usually selected automatically as a function of the operating range. The pulse length is responsible for the vertical resolution of the echo sounder, short pulses are necessary for a better resolution. It may be necessary to increase the pulse length in areas with poor reflectivity or with steep slopes.

In shallow waters, where resolution is more important, short pulses must be used. This will reduce the probability of false echoes due to strong reverberation.

- e) **Scale** – Corresponds to the depth scale of the echo sounder recording window. The width of the recording paper is fixed; therefore at small scales one will have a low vertical resolution.

⁴⁴ This corresponds to the production of small voids in the water. This phenomenon occurs when the acoustic pressure exceeds the hydrostatic pressure.

- f) **Phase scale** – The phase scale is one way to overcome limitations of the recording resolution imposed by the echo trace scale. The phase scale consists of recording just one depth window which should be changed, either manually or automatically, to maintain the seabed recording with a satisfactory vertical resolution no matter the water depth (Figure 3.21).
- g) **Draught** – This parameter corresponds to the immersion of the transducer; in order to record the depth with reference to the instantaneous water level, the draught should be set and verified before survey operations commence and regularly thereafter.
- h) **Paper's speed** – This speed is particularly important and should be selected to ensure good horizontal resolution from depth measurements.
- i) **Sound velocity** – This is the nominal value of sound velocity that should correspond to the mean sound velocity in the area of operation. In surveys with more demanding accuracies, the sound velocity may be set to the sound velocity at the transducer face or to 1500 m/s and then during data processing, the depth must be corrected by applying the actual sound velocity profile.

In classical analogue echo sounders, this parameter does not correspond to the sound velocity but to the value that calibrates the mechanical and electrical echo sounder components to measure the correct water depth.

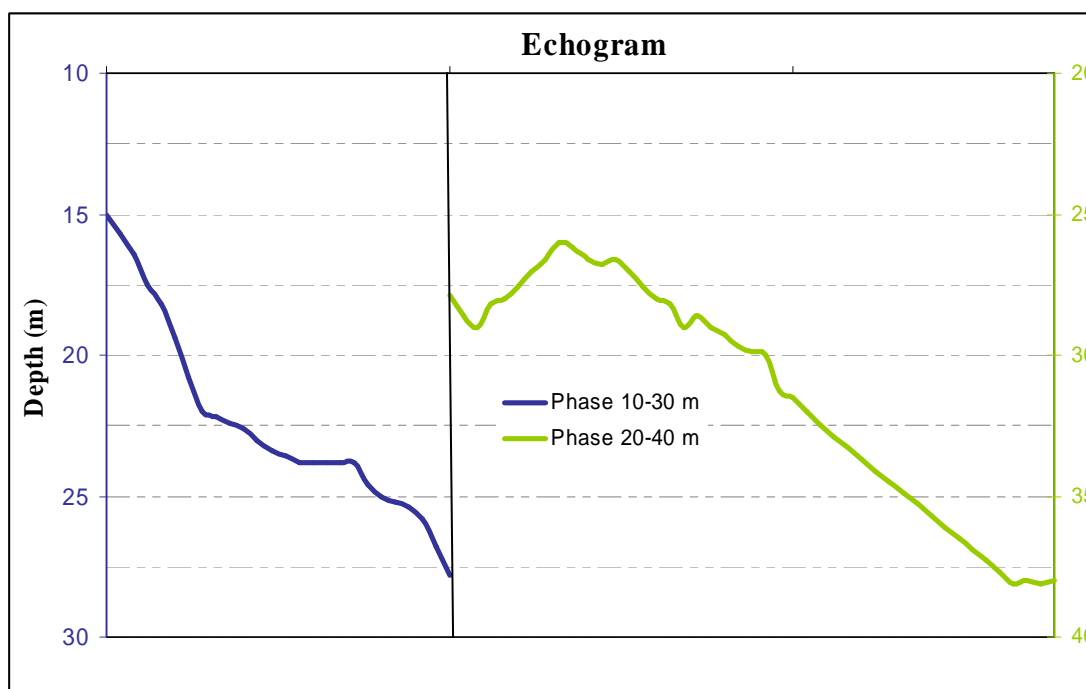


Fig. 3.21 "Recording scales"

The general working principles of SBES were referred to above. However, it is possible to identify two types of echo sounders, digital or analogue.

The traditional analogue echo sounder, whose diagram is presented in Figure 3.22, begins the cycle with the generation of an electrical pulse and the transmission of a burst of energy into the water. After the

echo reception and conversion into electrical energy, the low voltage signal is pre-amplified and passed to a recording amplifier, in order to be recorded on an echo trace, which is a graphic record of depth measurements obtained by an echo sounder with adequate vertical and horizontal resolutions. After the recording phase is completed, it is possible to initiate another cycle.

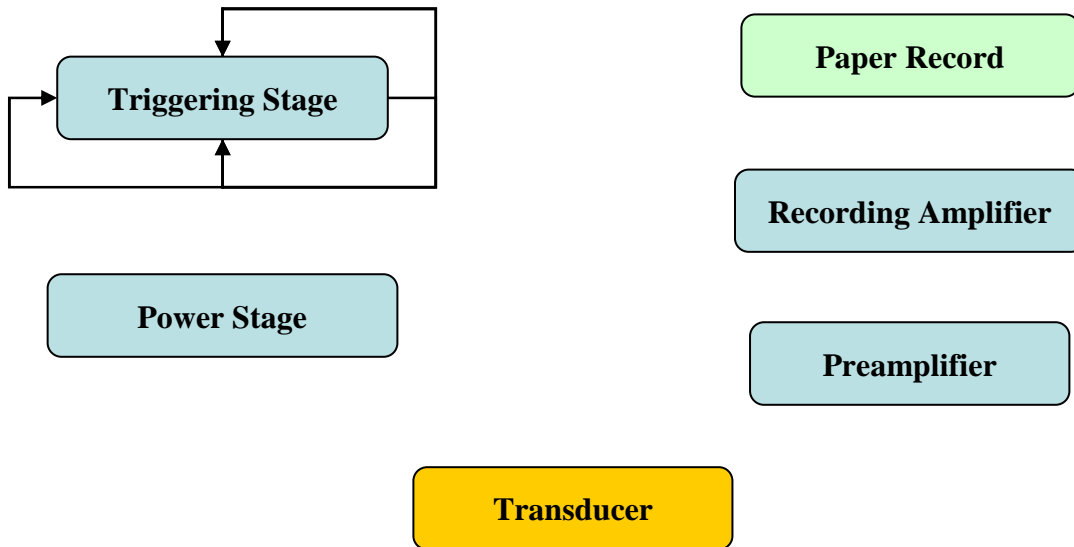


Fig. 3.22 "Analogue echo sounder – block diagram"

Hydrographic echo sounders for shallow waters are usually built with two channels (low and high frequency). The simultaneous recording of two frequencies allows the separation of the seabed return from the soft surface sediments and the underlying rock due to their different acoustic impedances.

The digital echo sounder, see Figure 3.23, works in a similar manner to the analogue echo sounder for the signal transmission. However, during the echo reception, the received signal is amplified as a function of time (time varying gain) and passed through an envelope detector where it is finally converted to digital format, which is the signal that is processed to determine the depth. This allows the information to be stored and displayed in several formats.

5.1.12 Accuracy in the depth measurement is a function of several factors, the echo sounder itself and the medium. Usually, it is necessary to calculate the error budget based on those factors (see 5.1.4).

5.1.1.3 Resolution is the ability to separate returns from two or more objects close together; it is generally expressed as the minimum distance between two objects that can be separated. In depth measurement, a major concern is the vertical resolution of the echo sounder which is dependent on:

- a) pulse length - larger pulses have smaller resolution (see 2.4.3). Two objects inside a narrow beam will be recorded as a signal target if they are less than half a pulse length apart; they will be resolved as two separate echoes if they are more than half a pulse length apart;
- b) sensitivity and resolution of the recording medium;
- c) transmit beam width.

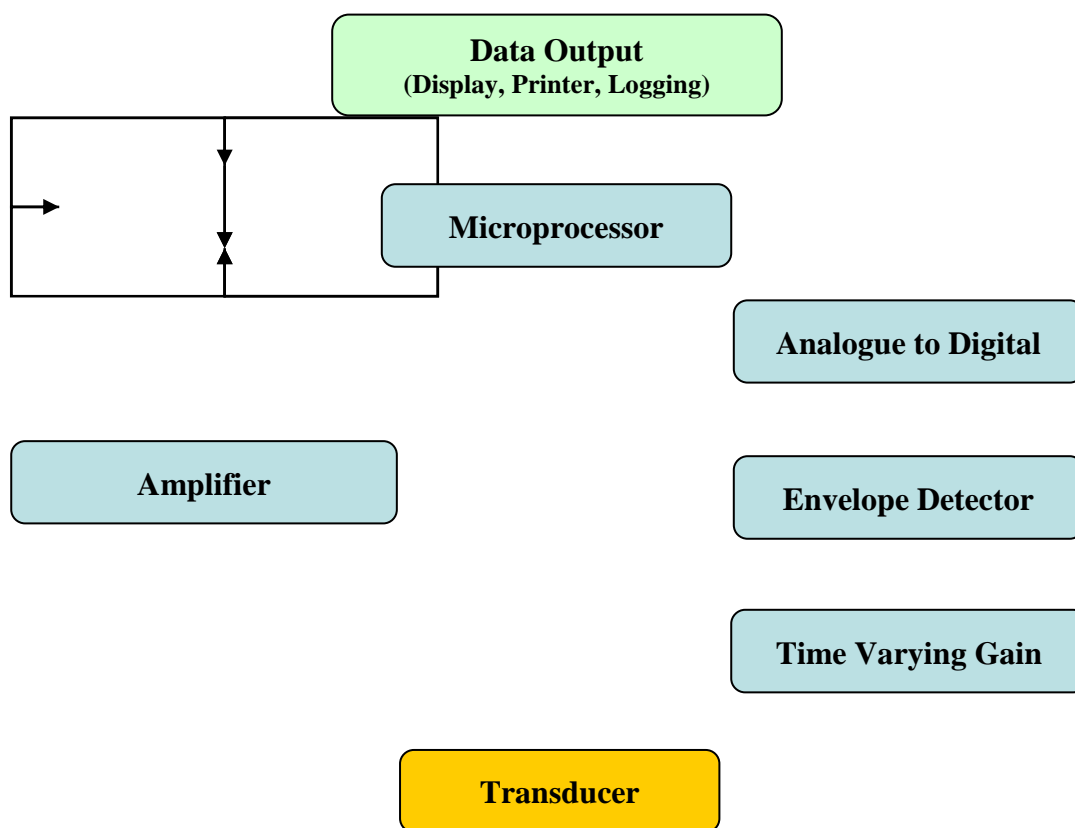


Fig. 3.23 "Digital echo sounder – block diagram"

5.1.1.4 Frequency of an echo sounder is selected based on the intended use of the equipment, i.e. the depth ranges. In some cases it is desirable to use the same device in several depths, for that purpose echo sounders may have more than one frequency and transducer in order to improve the data acquisition and data quality.

The frequencies are often allocated to channels. The echo sounders with two channels are mainly used in shallow and coastal waters; for deep waters, it is usual to use a single low frequency.

5.1.2 Installation and calibration

The transducer may be fixed under the hull or mounted on the side or over the bow. The relevant considerations are that the transducer should be placed, as far as possible, away from the vessel's own sources of noise, deep enough to avoid the surface noise and to stay submerged even in rough seas. It is

also very important that the transducer is securely fixed and vertically orientated. It is desirable for the heave compensator and the positioning antenna to be located in the same vertical axis as the transducer.

Echo sounder calibration is a routine task which consists of adjusting the equipment to ensure correct depth measurement. The calibration can be conducted with a bar check or with a special transducer. The purpose is to set the sound velocity parameter so as to adjust the mechanical and electrical components. It may also be possible to correct the measured depths during post processing with the application of the sound velocity profile.

In shallow waters, echo sounder calibration for the average sound velocity in the water column may be performed in the following ways:

- a) Bar check consists of lowering a bar or plate underneath the transducer at several depths (for instance, every two metres) either recording the depth error to apply afterwards during the data processing or forcing the echo sounder to record the correct depth from the bar or plate through the adjustment of the sound velocity parameter (Figure 3.24). In such cases the value adopted for calibration is the mean value of the observations. This method should be used down to 20-30 metres.
- b) Calibration transducer is an apparatus designed to perform the calibration knowing an exact path length. The calibration procedure consists of making the echo sounder record the correct two-way path inside the calibration transducer by the adjustment of the sound velocity parameter. The calibration transducer is lowered to several depths, each adjustment of the echo sounder, due to the performed measurement, is only valid for the corresponding depth. The calibration value used should be the mean of all the observations. This method should be used down to 20-30 metres.

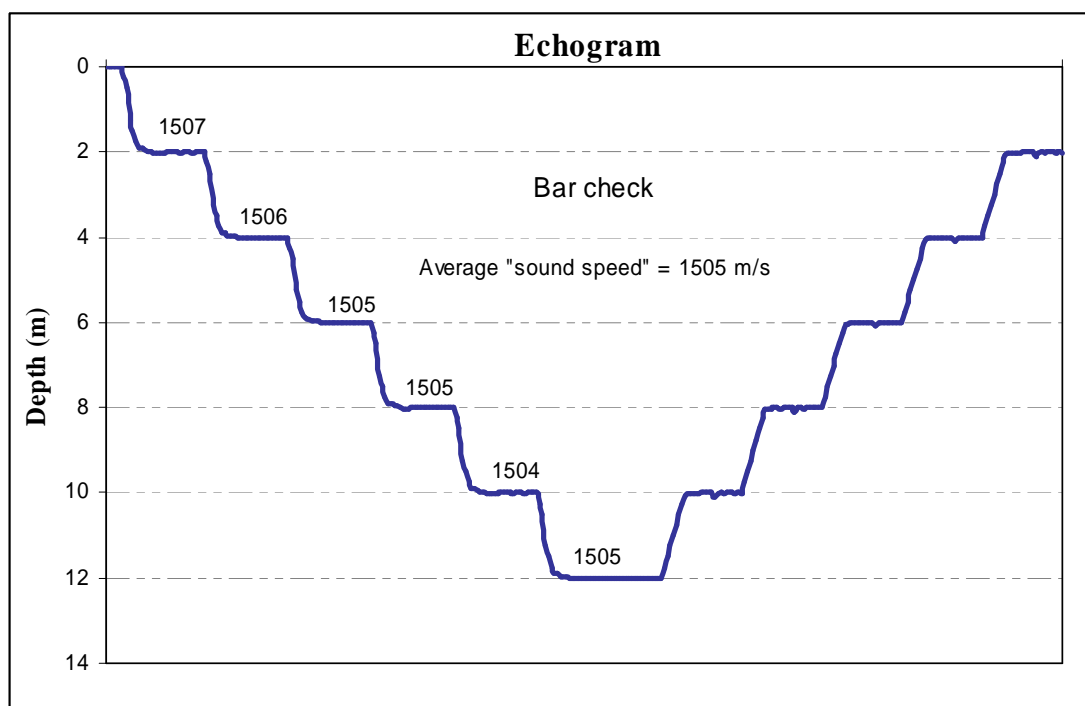


Fig. 3.24 "Bar check illustration"

- c) A combined method may also be used with a calibration transducer and a sound velocity profiler. This method is usually used for depths greater than those detailed above. With a sound velocity profile and the adjustment of the true sound velocity at the transducer draft, a similar procedure to that described in b) above is followed. In more modern echo sounders, the sound velocity parameter is set to the actual sound velocity.

The depth correction is computed during data processing, with the assumption that data was collected using the true sound velocity at the transducer draft. The depth correction is based on the difference between the sound velocity used during data collection and the harmonic mean sound velocity computed from the sound velocity profile.

For depths greater than 200 metres, it is not required to correct the measured depths for sound velocity, a standard sound velocity of 1500 m/s is usually used or values may be selected from the Mathews Tables (N.P. 139).

5.1.3 Operation and data recording

Operation of individual echo sounders should be referred to their operator's manual. Nevertheless, it is important to stress the following aspects:

- Prior to the start of the survey it is necessary to calibrate the echo sounder for the actual sound velocity;
- A general scale, adequate for the expected depths, should be selected;
- The frequency channel should be chosen according to their range capability;
- When using an analogue echo sounder, it is essential to set the gain and the recording intensity to produce a legible trace.

5.1.4 Sources of errors and quality control techniques

Errors in depth determination can be divided into three categories: large errors (blunders), systematic errors and random errors.

Blunder is the terminology used to define errors made by machines; these are caused by defective mechanical or electronic components.

Systematic errors are mainly the result of the offsets (fixed errors) or biases (errors that vary under different conditions) in motion sensing of the survey vessel, misalignment of the transducer and other sensor mounting angles. These errors can be easily corrected if the sign and size of the systematic error can be identified. This category of errors can be determined and removed during calibration of the system.

After removing blunders and systematic errors in the depth data, random errors will remain and these can be analysed using statistical techniques.

Hydrographers should be aware of the sources which contribute to the depth error and their individual impact. This section identifies several sources of errors and presents the usual techniques used for quality control.

5.1.4.1 Due to bottom slope - Taking into consideration the different seafloor slopes, in Figure 3.25, the error on the depth measurement, dz , depends on both beam width and slope. If no correction is applied, the error in depth will be given by:

$$dz = \begin{cases} z_m (\sec(\zeta) - 1) & \text{if } \zeta < \frac{\phi}{2} \\ z_m \left(\sec\left(\frac{\phi}{2}\right) - 1 \right) & \text{if } \zeta > \frac{\phi}{2} \end{cases} \quad (3.40)$$

where $\frac{\phi}{2}$ is half beam width and ζ is the slope of the seafloor.

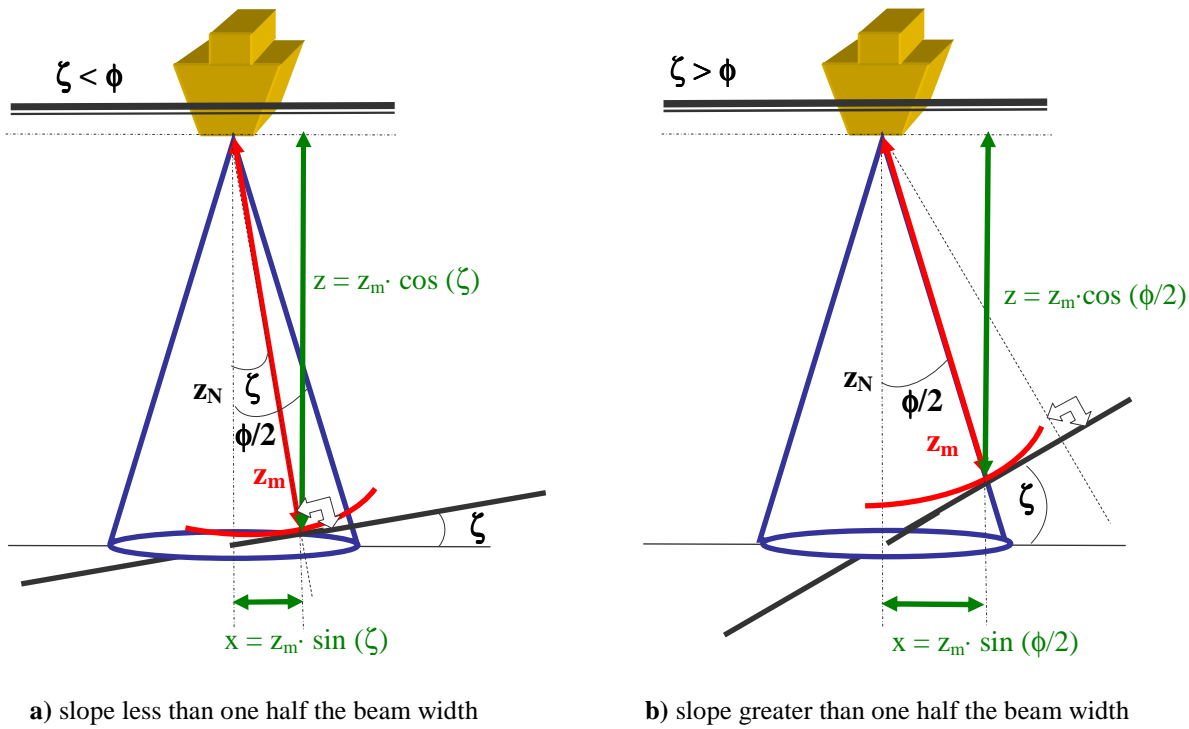


Fig. 3.25 "Effect of beam width and seafloor slope on depth measurement and positioning"

5.1.4.2 Due to sound velocity. Sound velocity variation is difficult to monitor and produces, in single beam echo sounders, errors in the depth measurement (dz_m), proportional to the mean sound velocity error or variation (dc) and to the depth

$$dz_c = \frac{1}{2} \cdot t \cdot dc \quad (3.41)$$

or

$$dz_c = z \cdot \frac{dc}{c} \quad (3.42)$$

The magnitude of the sound velocity error varies with:

- a) accuracy of sound velocity determination;
- b) temporal variation of sound velocity;
- c) spatial variation of sound velocity.

Note that the depth variance, σ_{zc}^2 , due to sound velocity measurement error and to sound velocity variation is written as,

$$\sigma_{zc}^2 = \left(\frac{z}{c} \right)^2 (\sigma_{cm}^2 + \sigma_c^2) \quad (3.43)$$

where σ_{cm}^2 is the sound velocity measurement variance and σ_c^2 is the sound velocity variance due to spatial and temporal variations.

Sound velocity variation, temporal and spatial, is a major external contribution to depth measurement errors. It is important, that during survey planning or at the beginning of the survey, to carry out a number of sound velocity measurements or sound velocity profiles across the survey area distributed throughout the day to assist the hydrographer in deciding on the frequency and location of profiles to be conducted within the survey area during data gathering operations.

5.1.4.3 Due to time measurement. An echo sounder effectively measures time, converting the measurement to depth. The error in time measurement, dt , relates directly to depth error, dz_t . In modern echo sounders, time measurement error is usually small and constant. This error is also taken into consideration during calibration.

$$dz_t = \frac{1}{2} c \cdot dt \quad (3.44)$$

The major error is a function of identification of the measurement point within the echo, i.e. on the algorithms used for signal detection.

Note that the depth variance, σ_{tm}^2 , due to time measurement error is written as,

$$\sigma_{zt}^2 = \left(\frac{1}{2} c \right)^2 \sigma_{tm}^2 \quad (3.45)$$

where σ_{tm}^2 is the time measurement variance.

5.1.4.4 Due to roll, pitch, and heave. Roll and pitch contribute to the error in depth measurement when the magnitude of those angles is greater than one half the beam widths, $\frac{\phi}{2}$. Figure 3.26 depicts the error in depth measurement and in positioning due to roll, θ_R ; this figure can be adapted for pitch changing θ_R by θ_P .

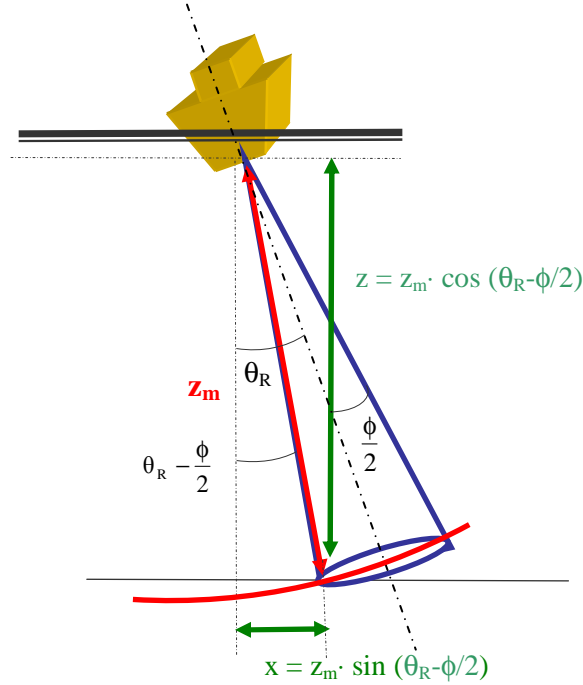


Fig. 3.26 "Effect of beam width and seafloor slope on depth measurement and positioning"

Wide beam echo sounders are usually immune to the roll and pitch of the survey vessel.

For narrow beam echo sounders, this effect may be compensated with beam stabilisation, i.e. keeping the beam vertical regardless of the vessel's attitude or correcting the measured depth and position as follows:

$$dz_{\text{roll}} = \begin{cases} z_m \left(1 - \sec \left(\theta_R - \frac{\phi}{2} \right) \right) & \text{if } \theta_R > \frac{\phi}{2} \\ 0 & \text{if } \theta_R < \frac{\phi}{2} \end{cases} \quad (3.46)$$

The heave (**h**), effect caused by the action of sea and swell on the survey vessel, is measured with inertial sensors or heave compensators. The heave compensator should be placed over the transducer to measure the heave in the same vertical axis.

When using inertial sensors, installation should be close to the centre of gravity of the survey vessel with the known lever arms from the centre of gravity to the transducer; with the roll and

pitch instantaneous angles, the measured heave, \mathbf{h}_m , can be transferred to the transducer position, \mathbf{h}_t , through the application of the induced heave, \mathbf{h}_i , (Figure 3.27).

$$\mathbf{h}_t = \mathbf{h}_m + \mathbf{h}_i \quad (3.47)$$

To calculate the induced heave, consider the vessel to be a rigid body which is free to rotate around the three axes (x, y & z) as mentioned in 3. The rotation about the centre of gravity (roll and pitch), near which heave is usually measured, corresponds to a transducer depth variation, from the vessel reference frame (identified with the script \mathbf{V}) to a local co-ordinate system (identified with the script \mathbf{L}). This difference is called induced heave.

The induced heave, adapted from Hare [1995] for the reference frames defined in 3 and Annex A, is given by:

$$h_i = z_t^L - z_t^V = -x_t^V \sin(\theta_P) + y_t^V \cos(\theta_P) \sin(\theta_R) + z_t^V (\cos(\theta_P) \cos(\theta_R) - 1) \quad (3.48)$$

where θ_R is the roll angle, θ_P is the pitch angle and $(x_t, y_t \text{ \& } z_t)$ are the transducer co-ordinates.

The total error on the depth measurement due to heave is therefore,

$$dh = dh_m + dh_i \quad (3.49)$$

where dh_m is the error in heave measurement and dh_i is the error in the induced heave determination.

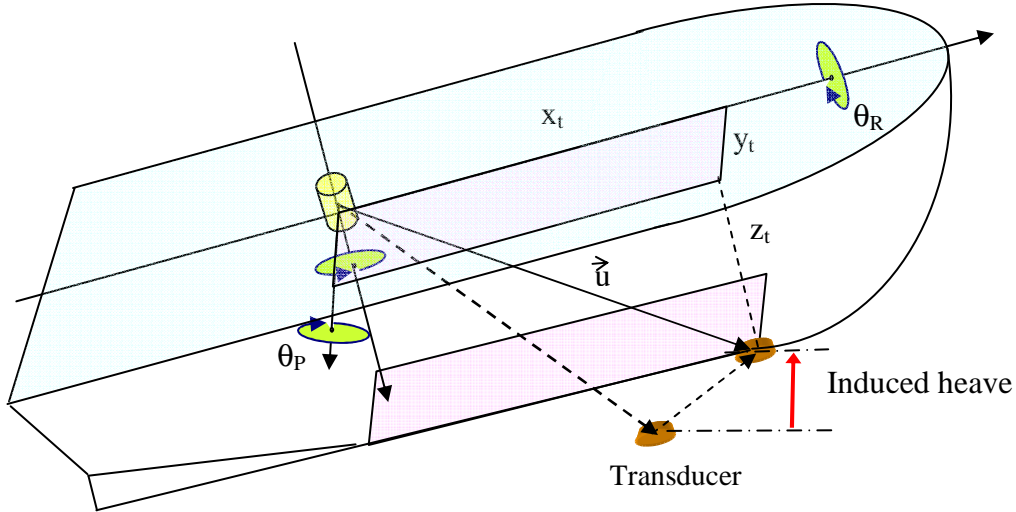


Fig. 3.27 "Induced heave"

Note that the induced heave variance is dependent upon the accuracy of the transducer offsets from the motion sensor and from the accuracy of the roll and pitch angles [Hare, 1995].

The total heave variance corresponds to the depth variance, σ_h^2 , i.e.

$$\sigma_h^2 = \sigma_{h_m}^2 + \sigma_{h_i}^2 \quad (3.50)$$

where $\sigma_{h_m}^2$ is the heave measurement variance and $\sigma_{h_i}^2$ is the induced heave variance. This latter error is typically negligible when compared to the heave measurement error.

When no heave compensator is available, it is possible manually to smooth the data in the echo trace. This task requires considerable experience in the interpretation of the echo trace in order to preserve seafloor features. The general procedure, in non significant roll conditions, is that the echo trace should be smoothed half way between crests and troughs (Figure 3.28).

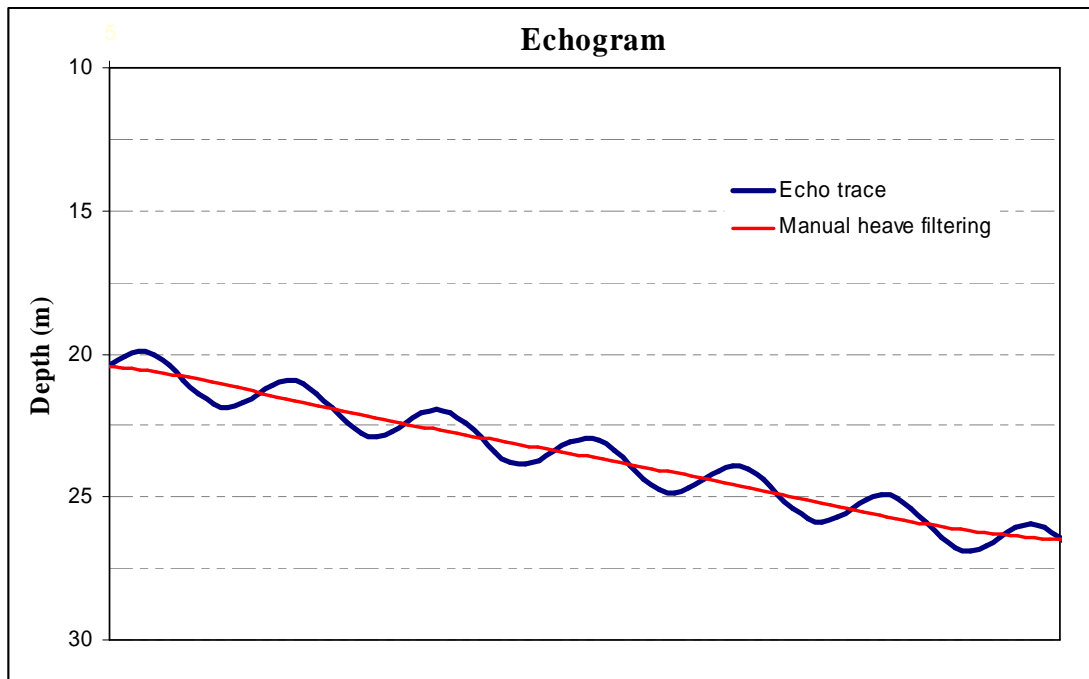


Fig. 3.28 "Manual heave filtering"

5.1.4.5 Due to draught, settlement, squat and relative position of transducer. The accurate measurement of the transducer draught is fundamental to the accuracy of the total depth. Even so it is generally necessary to update that value during the survey. The reasons for the draught variation are mainly due to the fuel and water consumption. The draught variation, for the same displacement, increases with the decrease of the float area at the sea surface. The draught error propagates directly as a depth error, $dz_{draught}$.

Settlement is the general lowering in level of a moving vessel, relative to its motionless state level. This effect, particularly noticeable in shallow waters, is due to the regional depression of the surface of the water in which the vessel moves. The depth error due to settlement is referred to $dz_{settlement}$.

Squat is another effect that takes place under dynamic conditions, the change in level of the bow and stern from the rest condition in response to the elevation and depression of the water level about the hull resulting from the bow and stern wave systems. In surveying vessels where the change in squat is significant, it is usually computed in a table of squat versus vessel speed. The depth error due to squat is referred to $\mathbf{dz}_{\text{squat}}$.

The relative position of the transducer from the motion sensor or heave compensator needs to be taken into consideration to correct the measured depth for induced heave, see 5.1.4.4.

The total error due to transducer position to the water line, \mathbf{dz}_i is:

$$\mathbf{dz}_i = \sqrt{\mathbf{dz}_{\text{draught}}^2 + \mathbf{dz}_{\text{settlement}}^2 + \mathbf{dz}_{\text{squat}}^2} \quad (3.51)$$

Note that the total depth variance due to transducer immersion is written as:

$$\sigma_i^2 = \sigma_{\text{draught}}^2 + \sigma_{\text{settlement}}^2 + \sigma_{\text{squat}}^2 \quad (3.52)$$

where $\sigma_{\text{draught}}^2$ is the draught variance, $\sigma_{\text{settlement}}^2$ is the settlement variance and σ_{squat}^2 is the squat variance.

5.1.4.6 Record reading and resolution. The record reading and resolution for depth measurement is dependent on the operating principles of the echo sounder. In the case of analogue recording, the operator should select appropriate echo sounder parameters during survey operations in order to have, as far as possible, a clean echo trace and adequate resolution. On the other hand, the digital record no longer has such a degree of dependence on the operator during the survey but supervision is required during data acquisition.

When the data is recorded on paper, it is necessary to select the gain and intensity for a legible record; it is also necessary to have a vertical scale with sufficient discrimination. It is common to use scale phases for that reason (see 5.1.1.1).

The echo trace should be prepared for reading; this task consists of identifying the points on the seabed that will be selected for depth reading. This is usually performed with the aid of a digitising table.

The error associated with record reading depends on the experience and care of the hydrographer. Consider a paper record width of 20 centimetres and scale 0-200 metres, an error reading of 0.5 mm will produce an error in the depth of 0.5 metres. Therefore, this scale is not adequate for depth recording in shallow waters. The reading error is referred to $\mathbf{dz}_{\text{read}}$, with variance σ_r^2 .

5.1.4.7 Interpretation of the echo trace is a hydrographer's responsibility. The interpretation requires experience to identify particular shapes, multiple echoes and false echoes.

a) **False echoes** – are caused by foreign matter such as kelp or fish in the water column (Figure 3.29), by layers of water separated by sudden changes of temperature or salinity or both.

False echoes are occasionally recorded by echo sounders and might be interpreted erroneously as correct depths. In cases of doubt over the validity of measured depths, an investigation of that sounding should be performed and the particular part of the survey line re-run if necessary.

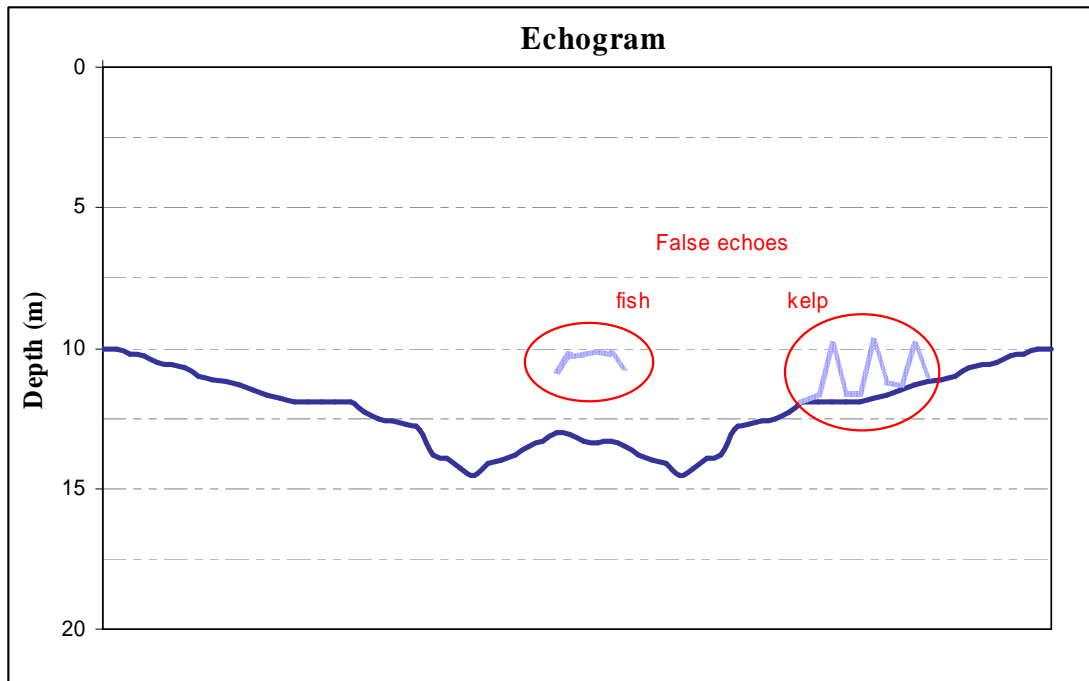


Fig. 3.29 "False echoes"

- b) Multiple echoes** – are echoes received subsequent to the very first one due to a multiplicity of reflections back and forth between the seafloor and the surface. These reflections are often recorded as multiples of the first depth (Figure 3.30).

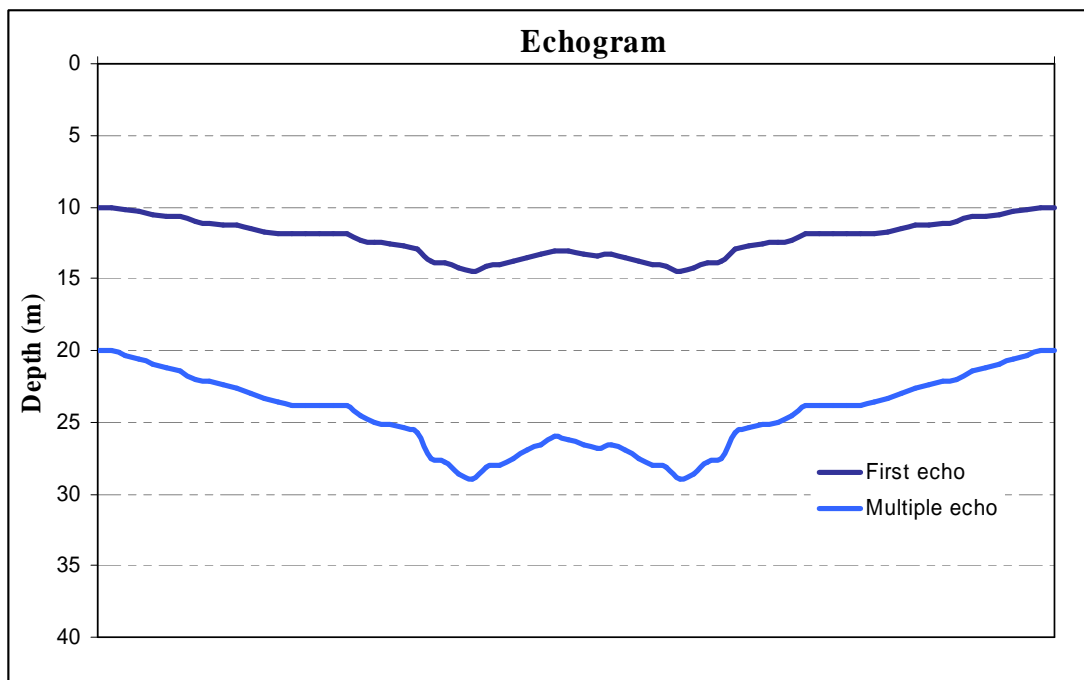


Fig. 3.30 "Multiple echoes record"

- c) **Heave** - the oscillatory rise and fall of a vessel due to the entire hull being lifted by the force of the sea, may be compensated during acquisition by a heave sensor or may be filtered manually afterwards. The hydrographer's experience is the tool used for that purpose, even though; it is sometimes difficult to differentiate the heave in an irregular seabed.
- d) **Side echoes** – are also false echoes but they are the result of echo detection in the side lobes which results in errors in depth measurement and positioning (see 4.2).
- e) **Unconsolidated sediments** – are usually detected by high frequency echo sounders. In shallow waters, it is recommended that two frequencies are used at the same time to differentiate soft sediments from the bed rock (Figure 3.31).

5.1.4.8 Depth reduction. The measured depths, corrected for the attitude of the surveying vessel, are reduced to the vertical datum by the application of the tide. The depth error due to tide error measurement is referred to $\mathbf{dz_{tide}}$.

In addition to the error in tide measurement, sometimes a more significant error is the co-tidal correction which results from the difference of the actual tide in the survey area and in the tide gauge. The depth error from co-tidal error is $\mathbf{dz_{co-tidal}}$. This may be quite significant several miles away from the tide gauge (see Chapter 4). A co-tidal model or weighted averages from two or more tide gauges may be required.

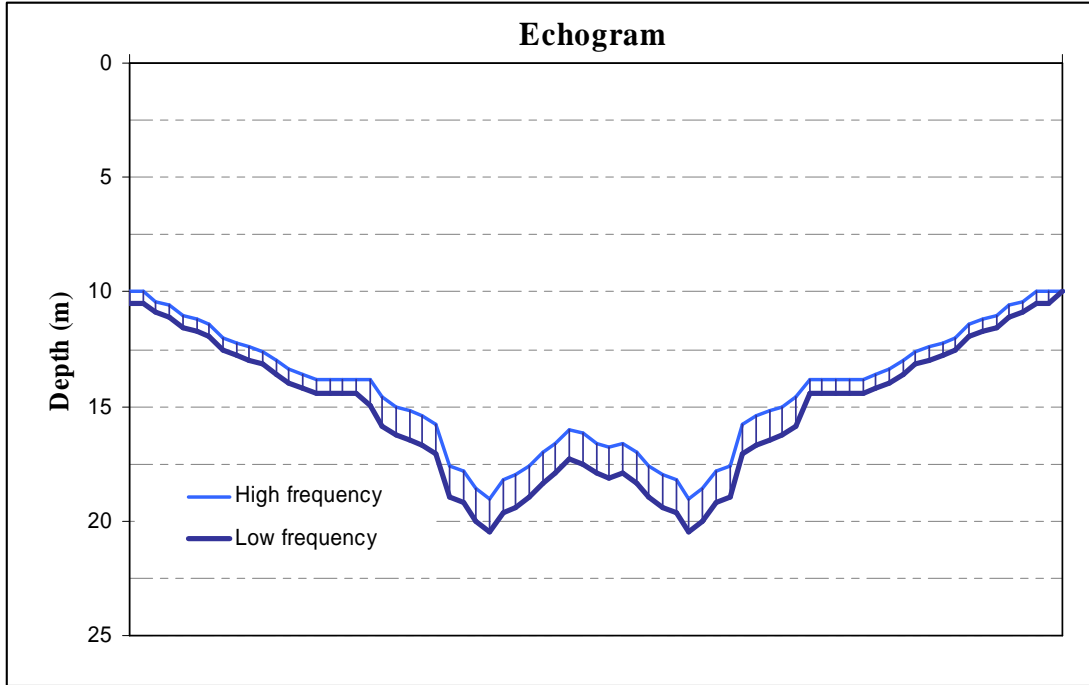


Fig. 3.31 "Dual channel recording"

Note that the tide variance, σ_{tide}^2 , due to measurement error and co-tidal variation is written as,

$$\sigma_{\text{tide}}^2 = \left(\sigma_{\text{tide m}}^2 + \sigma_{\text{co-tidal}}^2 \right) \quad (3.53)$$

where $\sigma_{\text{tide m}}^2$ is the tide measurement variance and $\sigma_{\text{co-tidal}}^2$ is the co-tidal component variance.

The tide determination using GPS-RTK (Real Time Kinematic) will provide accurate local tide determination, however, the tidal computation requires a model of the differences between the reference ellipsoid, the WGS84, and the vertical datum.

The quality control is performed by statistical calculations based on the comparison of soundings from the check lines against neighbouring soundings from the survey lines. The statistical results of the comparison should comply with the accuracy recommendations in the S-44 (Figure 3.32).

According to the errors presented above, the estimated reduced depth variance is written as follows,

$$\sigma_z^2 = \sigma_{z_c}^2 + \sigma_{z_t}^2 + \sigma_h^2 + \sigma_i^2 + \sigma_r^2 + \sigma_{\text{tide}}^2. \quad (3.54)$$

The estimated error on the reduced depth, at the 68 percent (or 1σ) confidence level, is obtained by the square-root of equation 3.54. Assuming that the component errors follow approximately a normal distribution, the estimated error on the reduced depth, at the 95 percent (or 2σ) confidence level, is obtained by substituting each variance σ^2 with $(2\sigma)^2$.

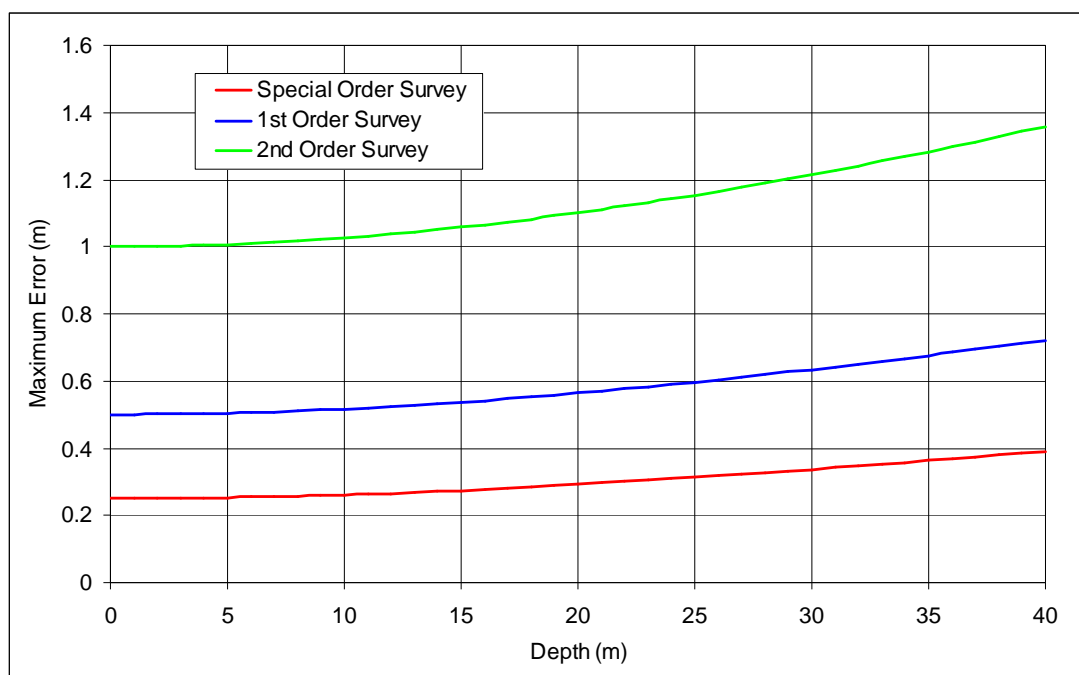


Fig. 3.32 "Minimum depth accuracy requirements for Special Order, Order 1 and Order 2 (S-44)"

For each surveying system it is recommended an error budget is created to assess compliance with the S-44 requirements. Figure 3.33 represents the error estimation for a particular echo sounder and operating conditions.

Echo sounder Characteristics:

Frequency = 200 kHz
 Beam width = 20° ($\beta = 10^\circ$)
 Pulse duration = 0.1 ms

Operating Conditions:

Mean sound speed = 1500 m/s
 Heave = 1 m
 Roll = 5°
 Vessel speed = 8 knots
 Settlement = N/A
 Squat = 0.05 m

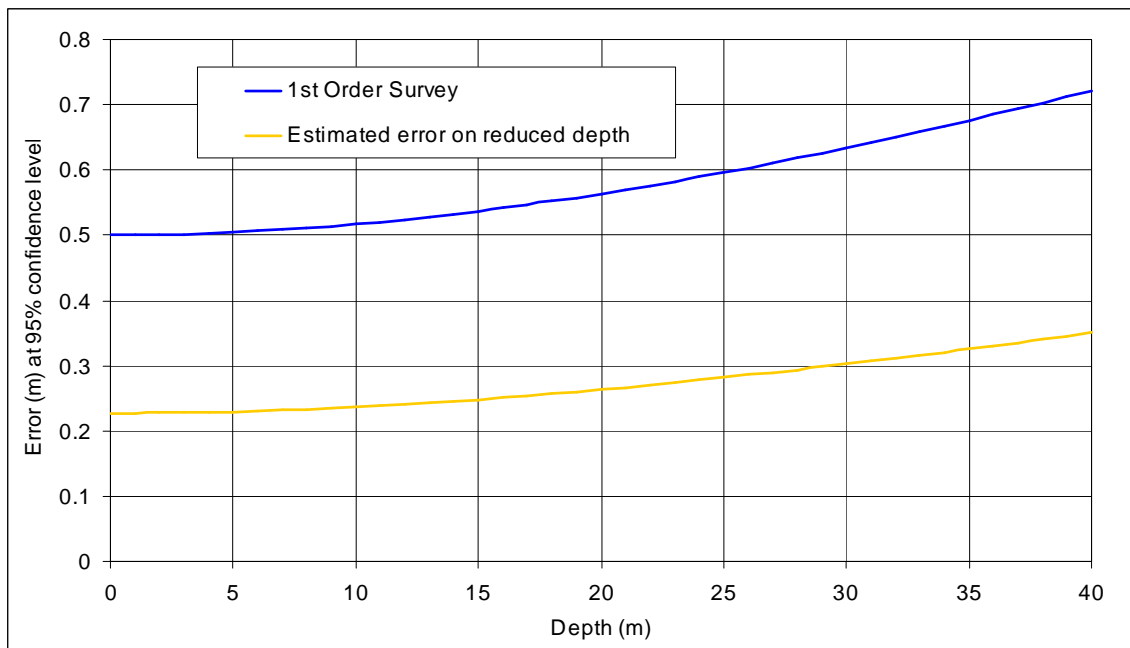
Estimated or standard errors (1 σ):

Draft error = 0.05 m
 Sound speed variation = 5 m/s
Depth errors due to:
 sound speed variation = $(5/1500)z$ m
 time measurement = 0.02 m
 squat = 0.05 m
 heave = 0.10 m
 tide error = 0.05 m
 co-tidal error = 0.05 m

**Estimated errors (2 σ):
(95% confidence level)**

Draft error = 0.10 m
 Sound speed variation = 10 m/s
Depth errors due to:
 sound speed variation = $(1/150)z$ m
 time measurement = 0.04 m
 squat = 0.10 m
 heave = 0.10 m
 tide error = 0.10 m
 co-tidal error = 0.10 m

$$\sigma_z = \sqrt{\sigma_{zc}^2 + \sigma_{zt}^2 + \sigma_i^2 + \sigma_h^2 + \sigma_r^2 + \sigma_{tide}^2}$$

**Fig. 3.33 "Depth error estimation"**

5.2 Swath Systems

Swath systems measure the depth in a strip of seafloor extending outwards from the sonar transducer. These systems are arranged in a way that the profile, line where measurements are performed, lies at right angles to the direction of survey vessel motion. As the vessel moves, the profiles sweep out a band on the seafloor surface, known as a swath.

This section describes the multibeam systems and interferometric sonars.

5.2.1 Multibeam systems

MBES are a valuable tool for depth determination when full seafloor coverage is required. These systems may allow complete seafloor ensonification with the consequent increase in resolution and detection capability.

5.2.1.1 Principles of operation. Multibeam principle of operation is, in general, based on a fan shaped transmission pulse directed towards the seafloor and, after the reflection of the acoustic energy by the seabed; several beams are electronically formed, using signal processing techniques, with known beam angles. The two-way travel time between transmission and reception is computed by seabed detection algorithms. With the application of ray tracing (see 5.2.1.8.1), it is possible to determine the depth and the transversal distance to the centre of the ensonified area.

The transmitted beam is wide across-track and narrow along-track; conversely, the beams formed during reception are narrow across-track and wide along-track. The intersections of those beams in the seafloor plan are the footprints (ensonified areas) for which the depths are measured.

Since depths are measured from a floating platform, with six possible degrees of freedom (three translations and three rotations), for accurate computation of depth measurement and its associated positioning, accurate measurements of latitude, longitude, heave, roll, pitch and heading are required.

A. Bottom detection is the process used in MBES to determine the time of arrival and the amplitude of the acoustic signal, representing a reflection from the seabed. The reliability of this process affects the quality of the measurements. Depth blunders can be, among other factors, related to a poor performance of the algorithms used for seabed detection. Seabed detection algorithms can be categorized into two main divisions: amplitude detection and phase detection algorithms.

a) Amplitude detection. The transducer array emits an acoustic pulse towards the seabed and then starts the listening period. In this phase, the returned signal is sampled in time for each beam angle. The travel time of the signal for the correspondent depth point is defined by the detected amplitude of the reflected signal (Figure 3.34).

The most common methods of amplitude detection are as follows:

- i) Leading Edge of the Reflected Signal. This method is commonly used when the angle of incidence of the acoustic signal to the seafloor is approximately zero degrees. The bottom detection time is defined for the first arrival inside the beam angle.

With the increasing angle of incidence, the returned signal loses its sharp form (short rise time) and the leading edge method no longer performs well. Two other methods can be employed, which take into account the variation of the reflected signal strength samples across the beam footprint.

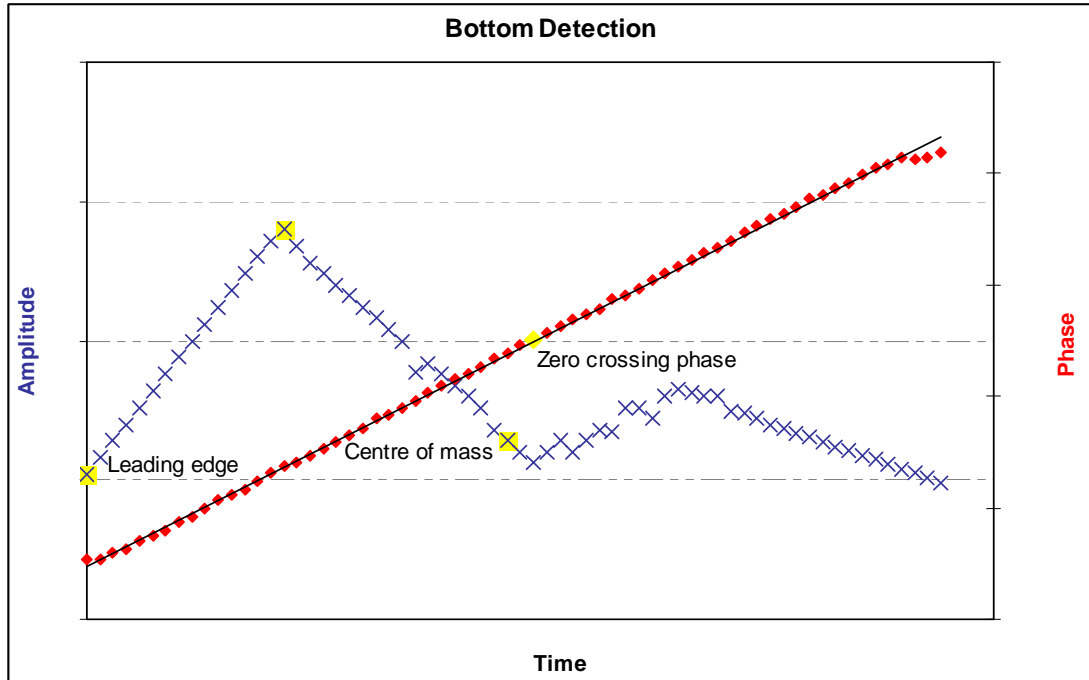


Fig. 3.34 "Bottom detection methods (signal detection)"

- ii) Maximum Amplitude of the Reflected Signal. The bottom detection is defined by the time of maximum backscatter amplitude.
 - iii) Centre of Mass of the Reflected Signal. This method consists of determining the time corresponding to the centre of gravity of the amplitude signal.
- b) Phase detection.** Amplitude detection is the technique used for the inner beams (close to nadir), where the backscatter amplitude has higher values and a smaller number of samples. For the outer beams, the backscatter amplitude decreases and the number of samples becomes very large. Consequently, the echo is so smeared out in time that amplitude detection methods obtain poor results. Against a sloping seabed in the across-track direction away from the source, the smear of the echo is also enhanced. Hence, the phase detection method is commonly used for large angles of incident.

In this technique, the transducer array for each beam is divided into two sub-arrays, often overlapping, with the centres of the sub-arrays a number of wavelengths apart. The angular directions are pre-determined and each sub-array forms a beam in that direction, the advantage being that in the case of the arrival of simultaneous echoes from different directions, the MBES system resolves only the echoes in the direction of the formed beam. The sequence of phase difference estimates are then used to estimate the time of arrival of the echo in the pre-determined direction by finding the zero crossing of the phase sequence [de Moustier, 1993]. Figure 3.35 depicts an example of the phase

detection method. The equivalent of the centre of the two sub-arrays are represented by A and B at a distance ℓ from each other, where θ is the angle of the received signal measured from the acoustical axis. A second order polynomial may be fitted to a limited sequence of differential phase estimates to refine the detection of the zero crossing phase.

When the signal return is from the acoustic axis direction, i.e. $\theta = 0$, the signals at the two sub-arrays are in phase, and this corresponds to the acoustic travel time.

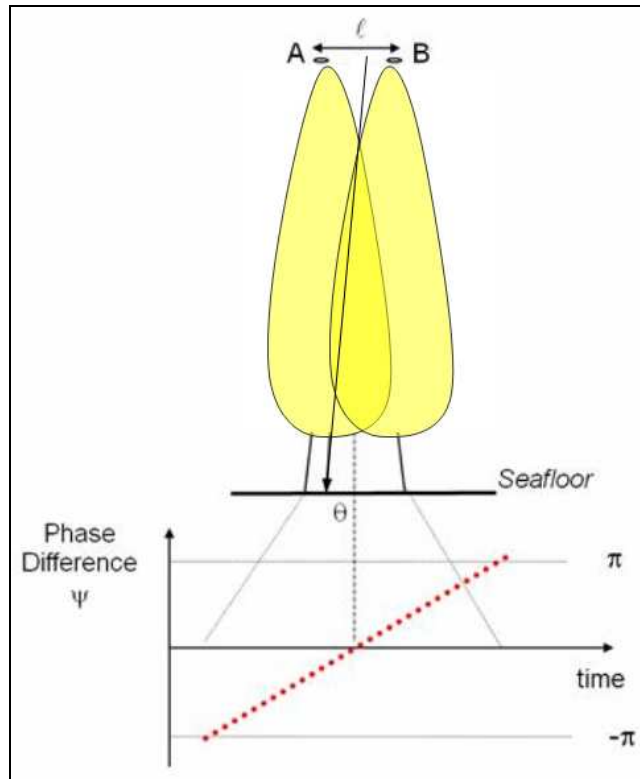


Fig. 3.35 "Bottom detection methods by phase difference (zero crossing phase)"

Across the swath, a combination of amplitude and phase detection is usually required for robust bottom detection. Near nadir, the amplitude detection should be used due to the fact that the time series for these beams is too short for a robust phase detection. Amplitude detection is also used in the case of steep slopes occurring well off-nadir, associated with bathymetric heights, except for the extreme case of a seafloor that is steeply sloping away from the transducer. Phase detection for the nadir beams is more likely to be the result of a gross error (blunder) due to mid-water column returns or due to higher returns from the side lobes. Off-nadir detections are better by phase, but amplitude detection may be chosen when a higher return is caused by the difference of the reflective properties of the target, by a near specula reflection or by a large variance of the curve fit. These conditions may occur due to features such as wrecks and boulders.

B) **Fast Fourier Transform (FFT)**

According to 4.1, during beam forming the signals from each element of the array are copied for each beam. The sum of the amplitude of the **N** transducer elements is itself a Fourier transform of the vector, with **N** elements, corresponding to the radiation pattern of the linear array. If **N** is a power of 2 the computation is less demanding and the Fourier transform is called Fast Fourier Transform⁴⁵. This method has the advantage to speed up the beam forming process.

Details on this method are addressed in de Moustier [1993].

- 5.2.1.1 Accuracy. Measurement of range and beam angle for multibeam systems is more complex than for single beam echo sounders. Consequently, there are a number of factors that contribute to the error in those measurements, including: beam angle, incident angle on the seafloor, transmit and receive beam widths, attitude and heave accuracy, bottom detection algorithms and sound speed profile variation.

It is usually necessary to calculate the error budget based on those factors (see 5.2.1.8.).

- 5.2.1.2 Resolution. Multibeam systems with their capability of full seafloor ensonification contribute to a better seafloor representation and, when compared to SBES, to higher mapping resolution. However, as far as the depth measurements are concerned, resolution will depend on the acoustic frequency, transmit and receive beam widths and on the algorithm used to perform seabed detection.

Resolution in depth measurement is a function of pulse length and of the dimensions of the ensonified area. The ensonified area of MBES echo sounders, near normal incidence, is relatively small, thus the resolution is higher than the single beam echo sounder.

- 5.2.1.3 Frequency of a MBES is selected based on the intended use of the equipment, basically depth ranges and resolution.

The frequencies of the MBES are typically:

- | | | |
|----|------------------------------------|----------------------------------|
| a. | Waters shallower than 100 metres: | frequencies higher than 200 kHz; |
| b. | Waters shallower than 1500 metres: | frequencies from 50 to 200 kHz; |
| c. | Waters deeper than 1500 metres: | frequencies from 12 to 50 kHz. |

- 5.2.1.4 System associated sensors and integrity

Multibeam systems, besides the echo sounder itself, include:

- motion sensor – for attitude (roll, pitch and heading) and heave measurement. Presently, these sensors comprise an inertial measurement unit (IMU) and a pair of GPS receivers with respective antennas. As a result of the technology involved this sensor is also capable of providing positioning with high accuracy;
- sound velocity profiler – to measure the sound velocity through the water column;
- sound velocity probe – to measure the sound velocity at the transducer face. This should be considered compulsory for flat arrays where beam steering is required;

⁴⁵ It is still possible to apply the FFT even when **N** it is not a power of 2 by adding virtual elements with zero amplitude (padded zeros), see de Moustier [1993].

- d) Positioning system – as stated above, positioning in new technology systems is integrated with motion sensors. GPS either in pseudo-differential mode or in Real Time Kinematic mode (RTK) is the system commonly used worldwide;
- e) Heading sensor – also integrated in motion sensors, the optimal and more accurate solution is the heading obtained by GPS dual receivers.

5.2.1.5 Installation and calibration (patch test)

The installation of multibeam transducers can be either fixed to the hull, on the side or over the bow. The hull installation is used in large vessels or when it is a permanent fixture, the other installations are used for temporary short term purposes in small vessels.

The calibration or patch test is an essential procedure which consists of determining the composite offset angles (roll, pitch and azimuth) for both transducer and motion sensor and the latency from the positioning system. Detailed analysis and procedures may be found in Godin [1996].

The calibration must be performed after the installation and either after long periods of inoperability or after appreciable changes in the installation.

Before calibration it is necessary to check the installation parameters and to perform a sound velocity profile to update the calculation of the refraction solution.

a) Positioning time delay

The time delay or latency is the time offset between depth measurement and positioning. The procedure to determine the time offset consists of running two pairs of survey lines at different speeds over a sloping seabed, the steeper the gradient the higher the resolution of this parameter will be. The slope should be regular and with enough extension to guarantee adequate sampling. Figure 3.36 illustrates the time delay calibration.

The time delay is obtained by measuring the longitudinal displacement of the soundings along the slope due to the different speeds of the vessel. To avoid any influence from the pitch offset the lines should be run on the same course.

The time delay, δt , may be obtained by the equation:

$$\delta t = \frac{\Delta x}{v_2 - v_1} \quad (3.55)$$

where Δx is the horizontal separation between the two sounding profiles near nadir, and v_1 and v_2 are the speeds of the vessel for line 1 and 2 respectively.

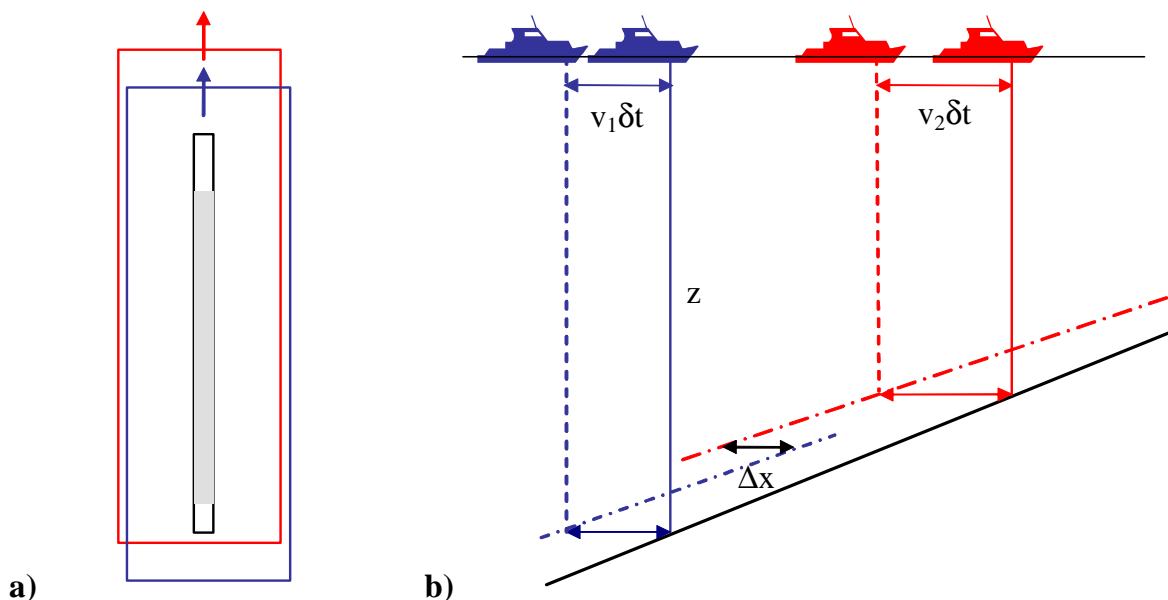


Fig. 3.36 "Time delay calibration.

- a) Top view of the two lines;**
b) Longitudinal section where the separation of the two sounding profiles from the actual seafloor is visible. "

b) Pitch offset

The pitch offset is the composite angle offset from the inertial measurement unit and from the transducer alignment with the local vertical in the longitudinal plane of the vessel. The procedure to determine the pitch offset consists of running two pairs of reciprocal survey lines at the same speed over a sloping seafloor, as mentioned in the time delay calibration, the steeper the gradient the higher the resolution of this parameter will be. The slope should be regular and with enough extension to guarantee adequate sampling. Figure 3.37 depicts the pitch offset calibration.

After the correct determination of time delay, the pitch offset is obtained by measuring the longitudinal displacement of the soundings along the slope due to the pitch offset. To avoid any influence from time delay the system should already be compensated for positioning latency.

The pitch offset, $\delta\theta_p$, may be obtained by the equation:

$$\delta\theta_p = \tan^{-1}\left(\frac{\Delta x}{2 \cdot z}\right) \quad (3.56)$$

where Δx is the horizontal separation between the two sounding profiles near nadir, and v_1 and v_2 are the speeds of the vessel for line 1 and 2 respectively.

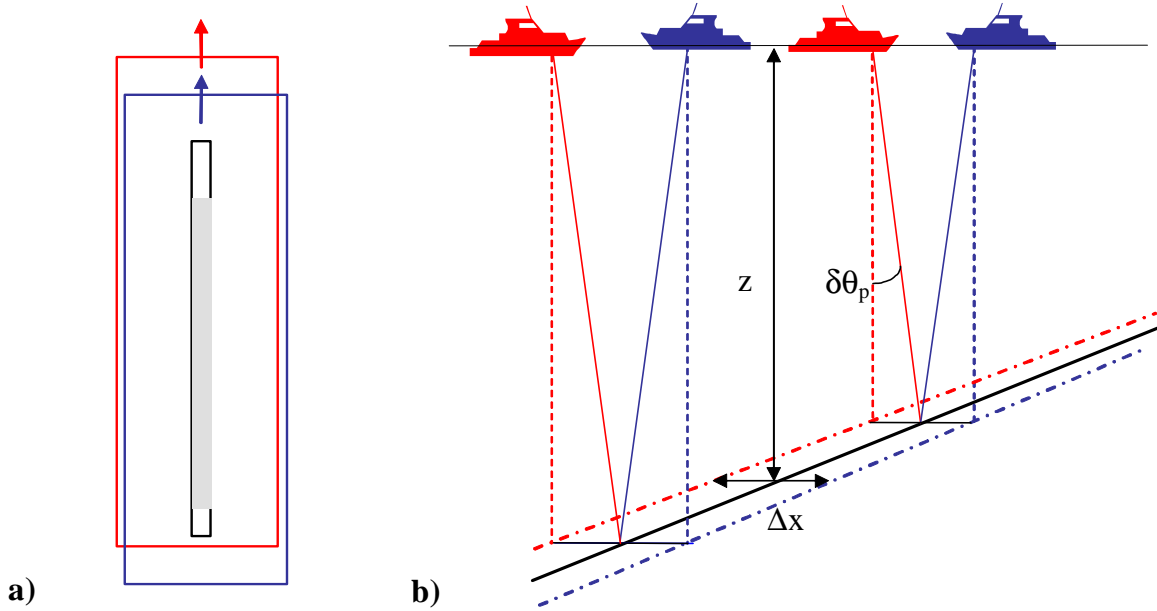


Fig. 3.37 "Pitch offset calibration.

a) Top view of the two lines;

b) Longitudinal section where the separation of the two sounding profiles from the actual seafloor due to pitch offset are visible."

c) Azimuthal offset

The azimuthal offset is the composite angle offset from the heading sensor and from the transducer alignment perpendicularly to the longitudinal axis of the vessel. The procedure to determine the azimuthal offset consists of running two adjacent pairs of reciprocal lines, at the same speed, in an area with a well defined bathymetric feature such as a shoal. The adjacent lines should overlap (not more than 20% the swath width) in the outer beams in the location of the bathymetric feature. Figure 3.38 depicts the azimuthal offset calibration.

After the correct determination of time delay and pitch offset, the azimuthal offset is obtained by measuring the longitudinal displacement of the bathymetric feature from adjacent lines. To avoid any influence from time delay and pitch offset the system should already be compensated for these offsets.

The azimuthal offset, $\delta\alpha$, may be obtained by the equation:

$$\delta\alpha = \tan^{-1}\left(\frac{\Delta x}{\Delta L}\right) \quad (3.57)$$

where Δx is the horizontal separation from the bathymetric feature from the adjacent reciprocal lines and ΔL is the distance between lines.

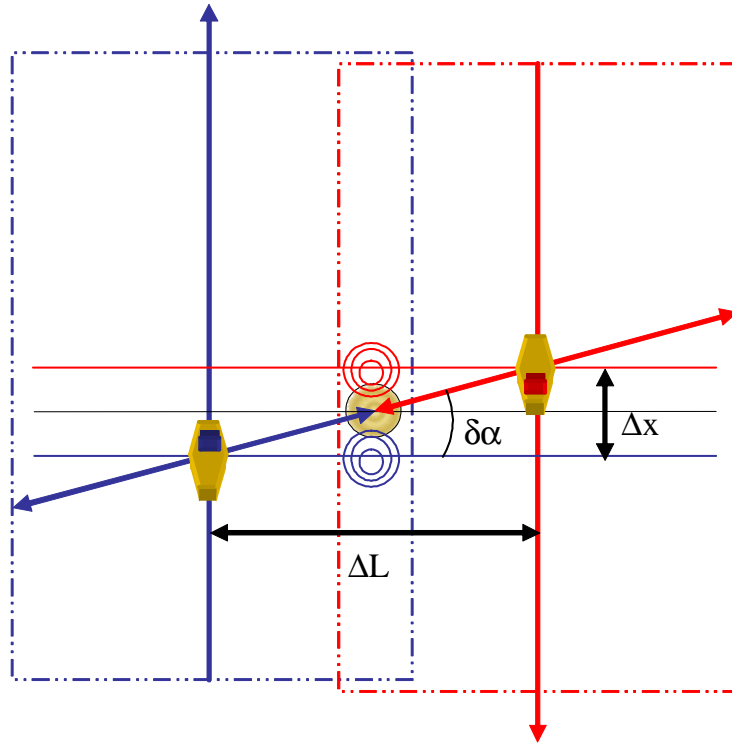


Fig. 3.38 "Azimuthal offset calibration"

d) Roll offset

The roll offset is the composite angle offset from the inertial measurement unit and from the transducer alignment with the local vertical in the transversal plane of the vessel. The procedure to determine the roll offset consists of running a pair of reciprocal survey lines, at the same speed, in a regular and flat seafloor. The lines should overlap each other. Figure 3.39 depicts the roll offset calibration.

After the correct determination of time delay, pitch and azimuthal offsets, the roll offset is obtained by measuring the vertical displacement of the outer beams from the reciprocal lines. To avoid any influence from time delay, pitch and azimuthal offsets the system should already be compensated for these offsets.

The roll offset, $\delta\theta_R$, may be obtained by the equation:

$$\delta\theta_R = \tan^{-1}\left(\frac{\Delta z}{2 \cdot \Delta y}\right) \quad (3.58)$$

where Δz is the vertical displacement between outer beams from reciprocal lines and Δy is half swath width or the distance from nadir to the point where vertical displacement is measured.

Calibration is usually performed by interactive tools. The adjustment or offset calculation should be done in several sampling sections in order to obtain an average. The offsets may have an uncertainty of the order of the motion sensor repeatability.

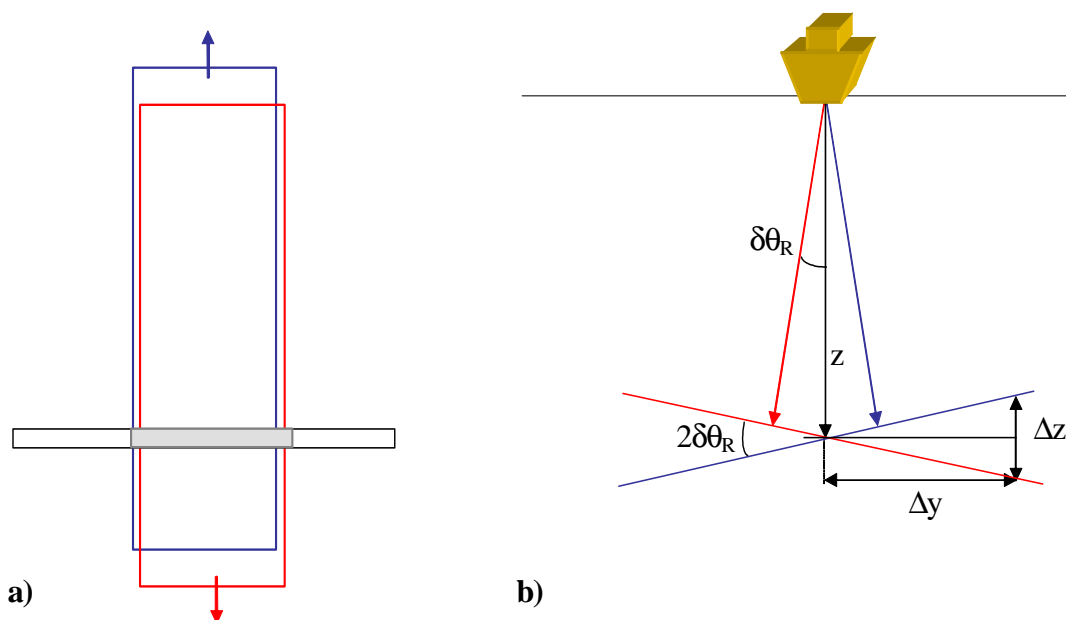


Fig. 3.39 "Roll offset calibration.

- a) Top view of the two reciprocal lines;**
- b) Cross section where the pronounced separation of the sounding profiles from nadir to the outer beams due to roll offset are visible."**

5.2.1.7 Operation and data recording

Vessel configuration and calibration parameters should be checked at the beginning of the survey. Some system parameters should also be checked. These are mainly the parameters used during data acquisition and may vary with each survey's location (e.g. maximum operating depth, expected depth, maximum ping rate, etc.).

At the beginning of the survey a sound velocity profile should be performed and transferred to the echo sounder to be used, generally, in real time. Sound velocity at the transducer face should be compared with the value given from the sound velocity probe. During the survey session several sound profile casts should be performed according to the pre-analysis of the temporal and spatial variation of sound velocity.

Whilst surveying, the systems are almost completely automatic, the hydrographer should, however, monitor the data acquisition and the data integrity. Full seafloor ensonification and overlap with the adjacent swaths must be guaranteed and monitored. It is most important to compare the overlapping outer beams of adjacent swaths and to check for any trend of curvature upward or downward of each ping.

At the end of every survey session it is strongly recommended that a back up of the collected data is created.

5.2.1.8 Sources of errors and quality control techniques

Sources of errors were discussed in 5.1.4 but these were for SBES. Hereafter the sources of errors are analyzed for MBES, some of the errors are common to both systems, i.e. they do not vary with beam angle. For this reason some of the errors are referred back to 5.1.4. Further details on multibeam uncertainty can be found in Hare [1995] and Lurton [2002].

5.2.1.8.1 Due to sound velocity. Errors in sound velocity or in its variation result in incorrect refraction solutions and, consequently, to errors in depth measurement and positioning.

The ray⁴⁶ tracing is based on Snell's law which states the relation between the ray direction and the acoustic wave velocity:

$$\frac{\sin \theta_0}{c_0} = \dots = \frac{\sin \theta_i}{c_i} = \kappa \quad (3.59)$$

where c_i is the sound velocity, θ_i is the incidence angle referred to the vertical at the depth z_i , and κ is the ray parameter or Snell constant.

Assuming that the sound velocity profile is discrete (Figure 3.40), it is reasonable to assume that the sound velocity gradient in a layer, between two measurements, is constant. Therefore sound velocity is represented as follows:

$$c^i(z) = c_{i-1} + g_i(z - z_{i-1}), \quad \text{for } z_{i-1} \leq z \leq z_i \quad (3.60)$$

where g_i is the constant gradient at layer i , given by:

$$g_i = \frac{c_i - c_{i-1}}{z_i - z_{i-1}} \quad (3.61)$$

In each layer the acoustic pulse travels a path with constant radius of curvature, ρ_i , given by:

$$\rho_i = -\frac{1}{\kappa g_i} \quad (3.62)$$

⁴⁶ The acoustic ray corresponds to a line drawn from the source, in each point is perpendicular to the wave front.

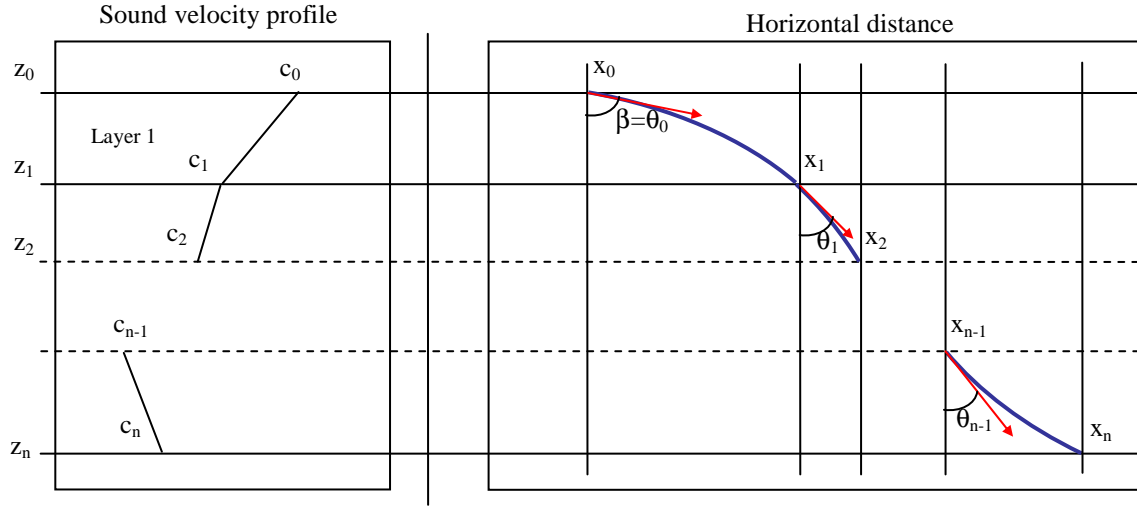


Fig. 3.40 "Ray tracing"

Considering the launching angle θ_0 (or β) in a depth with sound velocity c_0 , the horizontal distance travelled by the acoustic pulse to cross the layer i is:

$$\Delta x_i = \rho_i (\cos \theta_i - \cos \theta_{i-1}) = \frac{\cos \theta_{i-1} - \cos \theta_i}{\kappa g_i} \quad (3.63)$$

The replacement of $\cos(\theta_i)$ by $\sqrt{1 - (\kappa c_i)^2}$ produces:

$$\Delta x_i = \frac{\sqrt{1 - (\kappa c_{i-1})^2} - \sqrt{1 - (\kappa c_i)^2}}{\kappa g_i} \quad (3.64)$$

The travel time of the acoustic pulse in layer i , is obtained by:

$$\Delta t_i = \frac{1}{g_i} \int_{c_{i-1}}^{c_i} \frac{dc}{c \cdot \cos(\theta)} \quad (3.65)$$

which can be written:

$$\Delta t_i = \frac{1}{g_i} \ln \left(\frac{c_i}{c_{i-1}} \frac{1 + \sqrt{1 - (\kappa c_{i-1})^2}}{1 + \sqrt{1 - (\kappa c_i)^2}} \right) \quad (3.66)$$

To obtain the total horizontal distance travelled by the acoustic signal and the travel time, it is necessary to sum the distances Δx_i and the times Δt_i from the transducer to the seabed,

$$x = \sum_{i=1}^n \frac{[1 - (\kappa c_{i-1})^2]^{1/2} - [1 - (\kappa c_i)^2]^{1/2}}{\kappa g_i} \quad (3.67)$$

$$t = \sum_{i=1}^n \frac{1}{g_i} \ln \left(\frac{c_i}{c_{i-1}} \frac{1 + \sqrt{1 - (\kappa c_{i-1})^2}}{1 + \sqrt{1 - (\kappa c_i)^2}} \right) \quad (3.68)$$

Depth determination and sounding positioning are the result of the integration of the echo along each direction, fixed by the beam pointing angle, using the updated sound velocity profile between the transmission and one-way travel time ($\Delta t/2$).

Taking one sound velocity profile with constant gradient, \mathbf{g} , the depth is obtained as:

$$z = \int_0^{\Delta t/2} (c_0 + \mathbf{g} \cdot \mathbf{z}) \cdot \cos(\theta) dt \quad (3.69)$$

The depth error, \mathbf{dz}_c , due to the gradient variation, \mathbf{dg} , and surface sound velocity variation, \mathbf{dc}_0 , by differentiation of equation 3.69 can be approximated by:

$$dz_c = \frac{z^2}{2c_0} (1 - \tan^2(\beta)) dg + \frac{z}{c_0} dc_0 \quad (3.70)$$

where β and \mathbf{c}_0 are respectively the beam pointing angle and the sound velocity from the sound velocity profile at the transducer face. In equation 3.70 the first term corresponds to both the range and ray bending errors due to the variation of the profile gradient, whereas the second term corresponds to depth error due to the sound velocity profile offset at the transducer depth. Assuming there is no correlation of these errors, the depth variance due to sound velocity errors is written as:

$$\sigma_{z_{c_profile}}^2 = \left(\frac{z^2}{2c_0} \right)^2 (1 - \tan^2(\beta))^2 \sigma_g^2 + \left(\frac{z}{c_0} \right)^2 \sigma_{c_0}^2 \quad (3.71)$$

where σ_g^2 corresponds to the variance of the gradient of the sound velocity profile and σ_{c_0} corresponds to the variance of the initial value of the sound velocity profile used for depth calculation.

Sound velocity errors are, in practice, difficult to quantify and the problems with temporal and spatial variations may sometimes be so significant that the only practical solution is to limit multibeam angular coverage.

There is another error component due to sound velocity error or variation at the transducer face; this component introduces an error on the beam pointing angle which also introduces errors in depth measurement and positioning.

For beam steering or stabilization it is necessary to introduce time delays in the transducer elements (4.2). To compute the delays it is necessary to know the sound velocity at the transducer draught, this is usually achieved by a sound velocity sensor installed close to the transducer. Any error in the sound velocity at the transducer face will be propagated as an error in the beam pointing angle (Figure 3.41).

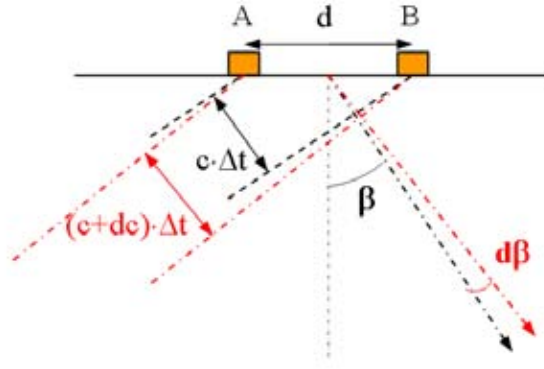


Fig. 3.41 "Beam steering error due to sound velocity variation"

The time delay to steer the beam by an angle β , is obtained by:

$$\Delta t = \frac{d}{c_0} \sin(\beta) \quad (3.72)$$

hence:

$$\beta = \arcsin\left(\frac{c_0 \cdot \Delta t}{d}\right) \quad (3.73)$$

by differentiation and the appropriate simplification gives:

$$d\beta = \frac{\tan(\beta)}{c_0} dc_0 \quad (3.74)$$

The error in beam steering propagates to an error in depth, given by:

$$dz_\beta = -\frac{z}{c_0} \cdot \tan^2(\beta) dc_0 \quad (3.75)$$

The depth variance due to beam steering is therefore:

$$\sigma_{z_\beta}^2 = \left(\frac{z}{c_0}\right)^2 \tan^4(\beta) \sigma_{c_0}^2 \quad (3.76)$$

where $\sigma_{c_0}^2$ corresponds to the variance of the sound velocity used for beam steering, usually obtained by a sound velocity sensor.

Note that the estimated total depth variance due to sound velocity errors is written as:

$$\sigma_{zc}^2 = \sigma_{zc_profile}^2 + \sigma_{zc\beta}^2 \quad (3.77)$$

The errors mentioned above may be detected by visual inspection of the data by trying to detect abnormal curvature of the profiles (set of beams).

5.2.1.8.2 Due to motion sensing. The depth measurement is dependent on pitch error and roll error, the contribution being given as follows:

$$dz_{\theta_R} = R \cdot \cos(\theta_P) \cdot \sin(\beta - \theta_R) d\theta_R \quad (3.78)$$

and:

$$dz_{\theta_P} = R \cdot \sin(\theta_P) \cdot \cos(\beta - \theta_R) d\theta_P \quad (3.79)$$

The depth variances are respectively:

$$\sigma_{z\theta_R}^2 = (z \cdot \cos(\theta_P) \cdot \tan(\beta - \theta_R))^2 \sigma_{\theta_R}^2 \quad (3.80)$$

and:

$$\sigma_{z\theta_P}^2 = (z \cdot \sin(\theta_P))^2 \sigma_{\theta_P}^2 \quad (3.81)$$

The total depth variance due to vessel attitude and heave is:

$$\sigma_{z\ motion}^2 = \sigma_{z\theta_R}^2 + \sigma_{z\theta_P}^2 + \sigma_h^2 \quad (3.82)$$

where σ_h^2 is the heave variance.

5.2.1.8.3 Due to draught, settlement, squat and relative position of transducer. The accurate measurement of transducer draught and knowledge of vessel behaviour in dynamic conditions, settlement and squat, are fundamental to the accuracy of the measured depths. These errors will contribute to the depth error independent of the beam angle.

The total depth variance due to transducer immersion, see 5.1.4.4, is written as:

$$\sigma_i^2 = \sigma_{draught}^2 + \sigma_{settlement}^2 + \sigma_{squat}^2 \quad (3.83)$$

where $\sigma_{draught}^2$ is the draught variance, $\sigma_{settlement}^2$ is the settlement variance, and σ_{squat}^2 is the squat variance.

5.2.1.8.4 Depth reduction. This issue was previously analysed in 5.1.4.8.

The QC may be performed by statistical calculations based on the comparison of soundings from the check lines against the bathymetric surface generated from the main survey lines. The statistics generated by the comparison should comply with the accuracy recommendations in the S-44.

According to the errors presented above, the estimated reduced depth variance is written as follows:

$$\sigma_z^2 = \sigma_{z_c}^2 + \sigma_{h_{motion}}^2 + \sigma_i^2 + \sigma_{tide}^2 + \sigma_{z_{detection}}^2 \quad (3.84)$$

where $\sigma_{z_{detection}}^2$ corresponds to the depth variance due to the seabed detection algorithm implemented in the MBES system [Lurton, 2002].

The estimated error on the reduced depth, at the 68 percent (or 1σ) confidence level, is obtained by the square-root of equation 3.84. Assuming that the component errors follow approximately a normal distribution, the estimated error on the reduced depth, at the 95 percent (or 2σ) confidence level, is obtained by substituting each variance σ^2 by $(2\sigma)^2$.

5.2.2 Interferometric sonars

5.2.2.1 Interferometric sonar systems apply the phase content of the sonar signal to measure the angle of a wave front returned from the seafloor or from a target. This principle differs from MBES which forms a set of receive beams and performs seabed detection for each beam, either by amplitude or phase, to detect the returning signal across the swath [Hughes Clarke, 2000].

These sonars have two or more horizontal arrays, each array produces a beam that is narrow along track and wide across track. One of these arrays is used for transmission, ensonifying a patch of the seafloor, scattering acoustic energy in all directions. Part of the scattered energy will return back towards the transducers, which measure the angle made with the transducers. The range is also calculated from the observed two-way travel time.

The method used for angle measurement can be diverse. The simplest method is to add the signal copied from the two arrays together, being the resultant amplitude “fringes“, corresponding to variations in signal strength. If the transducer arrays are separated by half a wave length, there will only be one fringe, being the zero phase direction perpendicular to the transducer array axis and the direction can be unambiguously determined. If the transducer arrays are separated by several wave lengths, the angle of the detected wave front may be derived from directions where maxima (or minima) of the received signal occur (Figure 3.42). However, this method, when used alone, produces only a few measurements. Using the gradient of the fringes to produce more measurements extends this method.

5.2.2.2 Forward looking sonars. Horizontal aperture sonars are used to detect obstructions ahead of the vessel by mechanical or electronic scanning in the horizontal plane. These systems are especially appropriate for the detection of obstructions in unsurveyed or poorly surveyed areas.

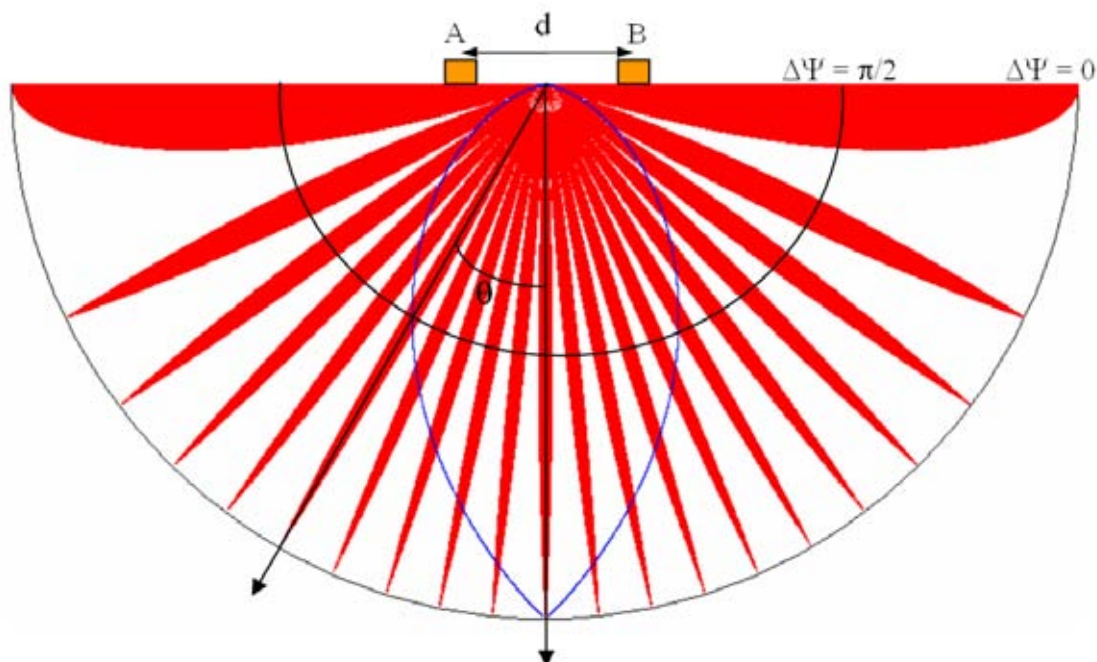


Fig. 3.42 "Pattern resulting from the interference, either constructive or destructive, from signals received at two arrays, separated by a distance (d) 10 times the acoustic wave length (red) and half wave length (blue)"

6. NON ACOUSTIC SYSTEMS

In addition to the acoustic systems, presented in previous sections, there are some electromagnetic systems which may be used for depth determination, such as the airborne laser and electromagnetic induction systems, as well as depth determination derived from satellite altimetry. These systems and the traditional mechanical methods for depth measurement and sweeping are described below.

6.1 Airborne Laser Systems

Laser⁴⁷ systems offer both an alternative and a complement to surveys with acoustic systems in shallow waters [Guenther et al., 1996].

A laser system is composed of a laser scanning system, global positioning system (GPS) and an inertial measurement unit (IMU).

6.1.1 Principles of operation

Hydrographic airborne laser sounding, LIDAR (Light Detection And Ranging), is a system for measuring the water depth. This system emits laser pulses, at two frequencies (blue-green and infrared), in an arc pattern across the flight path of the airborne platform; it records both signal arrivals from the light pulse

⁴⁷ Laser is the acronym for Light Amplification by Stimulated Emission of Radiation. The laser basically consists of an emitting diode that produces a light source at a specific frequency.

reflected by the sea surface and by the seafloor (Figure 3.43). The measured time difference, between the two returns, is converted to distance.

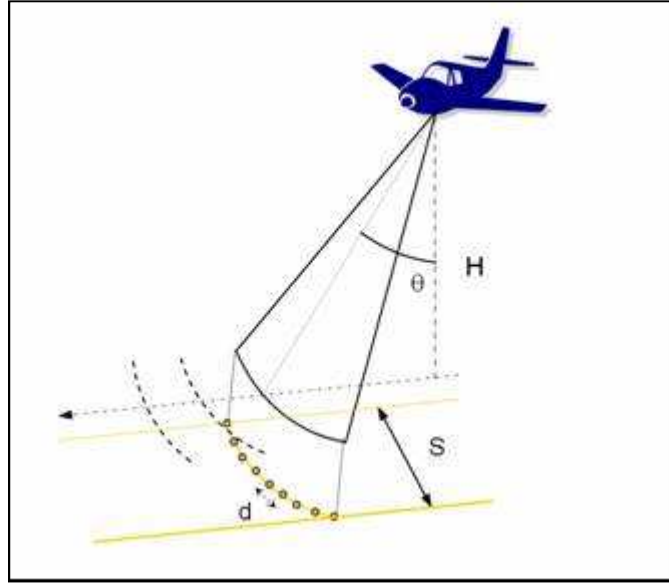


Fig. 3.43 "Geometry of Lidar measurements"

Propagation of light through sea water, like the propagation of acoustic energy, depends on the temperature, pressure and salinity. The sea water is, to some extent, transparent to light. In ideal conditions, no material in suspension, the attenuation is a function of the absorption and scattering.

The transparency of sea water to the infrared and optical regions of the electromagnetic spectrum is a function of the quantity of material suspended in the water. Therefore, water transparency⁴⁸ is a constraint to the use of laser sounding systems. Lidar maximum depth operation is about 2 to 3 times observed Secchi disk⁴⁹ depth.

A pulse of light of two different frequencies is transmitted in the direction of the sea; part of the energy from the infrared beam is reflected by the sea surface back towards the aircraft, the blue-green laser beam is transmitted to the water and partly reflected by the seafloor, also to be detected by the receiver. Using accurate timing, the distance to the seafloor can be measured knowing the speed of light in the water. The depth calculation requires, in addition, knowledge of the geometry of measurements according to Snell's law (Figure 3.44).

$$\frac{\sin \theta_a}{c_a} = \frac{\sin \theta_w}{c_w} \quad (3.85)$$

where θ_a and θ_w are the incidence angles in the air and into the water and c_a and c_w the respective speeds of light in the air and the water.

⁴⁸ The transparency of the sea water, i.e. the transmission of visible light through the water, can be measured quantitatively by determining the Secchi disk depth.

⁴⁹ The Secchi disk is a simple device to measure the water transparency. The disk is a white plate, approximately 30 cm in diameter, fastened horizontally on the end of a rope marked in metres. The disk is lowered into the sea water and the depth at which it is lost to sight is noted.

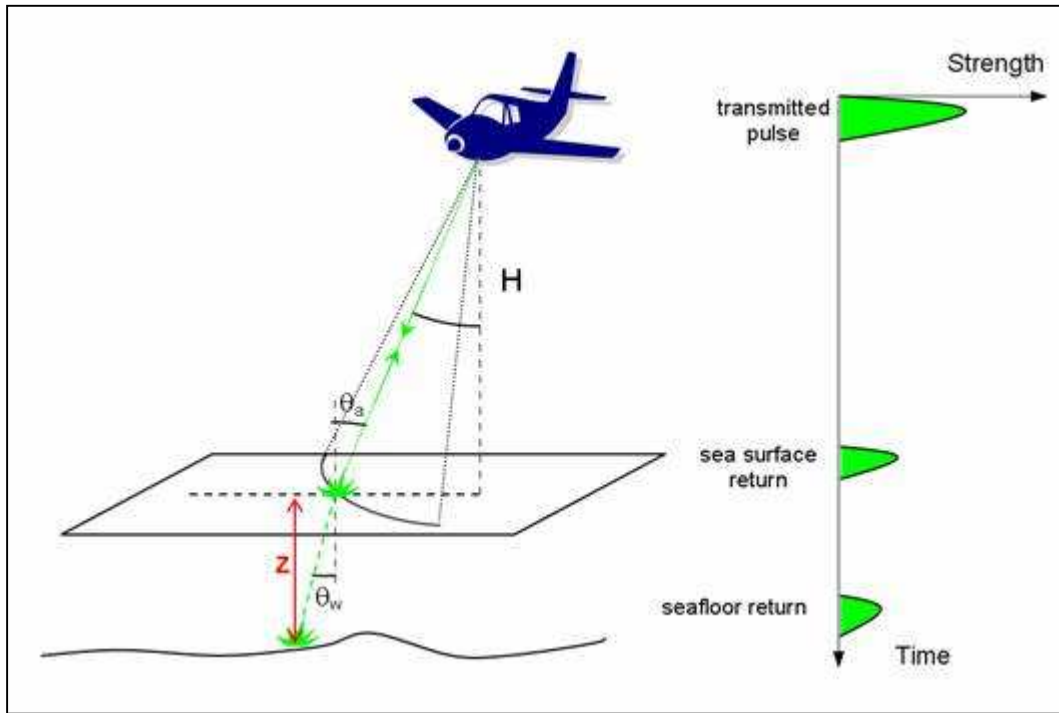


Fig. 3.44 "Lidar working principle"

6.1.2 Capabilities and limitations

Laser systems are efficient in shallow waters due to their outstanding productivity [Axelsson and Alfredsson, 1999]. This productivity results from the high surveying speed and the swath width, which is independent of water depth. In contrast, multibeam systems are operated at low surveying speed and the swath width is proportional to the water depth (usually 3 times the water depth).

Laser systems give good coverage, close to full coverage, in extreme conditions of salinity and temperature, where acoustic systems may produce poor quality data.

Undoubtedly, safety is a major advantage of laser system operation, particularly where under water hazards may be risky for surface navigation.

Despite the capabilities mentioned above, laser systems are very sensitive to suspended material and turbidity in the water column. The maximum operating depths, in optimal operation conditions, i.e. in very clear waters, is about 50-70 metres.

6.2 Airborne Electromagnetic Systems

Airborne electromagnetic induction systems have been used for over 40 years to detect highly conductive metallic mineral deposits. Advances in this technology have allowed the use of electromagnetic induction principles for mapping seafloor formations in shallow water. Detailed information on airborne electromagnetic induction systems is referred to Zollinger et al. [1987] and Smith and Keating [1996].

6.2.1 Principles of operation

The operating principle of these systems is based on a geophysical survey technique for measuring the electrical conductivity of bedrock or the thickness of a conductive layer.

A magnetic dipole transmitter, placed on a helicopter or a fixed wing aircraft, produces a magnetic field, the primary field, and a towed receiver is used to detect the secondary magnetic field induced in the ground.

Assuming horizontal layers, signal processing in time or frequency domain can be used to determine the conductivity, σ_w , and thickness of the seawater column, i.e. the water depth, and conductivity, σ_s , of the seafloor (Figure 3.45).

6.2.2 Capabilities and limitations

This no-acoustic system, due to the low frequencies involved, has the capability of operating over thick ice. However, this system is limited to water depths of less than 100 metres and is, at present, for reconnaissance purposes only.

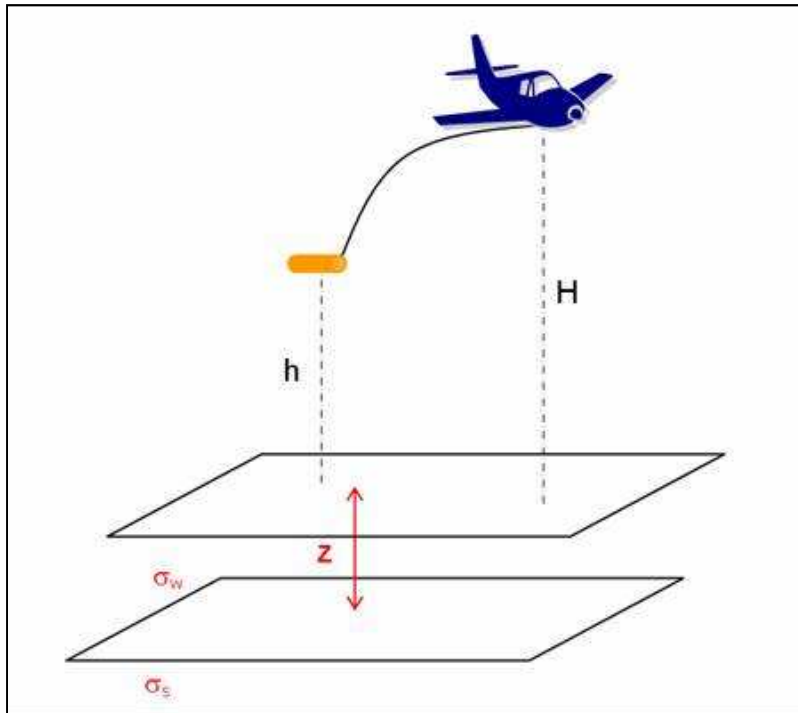


Fig. 3.45 "Electromagnetic airborne working principle"

6.3 Remote Sensing

This section presents depth estimation derived from aerial photography and from satellite altimetry, as an additional method for the coverage of extensive areas.

6.3.1 Photo-bathymetry

It is a common practise for aerial photography to be used to delineate the coast line and, sometimes, very helpful in reconnaissance, planning of hydrographic surveys, location of shoals and the creation of a qualitative description of the seafloor rather than a means by which to determine the water depth.

6.3.1.1 Principles of operation

Digital image processors have the ability to correlate light intensity with depth. However, variation in light intensity is also dependent on material in suspension and on the reflective properties of the seafloor. Thus a local calibration should be undertaken to account for these variations.

6.3.1.2 Capabilities and limitations

The application of photo-bathymetry, within the present limits of this technology, remains mainly a tool for reconnaissance and planning in areas where there is insufficient or no depth information.

6.3.2 Others

Satellite images in the visible band may be used in a similar way to photo-bathymetry. However, satellites may be equipped with high resolution altimeters for mapping the oceans' surface and, with the appropriate data processing, it is possible to estimate the depths all over the globe.

The ocean surface has an irregular shape which replicates, to some extent, the topography of the ocean floor. Seafloor features, such as seamounts, contribute to a local modification of the earth's gravity field, inducing a deflection of the vertical, which causes a slope in the sea surface and consequently the seawater is be pulled thus generating a bulge on the sea surface. The ocean surface can be mapped with an accurate satellite altimeter and the anomaly, i.e. the difference between the observed ocean surface and a theoretical surface, such as that created from WGS84 ellipsoid, can be determined and the water depth estimated (Figure 3.46).

The integration of satellite altimetry with bathymetric measurements may produce a more reliable data set which contributes to the knowledge of the seafloor topography in areas where hydrographic surveys are sparse [Smith and Sandwell, 1997].

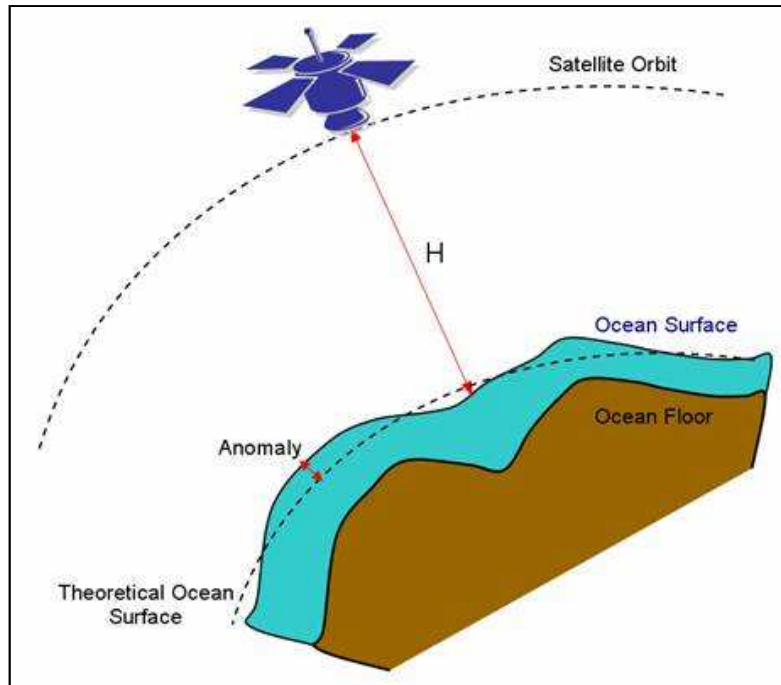


Fig. 3.46 "Satellite derived bathymetry"

6.4 Mechanic systems

Mechanic systems are the earliest tools used for depth measurement. Nonetheless, these systems are still valid and remain in use today.

The systems studied up until now perform indirect measurements and are sensitive to seawater characteristics. In typical conditions, gross errors in the depth measurements are likely to occur, these are generated by echoes from within the water column and therefore they do not related to the seafloor, for instance they can be caused by: kelp, schools of fish, deep scattering layer, thermal plumes and sediments in suspension. Additionally errors may occur near piers, where echo detection occurs from the returns of side lobes from the pier itself.

Mechanical methods (lead line or sounding pole) are not sensitive to these particular environmental conditions and may provide an alternatively method.

Bar or wire sweep methods are an unambiguous way to detect minimum depths over wrecks or over obstructions and to guarantee minimum depths throughout a navigation channel.

6.4.1 Lead line and sounding pole

The lead line aids the hydrographer in resolving echo sounder misinterpretation caused by spurious returns.

When the bottom is visible, a lead line or sounding pole can consistently be placed on the high points and the depth measured. In other areas, detection and measurement may be more difficult and sweeping methods may be preferred.

6.4.1.1 Description

A lead line is a graduated line with attached marks and fastened to a sounding lead. The line is used for determining the depth of water when sounding manually, generally, in depths of less than 50 metres.

A correction, to compensate for the shrinking and stretching of the line, may be applied to the depths obtained; this error source has, however, been overcome by inserting a wire heart inside the rope.

A sounding pole is a pole graduated with marks which is also used for determining the depth of water when sounding manually. It is generally used in depths of less than 4 metres.

As previously mentioned, at present, these tools are often used to check anomalous soundings gathered with acoustical systems which occur in shallow waters.

6.4.1.2 Sources of error

The sources of depth measurement error with lead line are mainly due to:

- a) Line curvature is induced by current and produces a depth error. The correction may be problematical and, for this reason, it is recommended only undertaking the measurements when the impact of the current will be negligible, the only remaining affect being the residual speed of the vessel.
- b) Heave will contribute to the error in the depth measurement. Heave leads to difficulty in reading the depth; this is overcome by taking an average of the reading between wave crests and troughs.

6.4.1.3 Operation, data recording, and processing

The direct depth measurement should be performed with the vessel dead in the water and, if possible, avoiding periods of strong currents and tidal flow. It is normal, between successive sounding positions, to keep the lead line in the water to check for any prominent seafloor features.

6.4.2 **Bar sweep**

Bathymetric coverage with SBES only measures the depth along the survey lines, leaving the seafloor between lines without coverage or detailed information, although side scan sonar is often used to search and locate any prominent seafloor features between the SBES lines. For rock pinnacles or wrecks, SBES may not detect the minimum depth when the echo is possibly too weak to be sensed by the receiver, this is particularly the case for masts or sharp pieces of metal.

For navigation safety purposes, the use of an accurate mechanical sweep, either bar sweep or wire sweep, is an adequate means to guarantee a minimum safe clearance depth throughout an area and, according to S-44, it may be considered sufficient for Special Order and Order 1 surveys.

6.4.2.1 Description

The sweep is made of a bar about 5-6 metres in length. Each end of the bar may be packed with lead, or other heavy material, to provide more weight and reduce lift when underway. The bar is suspended below the vessel by graduated lines.

This instrument is very easy to manufacture. Trial and error tests may be used to obtain the best solution.

This is often more effective and easier to handle than a wire sweep.

6.4.2.2 Operation methodology

The bar or rod should be suspended horizontally under a vessel. The sweep may be equipped with rockers or other sensors to record contact with the seabed.

The depth of the bar should be referred to the vertical datum, the tide height should be recorded during the sweep operation and depths reduced as appropriate.

A complete coverage of the navigation area at a safe clearance depth should be performed; in the event of an obstruction being detected, full coverage around the obstruction is recommended to confirm that the minimum depth is detected.

6.4.3 Wire sweep

As an alternative to the bar sweep, a wire sweep may be used to determine the least depth over a bathymetric feature when, from the general nature of the visible terrain, the existence of a rock pinnacle or obstruction is suspected.

Detailed information on wire sweeping may be found in NOAA [1976].

6.4.3.1 Description

The sweep is constructed from two small trawl boards or doors (identical to those used by fish trawlers). The trawl boards are connected by 40 to 60 metres of oval link chain. The sweep is bridled and towed so that the connecting chain is dragged along the seabed approximately 60 metres astern of the towing vessel NOAA [1976].

REFERENCES

- Artalheiro, F. (1996) *“Analysis and Procedures of Multibeam Data Cleaning for Bathymetric Charting”* Master’s Report, Department of Geodesy and Geomatics Engineering, University of New Brunswick, Fredericton New Brunswick, Canada.
- Axelsson, R. and M. Alfredsson (1999) *“Capacity and Capability for Hydrographic Missions”* US Hydrographic Conference 1999.
- Clay, C. e H. Medwin (1977) *“Acoustical Oceanography”* Wiley and Sons, Toronto.
- de Moustier, C. (1988) *“State of the Art in Swath Bathymetry Survey Systems”* International Hydrographic Review, LXV(2), p. 25.
- de Moustier, C. (1993). *“Signal Processing for Swath Bathymetry and Concurrent Seafloor Acoustic Imaging”* Acoustic Signal Processing for Ocean Exploration, J.M.F. Moura and I.M.G. Lourtie Eds., pp. 329-354.
- Godin, A. (1996). *“The Calibration of Shallow Water Multibeam Echo-Sounding Systems”* Proceedings of the Canadian Hydrographic Conference ‘96, Halifax, NS, Canada, pp. 25-31.
- Guenther, G., R. Thomas, and P. LaRocque (1996). *“Design Considerations for Achieving High Accuracy with the SHOALS Bathymetric Lidar System”* SPIE: Laser Remote Sensing of Natural Waters: From Theory to Practice. 15, pp. 54-71.
- Hare, R. (1995). *“Depth and Position Error Budgets for Multibeam Echosounding”* International Hydrographic Review (LXXII), Monaco, pp 37-69.
- Hughes Clarke, J. (2000). *“Present-day Methods of Depth Measurement”* In: P. Cook and C. Carlton (eds) Continental Shelf Limits - The Scientific and Legal Interface. Oxford University Press, New York.
- IHO (1994). *“Hydrographic Dictionary. Special publication No. 32, 5th edition”* International Hydrographic Organization, Monaco.
- IHO (1998). *“IHO Standards for Hydrographic Surveys. Special publication No. 44, 4th edition”* International Hydrographic Organization, Monaco.

- Kinsler, L., A. Frey, A. Coppens, and J. Sanders (1982). *“Fundamentals of Acoustics”*. Wiley and Sons, Toronto.
- Lurton, X. (2002). *“Acoustical Measurement Accuracy Modelling for Bathymetric Sonars”* Canadian Hydrographic Conference 2002.
- NOAA (1976). *“Hydrographic Manual. 4th edition”* National Oceanic and Atmospheric Administration. US Department of Commerce.
- Pföhner, F. (1993). *“Model for Calculation of Uncertainty in Multibeam Depth Soundings”* Report from Simrad Subsea AS, Horten, Norway, FEMME 93, 16 p.
- Pickard, G. and W. Emery (1990). *“Descriptive Physical Oceanography – An Introduction, 5th edition”* Pergamon Press, Oxford.
- Seippel, R. (1983). *“Transducers, Sensors and Detectors”* Prentice-Hall.
- Smith, R. and P. Keating (1996). *“The usefulness of multicomponent, time-domain airborne electromagnetic measurements”* Geophysics, Vol. 61, No. 1, pp. 74–81.
- Smith, W. and D. Sandwell (1997). *“Global Seafloor Topography from Satellite Altimetry and Ship Depth Sounding”* Science 277. pp. 1956-1962.
- OMG (1996). *“Multibeam Sonar Surveying Training Course. Ocean Mapping Group”* University of New Brunswick.
- Urlick, R. (1975). *Principles of Underwater Acoustics*. McGraw-Hill, Toronto.
- Zollinger, R., H. Morrison, P. Lazenby, and A. Becker (1987). *“Airborne Electromagnetic Bathymetry”* Geophysics, Vol. 52 no. 8, pp. 1172-1137.

BIBLIOGRAPHY

- Andersen, O. and P. Knudsen (1998). *“Global Gravity Field from ERS1 and GEOSAT Geodetic Mission Altimetry”* Journal Geophysics Research 103(C4), pp. 8129-8137.
- Arabelos, D. (1997). *“On the Possibility to Estimate the Bottom Topography from Marine Gravity and Satellite Altimetry Data Using Collocation”* In: R. Forsberg, M. Feissel, R. Dietrich (eds) Geodesy on the Move Gravity, Geoid, Geodynamics, and Antarctica IAG Symposia 119, Springer – Verlag Berlin Heidelberg, pp. 105-112.
- Burtch, R. (2002). *“Lidar Principles and Applications”* IMAGIN Conference 2002, Traverse City.
- Calmant, S. and N. Baudry (1996). *“Modelling Bathymetry by Inverting Satellite Altimetry Data: A Review”* Marine Geophysics Research 18, pp. 23-134.
- Collet, C., J. Provost, P. Rostaing, P. Pérez, and P. Bouthemy (2000). *“SPOT Satellite Data Analysis for Bathymetric Mapping”* IEEE, pp. 964-967.
- Denbigh, P. (1989). *“Swath bathymetry: Principles of operation and an analysis of errors”* IEEE Journal of Oceanic Engineering 14, pp. 289-298.
- Dixon, T., M. Naraghi, M. McNutt, and S. Smith (1983). *“Bathymetric Prediction from SEASAT Altimeter Data”* Journal Geophysics Research 88, pp. 1563-1571.
- Durey, L., G. Terrie, R. Arnone, and A. Martinez (1997). *“Bottom Reflectance Maps from Hyperspectral Sensors: An Application to AAHIS Data”* In Proceedings, ERIM Fourth International Conference on Remote Sensing for Marine and Coastal Environments, Orlando, pp. 17-19.
- Geng, X. and A. Zielinski (1999). *“Precise Multibeam Acoustic Bathymetry”* Marine Geodesy, 22, pp. 157-167.
- Guenther, G. (1985). *“Airborne Laser Hydrography: System Design and Performance Factors”* NOAA Professional Paper Series, National Ocean Service.
- Guenther, G., A. Cunningham, P. LaRocque, and D. Reid (2000). *“Meeting the Accuracy Challenge in Airborne Lidar Bathymetry”* Proceedings of EARSel Symposium 2000. Dresden, Germany.

- Guenther, G., M. Brooks, and P. LaRocque (1998). *"New Capabilities of the SHOALS Airborne Lidar Bathymeter"* Proceedings 5th International Conference on Remote Sensing for Marine and Coastal Environments, ERIM International, October 5-7, San Diego, CA, Vol. I, 47-55.
- Guenther, G., P. LaRocque, and W. Lillycrop (1994). *"Multiple Surface Channels in SHOALS Airborne Lidar"* SPIE: Ocean Optics XII, Vol. 2258, pp. 422-430.
- Guenther, G., R. Thomas, and P. LaRocque (1996). *"Design Considerations for Achieving High Accuracy with the SHOALS Bathymetric Lidar System"* SPIE: Laser Remote Sensing of Natural Waters from Theory to Practice, Vol. 2964, pp. 54-71.
- Hammerstad E. (1995). *"Simrad EM 950/1000 - Error Model for Australian Navy"* Extract of Report, Simrad Subsea AS, Horten, Norway, 4 p.
- Hare, R. and A. Godin (1996). *"Estimating Depth and Positioning Errors for the Creed/ EM 1000 Swath Sounding System"* Proceedings of the Canadian Hydrographic Conference '96. Halifax, NS, Canada, pp. 9-15.
- Herlihy, D., B. Hillard, and T. Rulon (1989). *"National Oceanic and Atmospheric Administration Sea Beam System - Patch Test"* International Hydrographic Review, Monaco, LXVI(2), pp. 119-139.
- Hughes Clarke, J. (1995). *"Reference Frame and Integration."* Lecture IV-1 in Coastal Multibeam Hydrographic Surveys. United States / Canada Hydrographic Commission Multibeam Working Group, St. Andrews, New Brunswick, Canada.
- Hughes Clarke, J. (1995a). *"Interactive Bathymetry Data Cleaning"* Lecture X-4 from Coastal Multibeam Hydrographic Surveys. United States / Canada Hydrographic Commission Multibeam Working Group, St. Andrews, New Brunswick, Canada.
- Ingham, A. (1992). *"Hydrography for the Surveyor and Engineer"* 3rd edition, BSP, Oxford.
- Irish, J. and W. Lillycrop (1999). *"Scanning Laser Mapping of the Coastal Zone: The SHOALS System"* ISPRS Journal of Photogrammetry and Remote Sensing, 54. pp. 123-129.
- Irish, J., J. McClung, and W. Lillycrop (2000). *"Airborne Lidar Bathymetry: the SHOALS System"* PIANC Bulletin. 2000 (103), pp. 43-53.
- Jung, W. and P. Vogt (1992). *"Predicting Bathymetry from Geosat ERM and Ship Borne Profiles in the South Atlantic Ocean"* Tectonophysics 210, pp. 235-253.

- Lillycrop W., L. Parson, and J. Irish (1996). *"Development and Operation of the SHOALS Airborne Lidar Hydrographic Survey System"* SPIE: Laser Remote Sensing of Natural Waters from Theory to Practice, Vol. 2964, pp. 26-37.
- Lillycrop, W. and J. Banic, (1993). *"Advancements in the US Army Corps of Engineers Hydrographic Survey Capabilities: The SHOALS System"* Marine Geodesy, Vol. 15, pp. 177-185.
- Lillycrop, W., J. Irish, and L. Parson (1997). *"SHOALS System: Three Years of Operation with Airborne Lidar Bathymetry - Experiences, Capability and Technology Advancements"* Sea Technology, Vol. 38, No. 6, pp. 17-25.
- Lillycrop, W., L. Parson, L. Estep, P. LaRocque, G. Guenther, M. Reed, and C. Truitt (1994). *"Field Test Results of the U.S. Army Corps of Engineers Airborne Lidar Hydrographic Survey System"* Proceedings of the 6th Biennial National Ocean Service International Hydrographic Conference, Norfolk, VA, pp. 144-151.
- Parson, L., W. Lillycrop, C. Klein, R. Ives, and S. Orlando (1996). *"Use of LIDAR Technology for Collecting Shallow Bathymetry of Florida Bay"* Journal of Coastal Research, Vol. 13, No. 4.
- Pope, R., B. Reed, G. West, and W. Lillycrop. (1997). *"Use of an Airborne Laser Depth Sounding System in a Complex Shallow-water Environment"* Proceedings of Hydrographic Symposium XVth International Hydro Conference. Monaco.
- Quinn, R., (1992), *"Coastal Base Mapping with the LARSEN Scanning Lidar System and Other Sensors"* Proceedings, 5th Biennial National Ocean Service International Hydrographic Conference, Baltimore.
- Riley, J. (1995). *"Evaluating SHOALS Bathymetry Using NOAA Hydrographic Survey Data"* Proceedings 24th Joint Meeting of UNIR Sea Bottom Surveys Panel, Tokyo, Japan.
- Sinclair, M. (1998). *"Australians Get on Board with New Laser Airborne Depth Sounder"* Sea Technology, June 1998, pp. 19-25.
- Sinclair, M. (1999). *"Laser Hydrography - Commercial Survey Operations"* Hydro 99.
- Smith, R. and M. Smith (2000). *"Airborne Lidar and Airborne Hyperspectral Imagery: A Fusion of Two Proven Sensors for Improved Hydrographic Surveying"* Proceedings Canadian Hydrographic Conference 2000.
- Thomas, R. and G. Guenther (1990). *"Water Surface Detection Strategy for an Airborne Laser Bathymeter"* SPIE: Ocean Optics X, Vol. 1302, pp. 597-611.

- | | | |
|---|--|---|
| USACE (2002). | <i>“Hydrographic Surveying Manual”</i> | U.S. Army Corps of Engineers,
Department of the Army,
Washington. |
| Vergos, G. and M.
Sideris (1998). | <i>“On Improving the Determination of the Gravity Field by Estimating the Bottom Ocean Topography with Satellite Altimetry and Shipborne Gravity Data”</i> | Department of Geomatics
Engineering, University of Calgary. |
| Whitman, E. (1996). | <i>“Laser Airborne Bathymetry - Lifting the Littoral”</i> | Sea Technology, August 1996, pp.
95-98. |
| Wozencraft, J.
(2001). | <i>“The Coastal Zone Revealed Through Shoals Lidar Data”</i> | Proceedings US Hydrographic
Conference 2001. |
| Wright, C. and J.
Brock (2002). | <i>“EAARL: A LIDAR for Mapping Shallow Coral Reefs and Other Coastal Environments”</i> | Seventh International Conference
on Remote Sensing for Marine and
Coastal Environments Proceedings
2002. |
| Yakima, W., Wilt
M., H. Morrison, K.
Lee, and N.
Goldstein (1989). | <i>“Electromagnetic Sounding in the Columbia Basin”</i> | Geophysics, Vol. 54, No. 8, pp.
952-961. |
-

CHAPTER 3 – ANNEX A

REFERENCE AND COORDINATE SYSTEMS

A. Reference and Coordinate Systems

Depth determination is performed in a vessel in dynamic conditions. Usually, a reference system (vessel coordinate system), three orthogonal axes, is used on board to locate the hydrographic sensors and to measure the vessel's attitude and heave.

The vessel's attitude consists of angular displacements about those axes, roll (transversally) about the x axis, pitch (longitudinally) about the y axis, and yaw (horizontally) about the z axis. Considering an orthogonal right-hand reference system with the z axis pointing downward; with the usual convention for most attitude sensors roll is positive when starboard side is down, pitch is positive when bow is up, and yaw is positive when rotating clockwise.

Considering Figure A.1, the rotation θ_1 in the yz plane, i.e., rotation about the x axis, can be expressed by the rotation matrix,

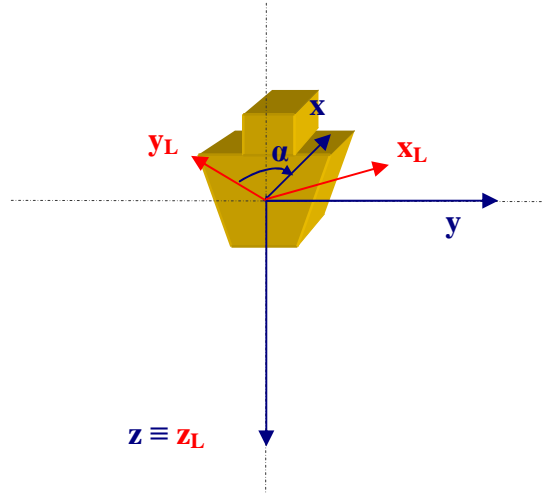


Fig. A.1. “Vessel reference system”

$$R_1(\theta) = \begin{bmatrix} 1 & 0 & 0 \\ 0 & \cos(\theta) & \sin(\theta) \\ 0 & -\sin(\theta) & \cos(\theta) \end{bmatrix} \quad (\text{A. 1})$$

and the rotations about the y and z axes are respectively:

$$R_2(\theta) = \begin{bmatrix} \cos(\theta) & 0 & -\sin(\theta) \\ 0 & 1 & 0 \\ \sin(\theta) & 0 & \cos(\theta) \end{bmatrix}, \quad (\text{A. 2})$$

$$R_3(\theta) = \begin{bmatrix} \cos(\theta) & \sin(\theta) & 0 \\ -\sin(\theta) & \cos(\theta) & 0 \\ 0 & 0 & 1 \end{bmatrix}. \quad (\text{A. 3})$$

The transformation which results from three sequential rotations is represented by the product of the rotation matrices. Successive rotations are applied to the left of this product.

Considering the successive rotations $(\theta_1, \theta_2, \theta_3)$ about the x, y and z axes, the transformation matrix is given by,

$$R_3(\theta_3) \cdot R_2(\theta_2) \cdot R_1(\theta_1) =$$

$$= \begin{bmatrix} \cos(\theta_3)\cos(\theta_2) & \sin(\theta_3)\cos(\theta_1) + \cos(\theta_3)\sin(\theta_2)\sin(\theta_1) & \sin(\theta_3)\sin(\theta_1) - \cos(\theta_3)\sin(\theta_2)\cos(\theta_1) \\ -\sin(\theta_3)\cos(\theta_2) & \cos(\theta_3)\cos(\theta_1) - \sin(\theta_3)\sin(\theta_2)\sin(\theta_1) & \cos(\theta_3)\sin(\theta_1) + \sin(\theta_3)\sin(\theta_2)\cos(\theta_1) \\ \sin(\theta_2) & -\cos(\theta_2)\sin(\theta_1) & \cos(\theta_2)\cos(\theta_1) \end{bmatrix}. \quad (\text{A. 4})$$

The measured depths, initially referred to the vessel's frame, need to be positioned in a local coordinate system. Considering an orthogonal left-hand local coordinate system; with the x axis pointing to East, y axis pointing to the geographic North, and the z axis pointing downward.

In a survey vessel with roll, pitch, and heading respectively: θ_R , θ_P , and α ; a beam with slant range R and angle β (Figure A.2), will be transferred from the tri-orthogonal, right-hand, vessel coordinate system $(x, y, z)_V$ to the tri-orthogonal, left-hand, local coordinate system $(x, y, z)_L$, with the rotation about the x axis the reciprocal of the roll angle $(-\theta_R)$, the rotation about the y axis the reciprocal of the pitch angle $(-\theta_P)$, and the rotation about the z axis the reciprocal of the heading angle $(-\alpha)$ and since the two z axes are both positive downward, but the vessel coordinate system is a right-hand system and the local coordinate system is a left-hand system, it is necessary to swap the x and y coordinates during the transformation from vessel to local coordinate systems. This is performed by applying the matrix R_{xy} .

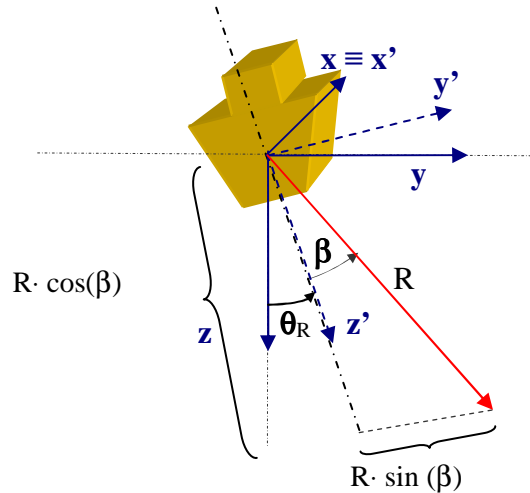


Fig. A.2 “Vessel and local level reference system”

$$\begin{bmatrix} x \\ y \\ z \end{bmatrix}_L = R_{xy} \cdot R_3(-\alpha) \cdot R_2(-\theta_p) \cdot R_1(-\theta_R) \begin{bmatrix} x \\ y \\ z \end{bmatrix}_V = T(\alpha, \theta_p, \theta_R) \begin{bmatrix} 0 \\ R \sin(\theta) \\ R \cos(\theta) \end{bmatrix}_V \quad (\text{A. 5})$$

where R_{xy} is given by,

$$R_{xy} = \begin{bmatrix} 0 & 1 & 0 \\ 1 & 0 & 0 \\ 0 & 0 & 1 \end{bmatrix}$$

$$T(\alpha, \theta_p, \theta_R) = \begin{bmatrix} \sin(\alpha)\cos(\theta_p) & \cos(\alpha)\cos(\theta_R) + \sin(\alpha)\sin(\theta_p)\sin(\theta_R) & -\cos(\alpha)\sin(\theta_R) + \sin(\alpha)\sin(\theta_p)\cos(\theta_R) \\ \cos(\alpha)\cos(\theta_p) & -\sin(\alpha)\cos(\theta_R) + \cos(\alpha)\sin(\theta_p)\sin(\theta_R) & \sin(\alpha)\sin(\theta_R) + \cos(\alpha)\sin(\theta_p)\cos(\theta_R) \\ -\sin(\theta_p) & \cos(\theta_p)\sin(\theta_R) & \cos(\theta_p)\cos(\theta_R) \end{bmatrix}$$

where $T(\alpha, \theta_p, \theta_R)$ is the transformation matrix from reference frame measurements into the local coordinate system.

$$\begin{bmatrix} x \\ y \\ z \end{bmatrix}_L = \begin{bmatrix} (\cos(\alpha)\cos(\theta_R) + \sin(\alpha)\sin(\theta_p)\sin(\theta_R)) \cdot R \sin(\beta) + (-\cos(\alpha)\sin(\theta_R) + \sin(\alpha)\sin(\theta_p)\cos(\theta_R)) \cdot R \cos(\beta) \\ (-\sin(\alpha)\cos(\theta_R) + \cos(\alpha)\sin(\theta_p)\sin(\theta_R)) \cdot R \sin(\beta) + (\sin(\alpha)\sin(\theta_R) + \cos(\alpha)\sin(\theta_p)\cos(\theta_R)) \cdot R \cos(\beta) \\ \cos(\theta_p)\sin(\theta_R) \cdot R \sin(\beta) + \cos(\theta_p)\cos(\theta_R) \cdot R \cos(\beta) \end{bmatrix}$$

Note that the beam angle is positive to starboard side and negative to port.